

Ministère de l'Enseignement Supérieur et de la Recherche Scientifique
Université Hassiba Benbouali de Chlef
Faculté de Technologie
Département de Génie Mécanique



THÈSE

Présentée pour l'obtention du diplôme de

DOCTORAT EN SCIENCES

Spécialité : Génie Mécanique

Par

Saliha MOHAMMED BELKEBIR

Thème:

CONTRIBUTION PAR HOMOGENÉISATION DE LA COMBUSTION DANS UNE CHAMBRE DE COMBUSTION D'UN MOTEUR DIESEL

Soutenue le 06/12/2021, devant le jury composé de:

HOCINE Abdelkader	Professeur	UHB-Chlef	Président
KHELIL Ali	Professeur	UHB-Chlef	Rapporteur
TOUAIBI Rabah	MCA	UDB-Khemis Miliana	Rapporteur
CHETTI Boualem	MCA	UDB-Khemis Miliana	Rapporteur
MANSOUR Cheikh	Professeur	USTO-MB Oran	Rapporteur
TAHAR-ABBES Miloud	Professeur	UHB-Chlef	Directeur de Thèse
KHELIDJ Benyoucef	MCB	UDB-Khemis Miliana	invité

Ministry of Higher Education and Scientific Research
Hassiba Benbouali University of Chlef
Faculty of Technology
Department of Mechanical Engineering



THESIS

OF DOCTORATE IN SCIENCES

Mechanical Engineering

Presented by

Saliha MOHAMMED BELKEBIR

Theme:

**CONTRIBUTION BY HOMOGENIZATION OF COMBUSTION
IN A COMBUSTION CHAMBER OF A DIESEL ENGINE**

Defended on December 06, 2021, in front of a committee composed of:

HOCINE Abdelkader	Professor	UHB-Chlef	President
KHELIL Ali	Professor	UHB-Chlef	Examinator
TOUAIBI Rabah	MCA	UDB-Khemis Miliana	Examinator
CHETTI Boualem	MCA	UDB-Khemis Miliana	Examinator
MANSOUR Cheikh	Professor	USTO-MB Oran	Examinator
TAHAR-ABBES Miloud	Professor	UHB-Chlef	Supervisor
KHELIDJ Benyoucef	MCB	UDB-Khemis Miliana	Guest

DEDICATIONS

I dedicate this work to:
In memory of my brother;
My dear parents who helped me a lot;
To my brothers and sister;
To the whole family and friends.

ACKNOWLEDGEMENTS

I owe this work to Allah almighty first and then to all my teachers from whom I learned a great deal from the very beginning of my early studies until this moment. Allah blesses them.

About this degree, there have been many people who have assisted, encouraged and supported me in my doctorate. I would like to show great appreciation to Pr. TAHAR ABBES Miloud for giving me excellent opportunities to study under his supervision. He was extremely supportive in every situation and it was my honor that he was my supervisor. I couldn't imagine having a better academic advisor for my Ph.D. thesis. I must express my gratefulness from the bottom of my heart for the supports that I believed I learned from one of the best experts in this field. I also would like to thank my supervising assistant Dr. KHELIDJ Benyoucef, who provided his valuable time and inputs to the research project and guided me from the beginning to the end. I also would like to thank him as he has been an indispensable source of advice and encouragement throughout my undergraduate and graduate career.

Next, I would like to graciously thank my committee members, Pr. HOCINE Abdelkader, Pr. KHELIL Ali, Dr. TOUAIBI Rabah, Dr. CHETTI Boualem and Pr. MANSOUR Cheikh for agreeing to judge this work.

I would also like to thank all my friends, F. GHABACHE, K. REDAOUIA, F. BOUDJEMAA, H. OULDARAB, H. DOUBA and R. MAHROUG for the support given to help me out finish writing my thesis!

Finally, I would like to give the utmost thanks to my family, who have been unwavering in their support and confidence during my entire academic career. Specifically, I would like to thank my parents effusively. Without their guidance, patience and sacrifice, I would not have been able to complete this journey.

My hope is one day to return the favor to all the people that helped me on this path.

Thanks for everything!

ABSTRACT

In order to investigate the concept that constitutes a viable approach to achieve high efficiencies and low emissions of nitrogen oxides (NO_x) and particulate (PM), this study was introduced by applying the operating conditions of the diesel engine to the homogeneous charge compression ignition (HCCI) engine. In this work, we present an analysis of the impacts of the equivalence ratio (ϕ), the intake charge temperature (T_{IVC}), the intake charge pressure (P_{IVC}), the compression ratio (CR) and the exhaust gas recirculation (EGR) rate on the combustion parameters. The results of these impacts were analyzed and discussed in detail. The ANSYS CHEMKIN-Pro software and the combined chemical kinetics mechanism were used to perform simulations for a closed homogeneous reactor under conditions relevant to HCCI engines. The calculation process is based on one single zone in the combustion chamber. The results show that HCCI combustion is more practical for very lean mixtures and the decreasing of mixing ratio lead to decreases engine emissions. Moreover, when the temperature T_{IVC} decreases from 277°C to 177°C , the indicated mean effective pressure (IMEP) increases from 6.34 bars to 8.62 bars. On the other hand, Diesel-RK software was used to study the effect of three different fuels, Heavy Diesel, Diesel No.2 and Hexadecane on engine performance and emissions. The results obtained were compared with those found with the baseline diesel fuel (Hexadecane). Simulation results relate to efficiency and power parameters such as piston engine power, torque and specific fuel consumption, as well as ecological parameters such as specific CO_2 and NO_x emissions. The results allow us to expect a decrease in NO_x emissions from Heavy diesel fuel used.

Keywords: combustion, numerical simulation, homogeneous charge compression ignition, exhaust gas recirculation, performance, emissions.

RÉSUMÉ

Afin d'étudier le concept qui constitue une approche viable pour atteindre des rendements élevés et de faibles émissions d'oxydes d'azote (NO_x) et de particules (PM), cette étude a été introduite en appliquant au moteur à allumage par compression à charge homogène (HCCI) les conditions de fonctionnement du moteur diesel. Dans ce travail, nous présentons une analyse des impacts du rapport d'équivalence (ϕ), de la température de la charge d'admission (T_{IVC}), de la pression de la charge d'admission (P_{IVC}), du taux de compression (CR) et du taux de recirculation des gaz d'échappement (EGR) sur les paramètres de combustion.

Les résultats de ces impacts ont été analysés et discutés en détail. Le logiciel ANSYS CHEMKIN-Pro et le mécanisme de cinétique chimique combiné ont été utilisés pour effectuer des simulations sur un réacteur homogène fermé dans des conditions pertinentes pour les moteurs HCCI. Le processus de calcul est basé sur une seule zone dans la chambre de combustion. Les résultats montrent que la combustion HCCI est plus adaptée pour les mélanges très pauvres et la diminution du rapport de mélange conduit à une diminution des émissions du moteur. De plus, lorsque la température T_{IVC} diminue de 277°C à 177°C , la pression effective moyenne indiquée (IMEP) augmente de 6.34 bars à 8.62 bars. D'autre part, nous avons utilisé le logiciel Diesel-RK pour étudier l'effet de trois carburants différents, le Diesel lourd (Fioul Lourd), le Diesel No. 2 et l'Hexadécane sur les performances et les émissions du moteur. Les résultats obtenus ont été comparés à ceux trouvés avec le carburant diesel de référence (Hexadécane). Les résultats de simulation sont relatifs aux paramètres d'efficacité et de puissance tels que la puissance du moteur à piston, le couple et la consommation spécifique de carburant, ainsi qu'aux paramètres écologiques tels que les émissions spécifiques de CO_2 et de NO_x . Ces résultats ont montré une diminution des émissions de NO_x pour le carburant diesel lourd utilisé.

Mots clés : combustion, simulation numérique, allumage par compression à charge homogène, recirculation des gaz d'échappement, performances, émissions.

المخلص

من أجل التحقيق في المفهوم الذي يعد نهجاً قابلاً للتطبيق لتحقيق كفاءات عالية وانبعاثات منخفضة من أكاسيد النيتروجين والجسيمات ، تم تقديم هذه الدراسة من خلال تطبيق شروط تشغيل محرك الديزل على الاشتعال بضغط الشحنة المتجانس (HCCI). نقدم في هذا العمل تحليلاً لتأثيرات كل من نسبة التكافؤ (ϕ) ، درجة حرارة شحنة المدخل (T_{IVC})، ضغط شحنة المدخل (P_{IVC}) ، نسبة الضغط (CR) ومعدل إعادة تدوير غاز العادم (EGR) على معالم الاحتراق. تم تحليل نتائج هذه الآثار ومناقشتها بالتفصيل. تم استخدام برنامج ANSYS CHEMKIN-Pro وآلية الحركة الكيميائية المدمجة لإجراء عمليات محاكاة لمفاعل متجانس مغلق في ظل ظروف ذات صلة بمحركات HCCI حيث تعتمد عملية الحساب على منطقة واحدة في غرفة الاحتراق. أظهرت النتائج أن احتراق HCCI أكثر عملية للمخاليط الهزيلة جداً والانخفاض في نسبة الخليط يؤدي إلى انخفاض في انبعاثات المحرك. بالإضافة إلى ذلك، عندما تنخفض درجة حرارة T_{IVC} من 277 درجة مئوية إلى 177 درجة مئوية، يزداد متوسط الضغط الفعال المشار إليه (IMEP) من 6.34 بار إلى 8.62 بار. من ناحية أخرى ، تم استخدام برنامج Diesel-RK لدراسة تأثير ثلاثة أنواع مختلفة من الوقود وهما الديزل الثقيل ، الديزل رقم 2 و الهكساديكان على أداء المحرك وانبعاثاته. تمت مقارنة النتائج التي تم الحصول عليها مع وقود الديزل المرجعي (هكساديكان). تتضمن نتائج المحاكاة بمعلمات الكفاءة والطاقة مثل قوة محرك المكبس وعزم الدوران واستهلاك الوقود المحدد ، بالإضافة إلى المعالم البيئية مثل انبعاثات ثاني أكسيد الكربون وأكاسيد النيتروجين. تسمح لنا النتائج بتوقع انخفاض في انبعاثات أكاسيد النيتروجين لوقود الديزل الثقيل المستخدم.

الكلمات المفتاحية: الاحتراق، محاكاة رقمية، الاشتعال بضغط الشحنة المتجانس، إعادة تدوير غاز العادم ، الأداء، الانبعاثات.

TABLE OF CONTENTS

DEDICATIONS	I
ACKNOWLEDGEMENTS	II
ABSTRACT.....	III
RÉSUMÉ	III
الملخص	IV
TABLE OF CONTENTS.....	V
LIST OF TABLES.....	VIII
LIST OF FIGURES.....	IX
NOMENCLATURE.....	XII
GENERAL INTRODUCTION	1
CHAPTER 1- LITERATURE REVIEW.....	4
1.1. INTRODUCTION	4
1.2. GENERAL OPERATION OF THE INTERNAL COMBUSTION ENGINE	5
1.2.1. Fuel injection system in diesel engine.....	6
1.2.2. Fuel injector	7
1.2.3. Fuel injector nozzle	7
1.2.4. Compression ignition background.....	7
1.2.4.1. Physical processes of compression ignition.....	8
1.2.4.2. Chemical processes of compression ignition	8
1.2.4.3. Complete ignition process	8
1.3. HCCI ENGINES	9
1.3.1. Principle and working of HCCI engines.....	9
1.3.2. Previous work HCCI	11
1.3.3. HCCI challenges and proposed solutions	13
1.3.4. Control of HCCI ignition timing.....	14
1.3.4.1. Mixture dilution for HCCI control	14
1.3.4.2. External exhaust gas recirculation (eEGR)	16
1.3.4.3. Internal exhaust gas recirculation (iEGR).....	17
1.3.4.4. Different fuels	18
1.3.4.5. Fast thermal management for HCCI control	19
1.3.4.6. Direct injection for HCCI control	20
1.3.4.7. Forced induction	21
1.3.4.8. Turbulence	22
1.3.5. Emissions of HCCI engines.....	23
1.3.5.1. CO Emissions.....	24
1.3.5.2. UHC Emissions	24
1.3.5.3. NO _x Emissions	24
1.4. ABOUT EXHAUST GAS RECIRCULATION (EGR)	25

1.5.	EMISSIONS AND REGULATIONS	28
1.5.1.	Heavy-duty vehicles	29
1.5.2.	Light-duty vehicles	30
1.6.	POST-TREATMENT OF POLLUTING EMISSIONS FROM INTERNAL COMBUSTION THERMAL ENGINES	31
1.6.1.	Exhaust gas recirculation (EGR).....	31
1.6.2.	NO _x trap type catalyts.....	32
1.6.3.	Diesel oxidation catalyst (DOC)	32
1.6.4.	Diesel particulate filters (DPFs)	33
1.6.5.	Selective catalytic reduction (SCR)	34
1.7.	CONCLUSION	35
CHAPTER 2- MODELING AND SIMULATION OF HETEROGENEOUS AND HOMOGENEOUS COMBUSTION.....		36
2.1.	INTRODUCTION	36
2.2.	COMBUSTION MODELLING	37
2.2.1.	Heterogeneous combustion	38
2.2.1.1.	Diesel-RK engine simulation software	38
2.2.1.2.	Model equations.....	50
2.2.2.	Homogeneous combustion	59
2.2.2.1.	CHEMKIN-Pro simulation software	59
2.2.2.2.	CHEMKIN Set Up	59
2.2.2.3.	Model description.....	60
2.2.2.4.	Charge compression ignition (HCCI) model (CHEMKIN-Pro Set-Up).....	61
2.2.2.5.	Structure of the calculation program (CHEMKIN-Pro).....	62
2.2.2.6.	Chemical kinetics model	65
2.2.2.7.	Governing equations.....	66
2.2.2.8.	Heat-transfer options for the IC-HCCI engine model.....	66
2.2.2.9.	Combustion reactions.....	68
2.2.3.	Thermodynamic analysis.....	69
2.2.3.1.	Governing equations.....	69
2.3.	CONCLUSION	74
CHAPTER 3- RESULTS AND DISCUSSION		75
3.1.	INTRODUCTION	75
3.2.	SIMULATION RESULTS (DIESEL-RK SOFTWARE).....	75
3.2.1.	Combustion parameters effect	75
3.2.1.1.	Cylinder pressure evolution	75
3.2.1.2.	Cylinder temperature evolution	76
3.2.1.3.	Ignition delay	76
3.2.2.	Performance parameters	76
3.2.2.1.	Indicated thermal efficiency (ITE)	76
3.2.2.2.	Brake torque	77
3.2.2.3.	Brake mean effective pressure (BMEP)	77
3.2.3.	Emission parameters.....	77
3.2.3.1.	NO _x emissions.....	77

3.2.3.2.	Specific carbon dioxide emissions	77
3.2.3.3.	Specific particulate matter (PM) emissions	78
3.3.	VALIDATION MODEL	80
3.4.	SIMULATION RESULTS (ANSYS CHEMKIN-PRO)	81
3.4.1.	Combustion parameters effect	82
3.4.1.1.	Cylinder temperature evolution	82
3.4.1.2.	Cylinder pressure evolution	83
3.4.1.3.	Net heat release rate (NHRR) evolution	85
3.4.2.	Engine performance parameters	86
3.4.3.	Emissions evolution.....	88
3.4.4.	EGR rate affect	90
3.5.	COMPARISON RESULTS (CHEMKIN-PRO/ DIESEL-RK SOFTWARE).....	92
	GENERAL CONCLUSION	93
	BIBLIOGRAPHY.....	95

LIST OF TABLES

Table 1. 1- Comparative parameters of SI, CI and HCCI engines [27]	11
Table 1. 2- Milestone achieved by the researcher in the development of HCCI engines [54]	13
Table 1. 3- Typical diesel exhaust composition [12]	29
Table 1. 4- US EPA Heavy duty diesel emissions standards.....	29
Table 1. 5- EU Heavy duty diesel emission standards in g/kWh	30
Table 1. 6- EU emission limits for private vehicles in g.km ⁻¹ [145].....	30
Table 2. 1-Properties of n-Hexadecane, Diesel No. 2 and Heavy diesel fuels	39
Table 2. 2-Simulated engine specifications.....	40
Table 2. 3-Coefficients C ₁ and C ₂ for Woschni correlation [172].....	67
Table 2. 4-Low-temperature (T<1000K) combustion products [187]	68
Table 2. 5- Engine parameters	70
Table 3. 1- Summary of relative change in engine parameters to the base fuel parameters	79
Table 3. 2- Comparison of the results between Diesel-RK software and MATLAB code at 1600 rpm.....	81
Table 3. 3- Engine performance parameters (cycle) with different EGR rates	90
Table 3. 4- Comparison between CHEMKIN and Diesel-RK software results	92

LIST OF FIGURES

Figure 1. 1- PCCI, LTC and HCCI concept on the ϕ -T map [29,15].	5
Figure 1. 2- Process in a four-stroke engine [30].	5
Figure 1. 3- Overall compression ignition [34].	8
Figure 1. 4- Schematic diagram of HCCI [43].	10
Figure 1. 5- High pressure EGR system with cooler.	26
Figure 1. 6- Effect of reducing oxygen concentration by different diluents on NO _x [8].	26
Figure 1. 7- The exhaust gas recirculation system [130,132].	27
Figure 1. 8- EGR systems in a turbocharged engine [133].	27
Figure 1. 9- Operation of a NO _x trap [150].	32
Figure 1. 10- Flow-through diesel oxidation catalyst [12].	33
Figure 1. 11- Ceramic monolith [12].	34
Figure 1. 12- Schematic representation of wall flow DPF [158].	34
Figure 1. 13- SCR layout in a heavy duty vehicle. Consists of the DOC (Diesel oxidation catalyst), DPF(Diesel particulate filter), Urea injector, SCR [161].	35
Figure 2. 1- Photo of an F8L413 diesel engine and its cross-section piston.	38
Figure 2. 2- FL413 F combustion chamber and position of the injection jets [169].	39
Figure 2. 3- Show the cylinder shape.	41
Figure 2. 4- The selection of engine cycle, fuel, and method of ignition.	42
Figure 2. 5- Selection of the basic engine design, number of cylinders, and type of cooling system.	42
Figure 2. 6- Engine geometrical dimensions (cylinder bore, stroke, engine speed and compression ratio).	43
Figure 2. 7- Options that selected ambient parameters (pressure and temperature) and engine application.	44
Figure 2. 8- Options selected for compressor pressure ratio and the number of valves per cylinder.	44
Figure 2. 9- Shows how to save the result file.	45
Figure 2. 10- Inlet valve timing parameters.	45
Figure 2. 11- Exhaust valve timing parameters.	46
Figure 2. 12- Fuel type and properties (Hexadecane).	46
Figure 2. 13- Design of the piston bowl (geometry of F8L413 engine).	47
Figure 2. 14- Operating mode table.	47
Figure 2. 15- Design of injector, orientation, and diameter of holes.	48
Figure 2. 16- Input injection profile.	49
Figure 2. 17- Run the program.	50

Figure 2. 18- Shows a run of the program.....	50
Figure 2. 19- Identification of the phases of the combustion, from heat release rate [8]	52
Figure 2. 20- Structure of CHEMKIN.....	60
Figure 2. 21- Typical HCCI with premixed fuel-air for F8L413 engine.....	61
Figure 2. 22- Choice of the reactor.....	62
Figure 2. 23- Chemistry set of Gas-Phase Kinetics file and Thermodynamics data file.....	63
Figure 2. 24- Engine basic and heat transfer parameters.....	63
Figure 2. 25- Reactor Physical Property for Woschni heat loss model.....	64
Figure 2. 26- Reactant species.....	64
Figure 2. 27- Model algorithm; CN—Cetane number; CC—Chemical composition; P—Pressure; T— Temperature; LHV—Lower heating value; IDP— Ignition delay period.....	74
Figure 3. 1- Variation of (a) cylinder pressure,(b) cylinder temperature, (c) combustion zone temperature and (d) concentration NO with crank angle according to the fuel type (engine speed=1600 rpm).....	78
Figure 3. 2- Results of engine torque and piston engine power.....	79
Figure 3. 3- Results of brake mean effective pressure and specific fuel consumption.....	80
Figure 3. 4- Comparison between model simulation results with those found in the literature [196].....	81
Figure 3. 5- Variation of cylinder temperature with crank angle according to the equivalence ratios ϕ ($P_{IVC}= 1.8\text{bar}$, $T_{IVC}= 500\text{K}$, $N= 2000\text{rpm}$).....	82
Figure 3. 6- Variation of cylinder temperature with crank angle according to the compression ratio ($P_{IVC}=$ 1.8bar , $T_{IVC}= 500\text{K}$, $\phi= 0.45$, $N= 2000\text{rpm}$).....	82
Figure 3. 7- Variation of cylinder temperature according to the intake charge temperature. Intake conditions ($P_{IVC}= 1.8\text{bar}$, $\phi= 0.45$, $\text{CR}= 18$, engine speed= 2000rpm).....	83
Figure 3. 8- Variation of cylinder pressure with crank angle according to the equivalence ratios ϕ ($P_{IVC}=$ 1.8bar , $T_{IVC}= 500\text{K}$, $N= 2000\text{rpm}$).....	84
Figure 3. 9- Variation of cylinder pressure with crank angle according to the intake charge temperature ($P_{IVC}= 1.8\text{bar}$, $\phi= 0.45$, $N= 2000\text{rpm}$).....	84
Figure 3. 10- Variation of cylinder pressure with crank angle according to the compression ratio. Intake conditions ($P_{IVC}= 1.8\text{bar}$, $T_{IVC}= 500\text{K}$, $\phi= 0.45$, engine speed= 2000rpm).....	84
Figure 3. 11- Variation of cylinder pressure with crank angle according to the pressure inlet. Intake conditions ($T_{IVC}= 500\text{K}$, $\text{CR}= 18$, $\phi= 0.45$, engine speed= 2000rpm).....	85
Figure 3. 12- Variation of net heat release with crank angle according to the equivalence ratios ϕ ($P_{IVC}=$ 1.8bar , $T_{IVC}= 500\text{K}$, $N= 2000\text{rpm}$).....	86
Figure 3. 13- Variation of net heat release rate according to the intake charge temperature ($P_{IVC}= 1.8\text{bar}$, $\phi= 0.45$, $N= 2000\text{rpm}$).....	86
Figure 3. 14- Engine performance parameters (cycle) according to the intake temperatures.....	87
Figure 3. 15- Engine performance parameters (cycle) according to the compression ratios.....	87

Figure 3. 16- Variation of CO molar fraction with crank angle according to the equivalence ratios ϕ ($P_{IVC}=1.8\text{bar}$, $T_{IVC}=500\text{K}$, $N=2000\text{rpm}$).....	88
Figure 3. 17- Variation of CO molar fraction with crank angle according to the intake charge temperature ($P_{IVC}=1.8\text{bar}$, $\phi=0.45$, $N=2000\text{rpm}$).	88
Figure 3. 18- Variation of unburned hydrocarbons with crank angle according to the equivalence ratios ϕ ($P_{IVC}=1.8\text{bar}$, $T_{IVC}=500\text{K}$, $N=2000\text{rpm}$).....	89
Figure 3. 19- Variation of unburned hydrocarbons with crank angle according to the intake charge temperature ($P_{IVC}=1.8\text{bar}$, $\phi=0.45$, $N=2000\text{rpm}$).....	89
Figure 3. 20- Variation of NO_x emissions with crank angle according to the equivalence ratios ϕ ($P_{IVC}=1.8\text{bar}$, $T_{IVC}=500\text{K}$, $N=2000\text{rpm}$).....	89
Figure 3. 21- Variation of NO_x emissions with crank angle according to the intake charge temperature ($P_{IVC}=1.8\text{bar}$, $\phi=0.45$, $N=2000\text{rpm}$).	89
Figure 3. 22- Variation of CO molar fraction with crank angle according to the compression ratio ($P_{IVC}=1.8\text{bar}$, $T_{IVC}=500\text{K}$, $\phi=0.45$, $N=2000\text{rpm}$).	89
Figure 3. 23- Variation of NO_x emissions with crank angle according to the compression ratio ($P_{IVC}=1.8\text{bar}$, $T_{IVC}=500\text{K}$, $\phi=0.45$, $N=2000\text{rpm}$).	89
Figure 3. 24- Evolution of (a) NHRR, (b) pressure, and (c) temperature cylinder for $\text{C}_{16}\text{H}_{34}$ fuel for different EGR rates.	91
Figure 3. 25- NO molar fraction evolution for different EGR rates.	91

NOMENCLATURE

Symbol	Designation	Unit
T	Temperature	K
B	Cylinder bore	m
S	Cylinder stroke	m
P	Cylinder pressure	Pa
h_g	Heat transfer coefficient	$W.m^{-2}.K^{-1}$
LHV	Lower heating value	$MJ.kg^{-1}$
C_v	Mean specific heat of the mixture	$J.kg^{-1}.K^{-1}$
V_d	Swept volume	m^3
R_c	Universal gas constant	$J/kg. mol^{-1}.K^{-1}$
\bar{U}_p	Mean piston speed	m/s
k_f	Forward rate constant	$m^3/mol. s$
k_r	Reverse rate constant	$m^3/mol. s$
CR	Compression ratio	-
θ	Instantaneous crank angle	degree
N	Engine speed	rpm
Q	Heat	J
M_1	Fresh load quantity	$kmol/kg-fuel$
M_2	Quantity of combustion products	$kmol/kg-fuel$
T_0	Normal atmosphere temperature	K
P_{IVC}	Cylinder pressure at IVC	bar
T_{IVC}	Cylinder temperature at IVC	K
IP	Indicated power	W
W_i	Indicated work	J
Tq	Torque	N.m
m	Mass	g

ALPHABET GREC

Symbol	Designation	Unit
u_{swirl}	Swirl velocity	m/s
ϕ	Equivalence ratio	-
$\dot{\omega}_k$	The chemical production rate	moles/cm ³ /sec
ρ	Fluid density	Kg/m ³
u	Specific internal energy	J/kg
λ	Coefficient of excess air	-

LIST OF ABBREVIATIONS

aTDC	after Top Dead Center
bTDC	before Top Dead Center
aBDC	after Bottom Dead Center
bBDC	before Bottom Dead Center
LNT	Lean NO _x Trap
SCR	Selective Catalytic Reduction
PCCI	Premixed Charge Compression Ignition
PPC	Partially Premixed Combustion
HCCI	Homogeneous Charge Compression Ignition
LTC	Low Temperature Combustion
EGR	Exhaust Gas Recirculation
BDC	Bottom Dead Center
TDC	Top Dead Center
CA	Crank Angle
EVO	Exhaust Valve Opening
IVC	Inlet Valve Closing
NO	Nitric Oxide (concentration, ppm)
WSF	Wall Surface Flow is a dense flow of air-fuel mixture moving along a wall

GENERAL INTRODUCTION

Today, pollutant emissions and global warming due mainly to the massive use of fossil fuels have become the most serious problems threatening the peaceful existence of humanity. Internal combustion engines, like the main engines of the automobile industry, consume a significant quantity of fossil fuel by combustion to develop their power and emit harmful exhaust gases such as unburned hydrocarbons (UHC), carbon monoxide (CO), carbon dioxide (CO₂), nitrogen oxides (NO_x) and fine particles (PM) [1]; which in turn absorb the infrared radiation emitted by the land surface and thus contribute to the greenhouse effect. The increase in atmospheric CO₂ concentration, known as the "additional greenhouse effect", is considered the main factor behind the recent rise in mean earth temperature [2]. The expected consequences of this global warming raise concerns (sea level rise, increased extinction of animal species, decrease in water resources,..., etc), and many countries have decided to reduce their greenhouse gas emissions greenhouse [3]. Therefore, the Paris Climate Conference 2015 (COP21) held from November 30 to December 11, 2015, resulted in an international climate agreement, applicable to all countries, to limit global warming to 2°C.

Modern direct injection diesel engines have a specific fuel consumption that is around 25% lower than that of modern gasoline engines [4]. In terms of emissions, diesel engines typically produce less carbon monoxide (CO) and unburnt or partially burned hydrocarbons (UHC), compared to gasoline engines [5,6]. Diesel engine emissions consist of a complex mixture of several hundred gaseous and particulate substances. The composition of diesel emissions has changed over time due to changes in diesel engine technology, fuel composition, engine type and age, engine speed and maintenance, treatment of exhaust gases and particles [7]. These developments mainly concern road vehicles, for which the emission standards introduced in Europe and the United States over the past 20 years have led to a gradual reduction in particle emissions [7,8]. A decrease in the size of the agglomerates has been observed, resulting in a reduction in the mass of particle emissions, but not in the number of particles.

Diesel engines are durable and reliable for their low cost of operation and higher efficiency. Due to the significant characteristics they offer, diesel engines are most preferred for

equipping heavy-duty vehicles [9]. In the transport sector case, heavy-duty vehicles contribute the most to climate change, as all or most vehicles on the roads are driven by internal combustion engines (ICE) and mainly diesel engines. This presumption is based on the fact that it will be very challenging in the near future to fully convert heavy-duty diesel transport to electric propulsion. Diesel engine exhaust has been classified as a human carcinogen [10]. Diesel particulate matter (DPM), known as fine particulate matter or particulate matter (PM), emitted by diesel engines, is a complex mixture. They have harmful effects on health and cause environmental problems [11]. Furthermore, the exhaust fumes emitted by diesel engines contain particulate (soot) emissions which are responsible for serious environmental and health problems [12]. The high gas temperature in the combustion chamber engine is one of the main factors in the NO_x formation and can be reduced when the oxygen (O₂) concentration in the combustion chamber is reduced. One of the main techniques for this is the use of exhaust gas recirculation (EGR). In this process, part of the oxygen is replaced by exhaust gas components such as CO₂ and H₂O.

In the context of the reduction of polluting emissions and fuel consumption of internal combustion engines, the researchers and engineers in the engine community pay more attention to the advanced combustion modes based on the conventional diesel (compression ignition) engine and spark ignition (SI) engine, such as homogeneous charge compression ignition (HCCI) [13-16], premixed charge compression ignition (PCCI) [17-19], reactivity controlled compression ignition (RCCI) [20,21] and CAI (controlled auto-ignition), are commonly used to denote specific variations of premixed combustion. The common feature of all these concepts is that they are all low-temperature combustion (LTC) processes that result in lower levels of nitric oxides and particulate matter than the spark ignition (SI) and direct injection (DI) combustion principles. The advanced combustion modes not only present superior thermal efficiency and ultra-low emissions of NO_x and PM but also demonstrate the high adaptability and flexibility to different kinds of fuels. The homogeneous charge compression ignition (HCCI) engine is one of several reliable alternative solutions for stationary and transportation applications. HCCI engines operate at high-intake temperatures and are probably more efficient than spark ignition (SI) engines due to their high compression ratio, which is also the case with compression ignition (CI) engines as well as they do not require spark plugs. In addition, they have lower maintenance costs than gasoline engines and produce very low emissions of NO_x [22].

The formation of pollutants such as nitrogen oxides in a combustion chamber is linked, among other things, to the existence of high flame temperatures. In order to assess the quantity of pollutants emitted by the F8L413 diesel engine mounted on TB230 vehicles of the national

mechanical construction company (SONACOME) in Algeria, we are interested in this work more particularly using ANSYS CHEMKIN-Pro software to perform simulations of a closed homogeneous reactor under conditions relevant to HCCI engines.

Objectives and scope of work

The objective of this thesis work is to allow a better understanding of the influence of certain operating parameters on combustion in HCCI mode. It is also a contribution to the study of tools allowing a reduction in pollutant emissions emitted during combustion. For this reason, in this study, a global model of HCCI combustion using the single-zone model and specific for the homogeneous combustion technical EGR is performed in order to reduce as much as possible the exhaust emissions in a diesel engine.

Thesis structure

The work developed on this thesis was accomplished by following steps:

The first chapter is a literature review concerning the technologies HCCI and EGR applied in internal combustion engines and emission characteristics of HCCI engines operating in various conditions. Moreover, we have added an after-treatment literature review of nitrogen oxides (NO_x) emissions from diesel engines and the emission regulations that drive their development.

The second chapter is involved a numerical simulation using the Diesel-RK and ANSYS CHEMKIN-Pro software, respectively. In this chapter, the HCCI combustion capability of running with different conditions parameters and exhaust gas recirculation (EGR) rates were investigated. This model was run in CHEMKIN using a detailed chemical kinetic mechanism; on the other hand, we have presented the formulation of the heterogeneous and homogeneous combustion models.

The third chapter is presented the main part of the simulation results obtained from Diesel-RK software that were compared against those obtained from the MATLAB software on the one hand. On the other hand, the simulation results obtained from CHEMKIN-Pro were presented and discussed in detail. Furthermore, a comparison between homogeneous and non-homogeneous model results was done.

Finally, we end this work with a general conclusion where we present the main results found.

CHAPTER 1- LITERATURE REVIEW

1.1. INTRODUCTION

Algeria is among the countries which are concerned by greenhouse gas emissions, of which the three most important gases in terms of emissions are carbon dioxide (CO_2), methane (CH_4) and nitrous oxide (NO_x). Air pollution in Algeria, especially in the capital, is becoming a major problem. This is no secret, but a reality confirmed by the latest World Health Organization (WHO) report which puts Algeria among the countries with the highest air pollution levels in the world. Within the framework of the Paris COP21 agreement, Algeria has committed to reducing greenhouse gas emissions by 7% by 2030. In this sense, Algeria reiterated in Amman (Jordan) its commitment to reduce its greenhouse gas emissions by 2021-2030 under the Paris climate agreement adopted in 2015 which aims to keep the rise in the average temperature of the earth below 2°C . The increase in the greenhouse-warming gases by carbon dioxide (CO_2), unburned hydrocarbon (UHC), carbon monoxide (CO) emissions, acid rain, particular matter (PM), haze and the photochemical smog from nitrogen oxides (NO_x) [23-25], anti-pollution standards are becoming more and more strict which pushed car manufacturers are constantly investing more money into the research and development sector in order to improve engine performance.

Given that HCCI is not the only candidate technology for obtaining a better fuel economy, it must be competitive in cost to the other solutions, as well as offering other benefits. A good argument for using the HCCI principle is that it can potentially eliminate the need for expensive after-treatment solutions that are otherwise required to remove emissions of particulate matter and nitric oxides. The only problematic emissions from HCCI combustion are unburned hydrocarbons and carbon monoxide. These are however easily removed by an inexpensive oxidizing catalyst. Such catalysts have a high conversion factor even at low exhaust temperatures, meaning that HCCI engines can easily meet current emission requirements.

Figure 1. 1 unveils the operating regions of different combustion modes [26,27]. As can be seen, the distribution of the soot and NO formation regions as a function of the local equivalence ratio (ϕ) and temperature (T) for the combustion of diesel fuel via LTC, PCCI, RCCI, HCCI and conventional diesel combustion. In 2001, Toyota and ExxonMobil used such a ϕ -T map to explain the effect of local temperature and equivalence ratio on NO_x and soot formation by applying chemical kinetics models [28].

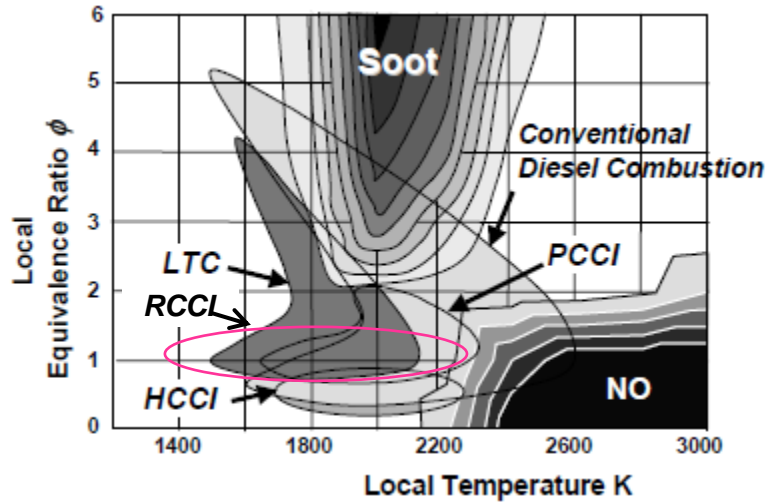


Figure 1. 1- PCCI, LTC and HCCI concept on the ϕ -T map [29,15].

1.2. GENERAL OPERATION OF THE INTERNAL COMBUSTION ENGINE

Combustion is a fundamental chemical process for releasing energy from an air-fuel mixture. The role of thermal engines is to transform thermal energy into mechanical energy. They are also called, internal combustion engines and are generally distinguished into two types; the spark-ignition gasoline engine and the compression ignition diesel engine. Most of them are four-stroke cycle engines, which means that it takes four strokes to complete a cycle. The cycle consists of four distinct processes: intake, compression, combustion-expansion and exhaust. In a spark-ignition engine, the air-gasoline mixture is formed in the carburetor outside the cylinder. Once the piston has compressed the air-fuel mixture, the spark ignites it and causes combustion. The expansion of the combustion gases pushes the piston during the power stroke. While, in a diesel engine, the air is first aspirated in and compressed, then the fuel is injected using an injector into the hot compressed air.

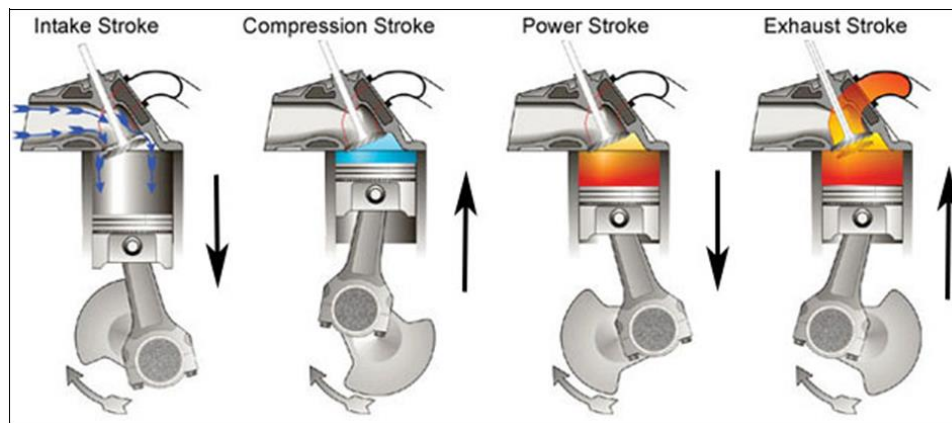


Figure 1. 2- Process in a four-stroke engine [30].

1.2.1. Fuel injection system in diesel engine

The diesel fuel injection system delivers fuel under extremely high injection pressures. This implies that the system component designs and materials should be selected to withstand higher stresses in order to perform for extended durations that match the engine's durability targets. The main purpose of the fuel injection system is to deliver fuel into the cylinders of an engine. For the engine to effectively the fuel must be injected at the proper time, that is, the injection timing must be controlled and the correct amount of fuel must be delivered to meet power requirements, that is, injection metering must be controlled. However, it is still not enough to deliver an accurately metered amount of fuel at the proper time to achieve good combustion.

Additional aspects are critical to ensure proper fuel injection system performance including fuel atomization, bulk mixing and air utilization [31].

Fuel atomization- Ensuring that fuel atomizes into very small fuel particles is a primary design objective for diesel fuel injection systems. Small droplets ensure that all the fuel has a chance to vaporize and participate in the combustion process. Any remaining liquid droplets burn very poorly or are exhausted out of the engine. While modern fuel injection systems can produce fuel atomization characteristics far exceeding what is needed to ensure complete fuel evaporation during most of the injection process, some injection system designs may have poor atomization during some brief but critical periods of the injection phase. The end of the injection process is one such critical period.

Bulk mixing- While fuel atomization and complete evaporation of fuel are critical, ensuring that the evaporated fuel has sufficient oxygen during the combustion process is equally as important to ensure high combustion efficiency and optimum engine performance. The oxygen is provided by the intake air trapped in the cylinder and a sufficient amount must be entrained into the fuel jet to completely mix with the available fuel during the injection process and ensure complete combustion.

Air utilization- Effective utilization of the air in the combustion chamber is closely tied to bulk mixing and can be accomplished through a combination of fuel penetration into the dense air that is compressed in the cylinder and dividing the total injected fuel into several jets. A sufficient number of jets should be provided to entrain as much available air as possible while avoiding jet overlap and the production of fuel-rich zones that are oxygen deficient.

1.2.2. Fuel injector

The injector is a device to deliver fuel intermittently into the engine cylinder at times that are synchronized with the engine camshaft position. The injector needle in an injector acts as a valve to open or close the passage to the injector hole(s). In a fuel pressure-activated injector, one end of the needle is preloaded with a spring force, and the other end is exposed to the fuel pressure. The needle is closed against the seat when the spring force is greater than the force due to fuel pressure.

Fuel injectors atomize the fuel into very fine droplets and increase the surface area of the fuel droplets resulting in better mixing and subsequent combustion atomization is done by forcing the fuel through a small orifice under high pressure [32].

There are two types of injectors in diesel injection systems namely mechanical fuel injectors and electronic fuel injectors. Which are categorized depending upon how the fuel is injected into the system.

1.2.3. Fuel injector nozzle

The nozzle is that part of an injector through which the liquid fuels are sprayed into the combustion chamber; the nozzle should fulfill the following functions:

- **Atomization-** This is a very important function since it is the first phase in obtaining proper mixing of the fuel and air in the combustion chamber.
- **Distribution of fuel-** Distribution of fuel to the required areas within the combustion chamber. The factors affecting the distribution of fuel are injection pressure, the density of air in the cylinder, and physical properties of fuel like self-ignition temperature, vapor pressure, viscosity, ..., etc [33].

1.2.4. Compression ignition background

When operating a compression ignition engine, a cylinder is filled with air through the intake valve. The intake valve is then shut and the piston's motion reduces the volume of air, compressing and heating the air to approximately 600°C. At this time, liquid fuel is injected into the cylinder through a nozzle. The fuel forms a spray of droplets, which vaporize, mix with hot air and ignite [34].

1.2.4.1. Physical processes of compression ignition

Hydrocarbon combustion occurs only in the gas phase. Thus, for liquid fuel, the first steps toward ignition involve transitioning from a liquid to a gas phase. The time required for this transition is the “physical delay” in the ignition and includes the time required for a droplet of fuel to heat, vaporize, and mix with hot air in the cylinder.

1.2.4.2. Chemical processes of compression ignition

Combustion is a sequence of chemical reactions in which the gas-phase fuel reacts with oxygen. These reactions proceed stepwise, through a mechanism involving free radicals (a free radical is a chemical entity containing an unpaired electron). For ignition to occur, the fuel must be heated to a temperature sufficient for some of the weaker bonds to break and form radicals. The finite rate of these radical-forming oxidation reactions is responsible for the chemical delay in compression ignition. Once a sufficient concentration of free radicals is reached, rapid oxidation occurs (ignition).

1.2.4.3. Complete ignition process

The role of these fuel properties in the various physical and chemical steps in the compression ignition process is summarized in figure 1. 3.

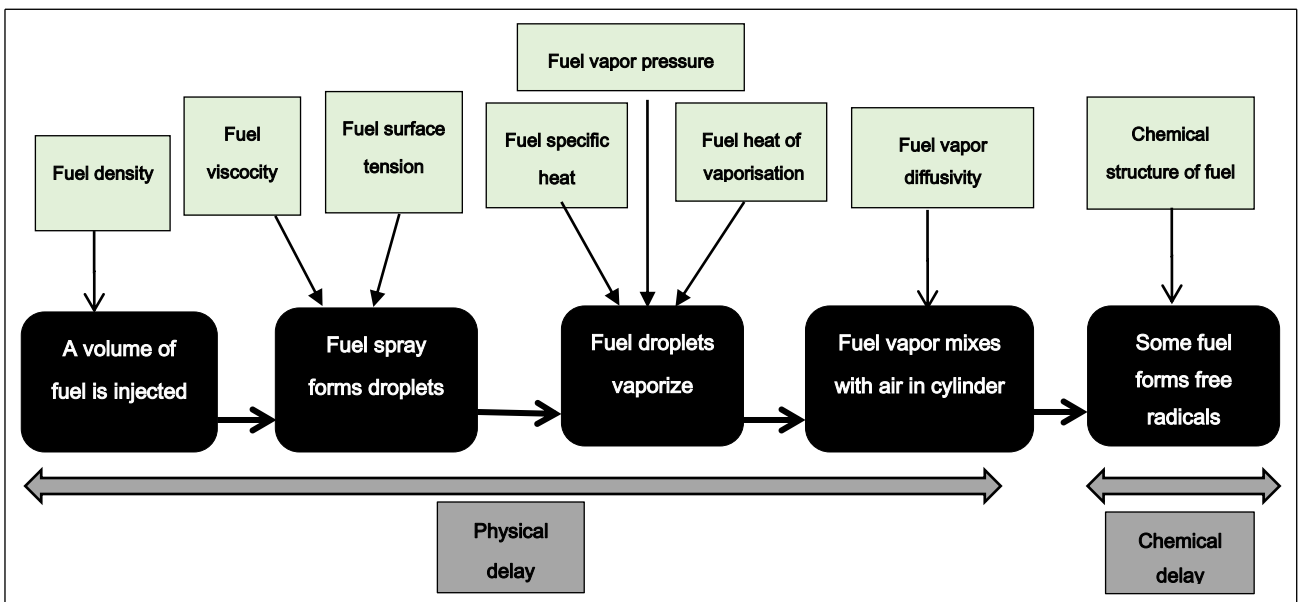


Figure 1. 3- Overall compression ignition [34].

1.3. HCCI ENGINES

1.3.1. Principle and working of HCCI engines

The basic principle behind HCCI combustion is to compress a homogeneous air-fuel mixture to a certain point so that it auto-ignites close to the top dead center (TDC). This operation can be described as a combination of SI and CI engines. A homogeneous charge is prepared in the inlet manifold where fuel and air are mixed before the engine's intake stroke—just like in an SI engine. After the intake stroke, the valves are closed and the onset of combustion is governed by compression of the pre-mixed charge – similar operation as in CI engines [35,36].

In HCCI engines, auto-ignition (a process dominated by the chemical kinetics of the air-fuel mixture), theoretically, occurs simultaneously as shown in figure 1. 4. That is, combustion happens at multiple points throughout the combustion chamber, resulting in simultaneous heat release events without any flame propagation. This process was verified through spectroscopic and imaging investigations by the Lund Institute of Technology [37,38]. Potentially, HCCI combustion is a third combustion principle for internal combustion engine applications.

In the definition of HCCI (Homogeneous Charge Compression Ignition) combustion, it is assumed that the air-fuel mixture is homogeneous, however in reality it is not. During the compression process, different parts of the charge mixture will have different heat capacities due to local inhomogeneities, which results in non-uniform temperature distribution throughout the combustion chamber. This is the practical deviation to the theoretical assumed homogeneous mixture. The first part of the mixture to ignite is the hottest region (may be constituted by only a few hot spots), which will then compress the rest of the charge, leading to the ignition of all the mixtures. Too fast burn durations lead to fast high heat release rates and consequently knock, which limits the upper load limit of HCCI operation. On the other hand, too slow-fast burn durations will cause incomplete combustion and misfire which will limit the lower load limit of HCCI [39-42].

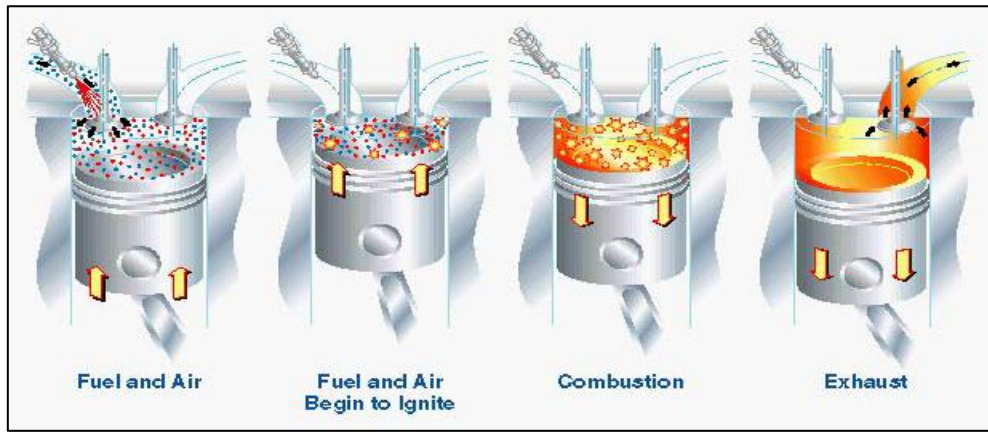


Figure 1. 4- Schematic diagram of HCCI [43].

HCCI combustion is achieved with very lean air-fuel mixtures that apart from contributing to minimizing fuel consumption, will also address the problem of fast high heat release rates. Due to the high dilution of the mixture, the gas temperature after combustion can ideally be lower than 1800-1900 K, so the formation of NO_x in the combustion chamber can be minimized. Also, due to the fact that the mixture in the cylinder is premixed, the formation of soot can be extremely low [42].

As just pointed, HCCI combustion has the potential to suppress the main problems that are currently associated with CI engines (the high emission formation of soot and NO_x) maintaining lower fuel consumption due to lean air-fuel mixture operation. There are, however, some disadvantages with this concept which are; high UHC and CO emissions (which can be easily removed using actual technology, namely the current range of catalytic converters), reduced operating range (due to high heat release rates on the upper limit and misfire on the lower limit), low power density per displacement (forced induction might be a solution) and difficulties in starting and controlling combustion. This represents a difficult problem in HCCI combustion, due to its extreme sensitivity to temperature, pressure and composition of the air-fuel mixture during the compression stroke. It is generally accepted that HCCI combustion is mainly chemically controlled.

Therefore a deep understanding of HCCI reaction chemistry is required to develop valuable control strategies. Consequently, the control system is fundamentally more complex than using a spark plug or fuel injector to determine the start of ignition [44,39,45,46].

Table 1. 1- Comparative parameters of SI, CI and HCCI engines [27]

Parameters	SI	HCCI	CI
Ignition method	Spark ignition	Auto-ignition	Compression ignition
Charge	Premixed homogeneous before ignition	Premixed homogeneous before ignition	In-cylinder heterogeneous
Ignition point	Single	Multiple	Single
Combustion flame	Flame propagation	Multi-point auto- ignition	Diffusive flame
Fuel economy	Good	Best	Better
Major emissions	UHC, CO and NO _x	UHC and CO	NO _x , PM and UHC
Equivalence ratio	1	<1	-
Max. Efficiency	30%	>40%	40%

1.3.2. Previous work HCCI

This is maybe the older concept of an internal combustion engine [47]. Ackroyd Stuart in the 1890s developed the so-called hot bulb engine. The operation of this engine is simple and does not require any advanced fuel system or spark ignition. The main feature of it is a hot bulb that must be heated externally before the engine start. Once the bulb is hot and the piston is rotating the principle is similar to a 4 stroke engine. During the intake stroke, the air is drawn into the cylinder and fuel is sprayed into the hot bulb. Due to the sprayer action and the temperature in the hot bulb the fuel is vaporized. On the compression stroke the air temperature inside the cylinder rises, the vaporized fuel is mixed (through an opening on the hot bulb) and ignition takes place. At the time of its invention, the main advantages were its economy, simplicity and tolerance to a large spectrum of fuels. The development of CI and SI engines made the hot bulb engine obsolete, especially for automotive applications, where its band of operation was too narrow [48,49].

Based on the auto-ignition concept of a homogeneous charge due to the air temperature in the cylinder (same fundamentals as the hot bulb engine), Onishi et al in 1979, reported a new combustion concept called "Active Thermo Atmosphere Combustion" (ATAC). This was the modern predecessor of HCCI combustion. This concept was developed as an alternative lean combustion mode for two-stroke internal combustion engines. The observations made concluded that ATAC was initiated by auto-ignition that occurs spontaneously at several different points within the combustion chamber. Stable combustion was achieved with lean air-fuel mixtures and exhaust emissions and fuel economy were remarkably improved [50]. At the

same time, another group of investigators led by Noguchi and Tanaka in 1979 was performing optical experiments to study this new concept. They observed that combustion could start at lower temperatures and pressures than those required for conventional diesel combustion, presumably by intermediate products. This special self-ignited combustion is named “TS (Toyota-Soken) combustion”. Apart from observing that ignition took place at numerous points inside the cylinder, they did not record any flame front being developed during combustion. Also, they realized that the combustion duration is much shorter than the one it takes place on conventional SI or CI engines. The spectroscopy methods employed allowed the detection of intermediate species such as formaldehyde (CH_2O), hydroperoxide (HO_2) and oxygen (O) that appeared in a specific sequence before auto-ignition occurs. These species served as ignition kernels for combustion. This sequence of events differs from conventional engines where all the radicals present appear simultaneously. Special self-ignited combustion was found to be different from the so-called “RUN-ON” combustion which presumably initiates from the deposits on the combustion chamber wall or other hot spots. It further differs from diesel combustion which is compression ignition combustion because it starts to burn at relatively low pressure and temperature in the cylinder. This self-ignited combustion process was named “TS combustion” [51].

In 1983, Najt and Foster’s work was the predecessor for the studies on modeling kinetics and fuel oxidation on HCCI combustion. They were also the first researchers to report HCCI combustion in 4-stroke engines. From their work, important contributions to the knowledge of the ignition and the energy release process were withdrawn. They found that chemical kinetics played a vital role in HCCI combustion and through temperature control and species concentration control; it was possible to control combustion. They found that two different temperatures were of major importance on HCCI; low-temperature hydrocarbon oxidation occurs below 950 K and is responsible for controlling ignition, and high-temperature hydrocarbon oxidation occurs above 1000 K, which controls the energy release process [52].

The studies were later extended by Thring (1989) [53] to examine the effect of external EGR and air-fuel ratio on the engine’s performance. In this work, Thring introduced the terminology homogeneous charge compression ignition (HCCI) that has since been adopted by many other researchers to describe this type of combustion process both in gasoline and diesel engines. The limitations of the HCCI operation were again noted by him and his team. The operating regime is restricted to part-loads and control of the auto-ignition timing is problematic. It was suggested in this work that HCCI could be potentially integrated into an engine operating strategy; at part loads, the engine operates on HCCI with a transition into SI flame propagation at higher engine loads.

Table 1. 2- Milestone achieved by the researcher in the development of HCCI engines [54]

	Work
1930s	Nikolai Semenov [55], generate the root of the HCCI combustion concept by doing the first chemical kinetics controlled combustion study for diesel engines.
1970s	Gussak, Karpov and Tikhonov, from the Academy of Sciences of the USSR [56], developed the first controlled combustion engine, using a partially burned mixture from a separate chamber.
1979	Onishi and Noguchi [50,51], HCCI research in 2 stroke engine.
1983	Najt and Foster, Univ of Wisconsin Madison [52], HCCI research in 4 stroke engine.
1989	Thring [53], tested the effects of air-fuel ratio and EGR on engine performance. Also, he introduces the name "Homogeneous Charge Compression Ignition (HCCI) Engine".
1992	V. Stockinher, H. Schapertons and U. Kuhkmann [57], first-time explorer the operating region (limited speed and load) of 4 stroke gasoline engine in auto-ignition mode by increasing compression ratio and heating intake air.
2001	Lund Institute of Technology [58], developed a 12 liter-6 cylinder largest gasoline engine running in auto-ignition mode by using a mixture of two fuels (heptane and iso-octane), increasing the compression ratio, heating intake air and booting intake air by a turbocharger.
2001	Lotus Engineering Ltd. [59], first to use exhaust valve closing (EVC) and negative valve overlap (NVO) for HCCI engine combustion, operating in limited speed and load range by using fully flexible variable valve actuation.
2003	AVL list GmbH [60], Explorer nature of residual gas fraction and exhaust rebreathing in order to achieve HCCI combustion in available production engines, stating best method for fuel consumption and most promising feature for HCCI to come closer to the production line.
2007	General Motors (GM) [61] demonstrated an HCCI engine working, in the powertrain of Opel Vectra and Saturn Aura with a maximum speed of 60 MPH.
2014	BOSCH et al. [62] developed a mode switching engine between SI and HCCI engine, named as SACI-HCCI engine.

1.3.3. HCCI challenges and proposed solutions

As already explained, HCCI is a combustion concept where neither a spark nor fuel injection initiates the ignition in the combustion chamber. In other words, HCCI is the auto-ignition of a homogeneous mixture by compression. The main challenge of the HCCI engine is to control ignition timing, which influences power and efficiency. Conventional engines have a direct mechanism to control the start of combustion. Unlike, spark timing in SI engines and fuel injection timing in CI engines, the HCCI engine lacks the start of combustion controlled by auto-ignition. The fuel-air mixture is premixed homogeneously, before the start of combustion initiated by the auto-ignition of time-temperature history. This phenomenon of auto-ignition leads

to the main combustion control which is affected by a few factors [63,64]: fuel auto-ignition chemistry and thermodynamic properties, combustion duration, wall temperatures, the concentration of reacting species, residual rate, degree of mixture homogeneity, intake temperature, compression ratio, amount of EGR, engines speed, engine temperature, convective heat transfer to the engine and other engine parameters. Hence, the HCCI combustion control over a wide range of speeds and loads is the most difficult task. Controlling combustion is the most important parameter because it affects the power output and engine efficiency. If combustion occurs too early, power drop in terms of efficiency and serious damage to the engine occurs, and if combustion occurs too late, the chance of misfire increases. Most of the researchers believe in the fact that HCCI combustion is governed by chemical kinetics [65-67]. The present part aims to introduce the impact of all these parameters.

1.3.4. Control of HCCI ignition timing

Several strategies have been investigated, with various levels of success, for controlling HCCI combustion timing and extending the load range [68,47]. Most of these strategies can be divided into the broad categories of mixture dilution, modifying fuel properties, fast thermal management and in-cylinder direct fuel injection. Many studies investigating HCCI control employ more than one method due to the complicated and highly coupled nature of the HCCI combustion problem [69].

1.3.4.1. Mixture dilution for HCCI control

In order to achieve HCCI combustion, high intake charge temperatures and a significant amount of charge dilution must be present. The in-cylinder gas temperature must be sufficiently high to initiate and sustain the chemical reactions leading to auto-ignition processes. Substantial charge dilution is necessary to control runaway rates of the heat-releasing reactions. Both of these requirements can be realized by recycling the burnt gases within the cylinder.

One approach to HCCI combustion phasing control is to advance or retard combustion timing by diluting the cylinder mixture. Najt and Foster showed that HCCI combustion in a four-stroke engine could be controlled by introducing recirculated exhaust gas into the cylinder intake mixture [52]. Christensen and Johansson showed combustion timing to be slower with higher amounts of EGR [70].

As stated previously, one of the requirements of HCCI combustion to reach the auto-ignition temperature is a higher initial temperature of the fuel-air mixture. This can be achieved

in several different ways; increasing the compression ratio, using auxiliary intake air heaters, or more simply and effectively by using residual gases, which are hot from previous cycles. There are two different strategies to use residual gases.

External EGR, where recirculation is achieved by driving the exhaust gases from the exhaust manifold into the inlet manifold. A control valve (EGR valve) within the circuit is used to control the gas flow in such a way so that the engine requirements are satisfied.

The most common strategy used, is by trapping the exhaust gases within the cylinder by not fully expelling them during the exhaust stroke. This is called internal EGR and it is achieved by changing the valve timing which is used to control the amount of residual gas. The exhaust valves close earlier and are totally shut before the intake valves open. This allows trapping exhaust residual gas in the cylinder on the latter stages of exhaust stroke with consequent compression and increases in temperature. As the piston subsequently descends on the induction stroke, the inlet valves open late, so that a fresh mixture of fuel and air is drawn into the cylinder that has already been partially filled with the trapped residuals. The cold fresh charge mixes with the hot residual gases and gains thermal energy. Shortly afterward the intake valves close and the in-cylinder charge is compressed by the ascending piston, the auto-ignition of the fuel/air mixture and the subsequent combustion around TDC occurs [71-74]. Furthermore, the effect of EGR was investigated and it was found to be a very effective tool to control HCCI combustion [75].

It is then possible to conclude that the use of EGR on HCCI combustion has the potential to extend its operation envelope. The burned exhaust gases from previous cycles will help raise the initial temperature of the charge which may help to enable auto-ignition conditions.

Work done by Cairns and Blaxill showed that by employing external exhaust gas, there was a 20 to 65% increase in the engine load. This increased efficiency is due to the reduced rate of heat release, with consequences such as prolonging combustion and extending the knock limit, especially at higher pressures. By external gas, these authors refer to the same exhaust gas but that is passed by an external circuit which has the effect of cooling down the gases. In the work done by these authors a combination of the use of internal EGR with external EGR is studied. This combined EGR technique proved to bring several benefits. Besides the advantage just pointed, the hotter internal EGR can help on the lower load conditions, where raising the air-fuel charge is essential to achieve auto-ignition. Another benefit of it is when the engine is transitioning from HCCI to SI conditions, as this transition seems to be smoother [72].

One other requirement of HCCI combustion is the need to use lean diluted mixtures. This demand is also attained with the use of EGR. The presence of residual gas increases the total thermal mass of the cylinder charge which results in increased heat capacity. This will lower the peak temperatures in the cylinder, slowing down combustion at high loads (avoiding knock) and consequently reducing the amount of NO_x that is produced (NO_x production is highly dependent on the temperature) [45,72,73,74,76]. This strategy for NO_x emissions abatement is nowadays of common use in diesel engines. It is worth referring that HCCI combustion is governed by three important temperatures. There is the auto-ignition temperature (low-temperature hydrocarbon oxidation), below 950 K. The temperature should then increase to at least 1500 K to allow good combustion efficiency (high-temperature hydrocarbon oxidation), but it should not be increased to more than 1800 K to prevent NO_x formation [35,72].

EGR or recycling of burned gases is the most effective way to moderate the pressure rise rate and expand the HCCI operation to higher load regions. The studies done related to EGR include both external EGR and internal EGR (residual combustion products) to achieve proper combustion phasing. External EGR is the more commonly utilized method for recycling exhaust gases. However, external EGR control has issues, such as slow response time and difficulties in handling transient operating conditions [77]. A second way of reintroducing exhaust gases is through internal exhaust gas recirculation where the amount of exhaust gas residual in the cylinder is varied by changing the timing of the intake and exhaust valve's opening and closing events.

1.3.4.2. External exhaust gas recirculation (eEGR)

External exhaust gas recirculation has been investigated by many researchers in the last decades. The study done by Thring investigated the effects of the EGR rate (between 13 and 33%) on the achievable HCCI operating range and engine-out emissions [58]. Their study found out that the maximum load of HCCI operating range for a four-stroke engine was less than that of a two-stroke engine under the selected conditions.

Christensen and Johansson observed that the upper load limit of a supercharged HCCI engine could be increased to an IMEP of 16 bars through the addition of approximately 50% EGR to the intake mixture, which retarded combustion and avoided knock [78]. In this study, high EGR rates were used in order to reduce the combustion rate. While external EGR is promising for load range and combustion phasing improvement, some drawbacks still exist. For recirculation of the exhaust gas into the intake mixture, the exhaust manifold pressure has to be increased to a level over that of the intake manifold pressure. This pressure increase is often

achieved by throttling the exhaust manifold, which can result in higher pumping losses and thus an overall lower net efficiency of the engine. Efficiency losses are also seen as a result of cooling the exhaust gases before reinduction to prevent early auto-ignition [78].

In 2001, Morimoto et al. [74] found similar results using a Natural Gas fueled engine. In this study, an external cooled EGR was used to control combustion phasing and extend the load range of an HCCI engine. He also concluded that the total hydrocarbon emissions were reduced at higher loads with the introduction of EGR.

Numerical studies conducted by Narayanaswamy and Rutland, using a multizone model coupled with GT-Power, confirmed that the effects of EGR (external) on diesel HCCI operation vary with different levels of EGR [79]. Interestingly they pointed out that ignition was advanced initially for low EGR cases and then began to retard with an increase in EGR percentage. The effect of cold EGR on the start of combustion was explained by competing effects, with the increase of the equivalence ratio advancing the ignition timing and the diluting effects retarding the combustion. As the EGR increases, the advancing effect prevails at first, and then evidently the retarding effect becomes dominant for further increase in EGR.

Atkins and Koch also observed that diluting the intake mixture using EGR is effective in retarding start of combustion (SOC) timing. Similarly, the introduction of EGR (around 62%) resulted in increasing maximum gross efficiency to 51%, much higher than that which could be achieved in an SI engine [80].

In 2011, Fathi et al. [81] investigated the influence of external EGR on combustion and emissions of HCCI engines. In his study, a Waukesha Cooperative Fuel Research (CFR) single-cylinder research engine was used to be operated in HCCI combustion mode fueled by natural gas and n-heptane. The main goal of the experiments was to investigate the possibility of controlling combustion phasing and combustion duration using various exhaust gas recirculation (EGR) fractions. The influence of EGR on emissions was discussed. Results indicated that applying EGR reduces mean charge temperature and has a profound effect on combustion phasing, leading to a retarded start of combustion (SOC) and prolonged burn duration. Heat transfer rate decreases with EGR addition. Under the examined condition, EGR addition improved fuel economy, reduced NO_x emissions and increased UHC and CO emissions.

1.3.4.3. Internal exhaust gas recirculation (iEGR)

Internal exhaust gas recirculation is another promising method for achieving stable HCCI combustion. By changing the valve timing of the engine, the amount of trapped residual gases

(TRG) in the cylinder can be changed, thereby changing the temperature, pressure, and composition of the cylinder mixture at IVC. In 2001, Law et al. found that it was possible to change the amount of internal EGR by varying valve timing, which in turn allows for control of combustion phasing of HCCI combustion [59].

Milovanovic et al. [82] studied the influence of a fully variable valve timing (VVT) strategy on the control of a gasoline HCCI engine and found that EVC and IVO timing have the greatest impact on the ability to control HCCI combustion timing. EVO and IVC timing was found to have little effect on HCCI combustion phasing control. Different research on fully VVT control of HCCI combustion was seen in the research of Urata et al. [83] where a combination of direct injection, fully VVT with an electromagnetic valve train, and intake boost was used to control HCCI. He hypothesized that injecting a small amount of fuel during negative valve overlap would allow unburned hydrocarbons in the internal residual to react, which could facilitate compression ignition during the following cycle.

1.3.4.4. Different fuels

The most obvious parameter which can influence the auto-ignition is the fuel and it is of main importance. One important characteristic of HCCI engines is their fuel flexibility [47]. This is of special interest, not only from the control point of view but also because of environmental considerations. Several studies have been performed with different fuels, from conventional gasoline and diesel to natural gas, methanol, ethanol, biodiesel, hydrogen, dimethyl ether (DME) and also their mixtures. Some of the early enthusiasm for this variety of fuels disappeared as the research increased and their limitations started to be exposed. Oxygenated fuels, methanol and ethanol can be produced from renewable raw materials and help to reduce fossil fuel dependency. As a setback, the fuel supply system of a conventional engine needs to change. Natural gas, in which methane is its main constituent, has a high auto-ignition temperature requiring high compression ratios and/or intake charge heating to achieve HCCI operating conditions. When hydrogen is used as the main fuel, theoretically at least, its combustion can result in zero emissions. However, it requires substantial intake heating and its rate of combustion is too rapid to be effectively controlled. Besides that, there are other relevant issues to consider regarding demand, production, storage and safety.

It has been seen that the combustion duration decreases with increased fuel octane number as the overall combustion temperature becomes higher. The high octane number means implies higher auto-ignition temperature, which gives a higher overall combustion temperature [84].

As pointed before, gasoline and diesel are two fuels with very different characteristics. With their wide availability, they were blended as an HCCI engine fuel. Some experimental results show that better combustion stability is obtained when gasoline/diesel blended fuel is used instead of gasoline-fuelled HCCI. As pointed in other studies the use of this mixture reduces the audible knocking limit and increases the HCCI operation envelope. It is possible to say that diesel fuel has a remarkable influence on gasoline HCCI combustion. Ignition timing is advanced, the combustion duration is shortened and the IMEP range achievable in the unheated negative valve overlap (NVO) mode is widened as diesel content increases. Exhaust emissions, especially UHC and NO_x, show a large improvement compared with gasoline HCCI [85].

1.3.4.5. Fast thermal management for HCCI control

Fast Thermal Management (FTM) is a controlling technique that involves rapidly changing the temperature of the intake charge to control the combustion phasing. Many studies have indicated that HCCI combustion timing is sensitive to intake air temperature.

↳ Intake temperature

The effects of intake charge temperature on HCCI combustion on-set have been widely reported by many researchers. In 1983, Najt and Foster showed that HCCI of lean mixtures could be achieved in a SI engine that has a low compression ratio with elevated intake charge temperatures (300–500°C) [52]. In general, the intake charge temperature has a strong influence on the HCCI combustion timing.

The study performed by Iida and Igarashi also indicated that an increase in intake charge temperature (from 297 K to 355 K) increased the peak temperature after compression and advanced the HCCI combustion on-set [86]. Furthermore, the authors found that the effect of intake charge temperature on combustion on-set was greater for higher engine speed (1200 rpm) compared to the lower engine speed (600 rpm). Aceves and his coworkers carried out some investigations including analysis as well as experimental work [39]. On analysis, they developed two powerful tools: a single zone model and a multizone model. On experimental work, they did a thorough evaluation of operating conditions in a 4-cylinder Volkswagen TDI engine. The engine had been operated over a wide range of conditions by adjusting the intake temperature and the fuel flow rate. They found out that it may be possible to improve combustion efficiency by going to a lower fuel flow rate and a higher intake temperature. For the high load operating points, the trend was that lower intake temperature results in higher brake mean effective pressure (BMEP).

↳ Variable compression ratio (VCR)

Experimental research done in HCCI combustion is often performed in experimental engines with variable compression ratio (VCR), several studies show that almost any liquid fuel can be used in an HCCI engine using this type of strategy [47]. On the work done by Christensen et al, it is shown that operation with pure n-heptane required a compression ratio of about 11:1 to get auto-ignition at TDC, without the use of inlet air preheating. Under the same conditions, iso-octane required 21.5:1. It was found that the increase in compression ratio (CR) did not impact negatively the formation of NO_x formation. However, the indicated efficiency did not improve with the increased compression ratio as expected. This parameter was studied by looking at the composition of the exhaust gases. More concentration in the exhaust gases of CO and UHC would translate to lower combustion efficiency [84]. Some previous work done in HCCI combustion showed that lower compression ratios were more suited for this kind of combustion concept. High CR offers the potential to enable HCCI at low loads at the expense of decreasing the higher load limit, due to excess pressure and heat release rates being created inside the cylinder, which ultimately leads to engine knock. A higher CR could be the solution to tackle the problem of the high initial temperatures required, but generally, research has gone in the direction of choosing the CR that allows better efficiency at upper limits [87,84]. An engine capable of dynamically changing its CR during cycles could offer good potential in terms of extending the HCCI operation limits. On lower load regions an engine like this would operate with high CR while when approaching higher load limits the CR would be decreased to prevent unwanted spontaneous detonations. As pointed by some researchers, it is possible to run HCCI mode during a complete drive cycle with this type of control. However, for driveability reasons (and power requirements, during specific situations) switching from HCCI mode to conventional SI will be desired/required [87]. The transitions between these two very different combustion modes present new challenges such as moving from a highly diluted environment to stoichiometric conditions. These transitions can be facilitated by adjusting the CR [87,84].

1.3.4.6. Direct injection for HCCI control

Fuel injection into the cylinder at different stages of the engine cycle allows HCCI combustion timing to be advanced by improving mixture ignitability or retarded by increasing fuel stratification, creating the possibility of expanding the low and high load operating limits. Direct injection can be a good way to control HCCI combustion, but it depends heavily on the type of fuel and the timing of the direct injection [69].

A numerical study by Gong et al. showed that the power density of an HCCI engine could be improved by the injection of a small amount of diesel fuel during the compression stroke of the engine. This pilot fuel injection also decreased the sensitivity of the HCCI combustion to intake conditions [88].

Dec and Sjöberg found that early direct fuel injection in the intake stroke produced near identical results to a premixed charge. However, injection close to TDC improved the combustion efficiency of very low fuel load mixtures [89]. Numerical models by Strålin et al. showed that fuel stratification caused by the injection of fuel around TDC results in pockets of rich fuel and air mixture, which promotes ignitability. Overall fuel stratification extended the combustion duration helping to avoid knock, thus extending the operating range of the engine [90]. Helmantel and Denbratt used multiple injection schemes of n-heptane to allow for sufficient mixing to operate a conventional diesel common passenger rail car engine with HCCI combustion [91].

1.3.4.7. Forced induction

Supercharging or turbocharging is used in HCCI engines to extend the domain of operation [92,78]. Supercharging in HCCI combustion increases the indicated mean effective pressure (IMEP) to 14 bars [93]. Supercharging has the capacity to deliver increased charge density and pressure at all engine speeds while turbocharging depends upon the speed of the engine. The in-cylinder density and volumetric efficiency can be improved with high boost pressure. The evaporation of the fuel is increased with a high intake pressure due to high in-cylinder temperatures. The mixing time can be decreased with the boost pressure is advantageous with all early injection systems. The combustion efficiency can be improved slightly at high boost levels, and cooled EGR rates were introduced [94]. But, Lee Taewon et al. [95] found, that the increase of intake boost pressure shortened ignition delay which is not favorable for the modulated kinetics combustion. Olsson et al. [96] extended the operating range of a 6-cylinder truck engine modified to a turbocharged HCCI engine. This study proves the possibility to achieve high loads, up to 16 bars brake mean effective pressure (BMEP), and ultra-low NO_x emissions. Due to the high levels of EGR and consequently lean mixtures that are used on HCCI combustion, the power density coming from this concept is low. To compensate for the charge dilution effect, one of the methods used to recover some of the power is to introduce more air into the engine allowing also more fuel while maintaining overall diluted mixtures. Forced induction is an effective solution to introduce an extra amount of air into the engine to increase power [47].

The work performed by Gharahbaghi et al proves that NO_x emissions are reduced considerably in the case of supercharged HCCI. The use of excess air which provides more thermal ballast without the regions of high temperature reduces the NO_x production (highly temperature-dependent). Besides the fact of reducing NO_x emissions formation, the excess air helps to reduce the high-temperature regions and consequently has a positive effect on decreasing knock occurrence. Lower combustion temperatures are preferable as they allow for heat release without reaching the NO_x -critical temperature. Summarizing the studies completed by this author it is possible to state that by boosting the engine and providing excess cold air to the combustion chamber, NO_x formation is decreased and the knock limits are improved [97]. There is published work where the exhaust gases were either recycled or rejected and the temperature of the mixture was increased or decreased as needed with the help of the supercharger and intercooler. This method has been shown to be effective in raising the usable HCCI operation load without any inlet heating required.

The limits of the load range are the maximum boost pressure and unstable combustion. At the maximum allowed boost pressure for the system used, the indicated mean effective pressure (IMEP) was approximately 75% of the total engine load possible in this same engine running in SI configuration. This represents a substantial increase over the engine load range for naturally aspirated HCCI combustion with residual gas trapping. Also, it was found that NO_x emissions can be low due to the advanced exhaust valve timings and high boost pressures. This will increase the charge dilution by exhaust residuals creating the necessary buffer in the combustion chamber that does not allow combustion peak temperatures to be too high. On the other hand, NO_x emissions can be relatively high when there is a smaller percentage of trapped residual coupled with low boost pressures, resulting in minimal amounts of dilution [98].

1.3.4.8. Turbulence

The auto-ignition timing is crucial to HCCI operation, and it is a function of complex chemistry, temperature, pressure and turbulence of the mixture fuel/air/residuals [99,100, 47]. It is reported in several papers that turbulence and mixing are important factors in HCCI combustion and they have an indirect effect on the auto-ignition timing by altering the temperature distribution within the cylinder, boundary layer thickness, heat losses and the charge homogeneity. Small temperature differences in the cylinder may have a considerable effect on combustion since chemical kinetics is very sensitive to temperature; therefore turbulence indirectly determines the speed of combustion. It is, however, accepted that once auto-ignition occurs, turbulence plays a minor role in combustion. After the ignition event,

combustion propagates from the initial ignition points as a pressure wave across the combustion chamber, without a flame front [100-102].

Christensen et al in 2002 used two different piston tops to study the influence of turbulence in HCCI combustion. A low turbulence flat-top piston and a high turbulence square-bowl piston were used. Several parameters were possible to be studied and compared by varying the levels of turbulence inside the combustion chamber with the two-piston designs. It was observed that with the flat-top piston (low turbulence inducer) the heat release rate was much higher than the one obtained with the square bowl piston. With such an increase in the heat release ratio, it was expected that the NO_x formation and emissions would be substantially higher for this case; however, the results obtained in the work performed only showed a slight increase in these emissions. It is worth highlighting that with late combustion timing, less than 1 ppm of NO_x was generated in all cases. Regarding UHC and CO emissions, their formation was more sensitive to combustion timing with the high turbulence combustion. The square bowl piston (high turbulence inducer), produced a longer combustion duration than the low turbulence piston. In some cases, this duration was almost twice as long. Also by using this piston, it was verified that the inlet air temperature required to achieve auto-ignition conditions (and the same combustion phasing) was lower than when using the low turbulence flat-top piston. This effect is seen probably due to the higher wall temperature and higher residual gas fraction [103].

It is possible to say that combustion chamber design, by increasing turbulence and with that allows different mixture formation, can be used as a tool for indirectly increasing and allowing better control of the HCCI load range and the start of combustion. This method offers another control mechanism over HCCI combustion.

Summarizing some of the trends seen, higher turbulence promotes a broader temperature distribution, which enhanced heat transfer with the result of longer burn duration, which in turn is reflected in a lower heat release rate. In some cases, the combustion duration for the high turbulence piston was twice as long as when a low turbulence piston was used, making the use of high turbulence systems more desired [100,101,104].

1.3.5. Emissions of HCCI engines

Emission from HCCI engines includes CO, UHC, NO_x and PM. In general, NO_x and PM emissions from HCCI engines are quite low [105]. However, HCCI produces high levels of unburned UHC and CO [105,106]. All these emissions depend on the engine operating

conditions, engine design and fuel quality [107]. Various emissions parameters of HCCI engines using various fuels are discussed below [108]:

1.3.5.1. CO Emissions

Literature reports that CO emissions of HCCI engines is higher than that from gasoline engines [109-111,41,87,112-114]. Kobayashi et al. [110] investigated the engine performance, combustion characteristics and emissions parameters of HCCI engines using both single and four-cylinder gasoline engines operating on gasoline. In their experiments, intake temperature was varied from 383 K to 413 K and equivalence ratios from 0.20 to 0.40. A huge amount of CO emissions was observed while the engine was running in HCCI mode compared to SI mode. Highest CO was measured as 6000 ppm at 413 K and 0.20 equivalence ratio, which is almost 10 times higher than the CO emissions achieved from SI mode. Aceves et al. [41] proposed a multi-zone model for predicting the combustion, performance and emissions characteristics of an HCCI combustion engine. From their prediction, it was found that CO was always higher than in conventional SI engines in any load condition. The combustion efficiency dictates the amount of CO₂ and CO and is defined as the ratio of CO₂ to the total fuel carbon present in the exhaust, including CO, CO₂ and UHC [115].

1.3.5.2. UHC Emissions

In general, HCCI combustion increases UHC emissions [116], which is another challenge for the broad application of HCCI engines. Kobayashi et al. [110] investigated the emissions characteristics of an HCCI engine by modifying a gasoline engine and using natural gas as fuel. They found UHC higher than in SI engines. Lemberger et al. [112] converted a single-cylinder, air-cooled, 4-stroke SI engine to run in HCCI mode by applying various combustion control systems. The authors used diethyl ether to operate the engine. Later they compared the emission result with an SI engine and found UHC higher than for SI. In their experiments, engine speed was varied from 1000 rpm to 4000 rpm and equivalence ratios from 0.30 to 0.75. A huge amount of UHC emissions was observed while the engine was running in HCCI mode compared to SI mode.

1.3.5.3. NO_x Emissions

NO_x formation generally occurs through an elevated temperature reaction between nitrogen and oxygen to form NO. Further reaction covers some of this NO into NO₂. The final flame temperature of HCCI engines is usually well below 2000 K as the engine mostly operates at the fuel-lean condition. Therefore, the chemical reactions that are responsible for NO_x

emissions remain mostly inactive [117]. As a result, compared to SI engines, NO_x emissions from HCCI engines is quite negligible [109,118,119,110,120,41,87,112,121]. Kobayashi et al. [110] observed much lower NO_x in HCCI engines than in SI engines. In every test condition, NO_x was below 2 ppm. Similarly, Lemberger et al. [112] reported similar results. Aceves et al. [41] proposed a multi-zone model for predicting the combustion, performance and emissions characteristics of an HCCI combustion engine and reported very low NO_x emissions (<2.5 ppm) compared to conventional SI engines in any test condition.

1.4. ABOUT EXHAUST GAS RECIRCULATION (EGR)

As we know vehicles are produced emissions. So the reduction of emissions such as EGR system was built on the engine. The first EGR system was built in the 1973s on the diesel engine [122-124].

NO_x emissions are closely related to temperature and oxygen content in the combustion chamber. Any process to reduce cylinder peak temperature and concentration of oxygen will reduce the oxides of nitrogen. It has been suggested several methods for reducing the level of nitrogen oxides. The main technology applied is EGR for reducing peak cycle temperature and thereby reducing NO_x emissions [125].

Exhaust gas recirculation (EGR) is a system that allows the exhaust gases to be recirculated back into the intake manifold. This process leads to a significant reduction in nitrogen oxides (NO_x) emissions because it reduces the two elements underlying its production: oxygen in excess and combustion temperature [126]. Figure 1. 5 shows this schematically. During combustion, the molecules of the fuel need more time to find an oxygen molecule to react with each other, when inert molecules are surrounding them. This slows down the rate of combustion. The combined effect of the high specific heat, due to the CO₂ and H₂O concentrations, and the reduction in the flame propagation speed, due to the presence of inert materials, lead to a significant reduction in the maximum flame temperature. Hence, it causes a reduction of NO_x levels. The displacement of the intake of oxygen leads to a reduction in the rate of excess air, which in turn increases the ignition delay. This greatly influences the temperature of the gas in the cylinder and the particle formation [127]. Besides, the kinetics of the elementary NO formation reactions is affected by the reduction in the oxygen partial pressure due to the dilution effect [128]. Figure 1. 6 shows how the NO_x concentrations decrease when the inlet airflow of the DI diesel engine is diluted for a constant fuel flow. Dilution is expressed in terms of the oxygen concentration in the mixture after dilution [8].

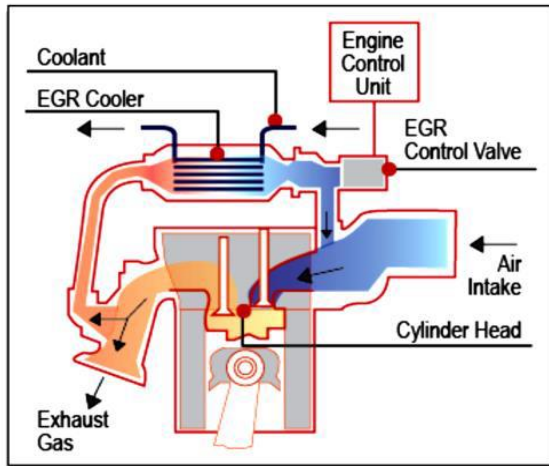


Figure 1. 5- High pressure EGR system with cooler.

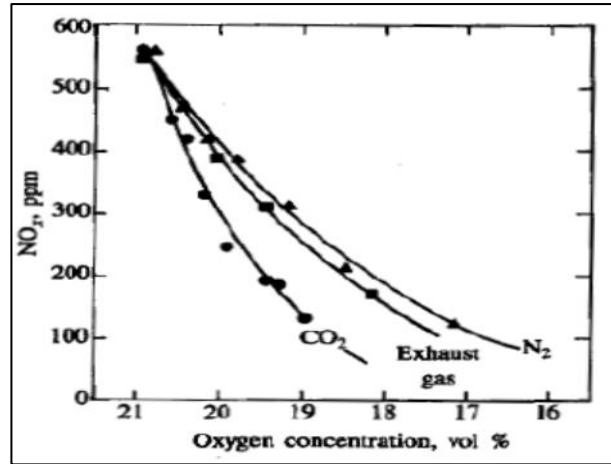


Figure 1. 6- Effect of reducing oxygen concentration by different diluents on NO_x [8].

Two parameters were found to be most responsible for the formation of NO_x emissions: (1) the presence of oxygen in the load and (2) the reaction temperature, which promotes chemical activity during both formation and destruction stages. During the formation phase, the reaction temperature is close to the temperature of the adiabatic flame, which is a consequence of the oxygen concentration in the charge, the initial temperature and pressure, and the local fuel-charge ratio. The EGR reduces the oxygen concentration in the charge and, therefore, the combustion temperature [129].

Considering the cooling system of the engine, the high-pressure EGR method that the exhaust gas is recirculated into the intake air before reaching the turbocharger is appropriate for the turbocharged inter-cooled diesel engine [130]. As shown in Figure 1. 7, the compressor and the intercooler could be avoided being polluted by the recirculated exhaust. If exhaust gases passed through the compressor and the intercooler, matters such as particulates, hydrocarbons, and sulfur in the exhaust may cause clog and corrode to the narrow passage of the cooling system. In addition, the turbocharged direct injection diesel engines applied to vehicles usually work under variable operating conditions, and the standard procedures testing emissions were also carried out under variable operating modes conditions [131]. The other EGR pattern that introduces exhaust gases into the intake air after reaching the turbocharger would delay the engine responses under the transient operating conditions, which would have an unfavorable effect on controlling the NO_x emissions.

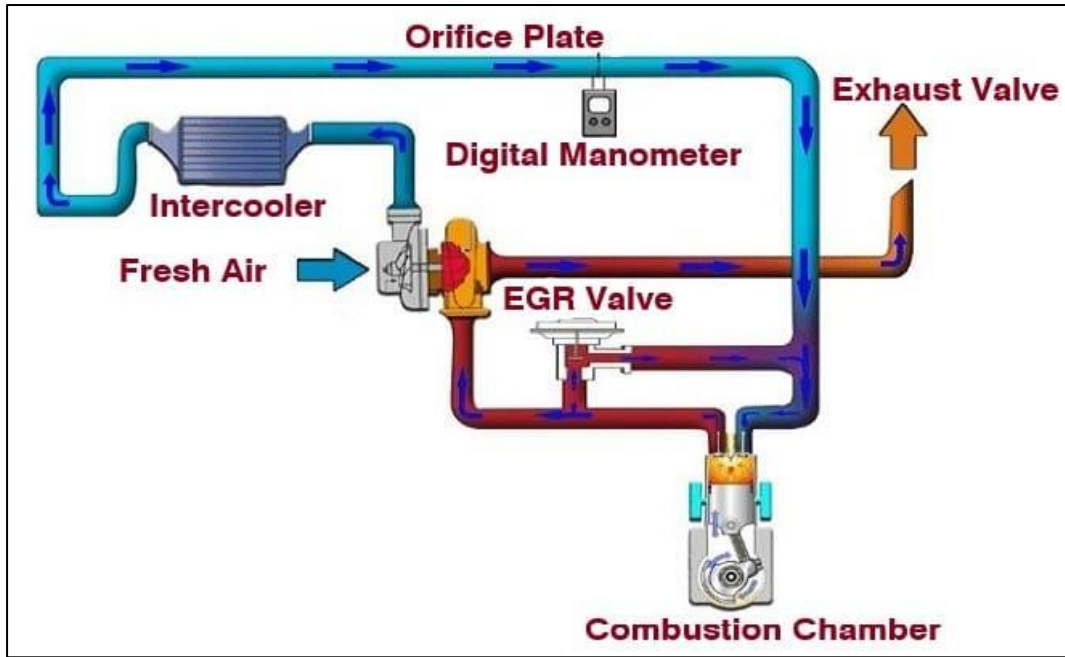


Figure 1. 7- The exhaust gas recirculation system [130,132].

The exhaust gases were regulated by a control valve and directly send to the inlet manifold. The above-shown system is also called hot EGR because it is not fitted with an EGR cooler which is used to cool the intake mixture.

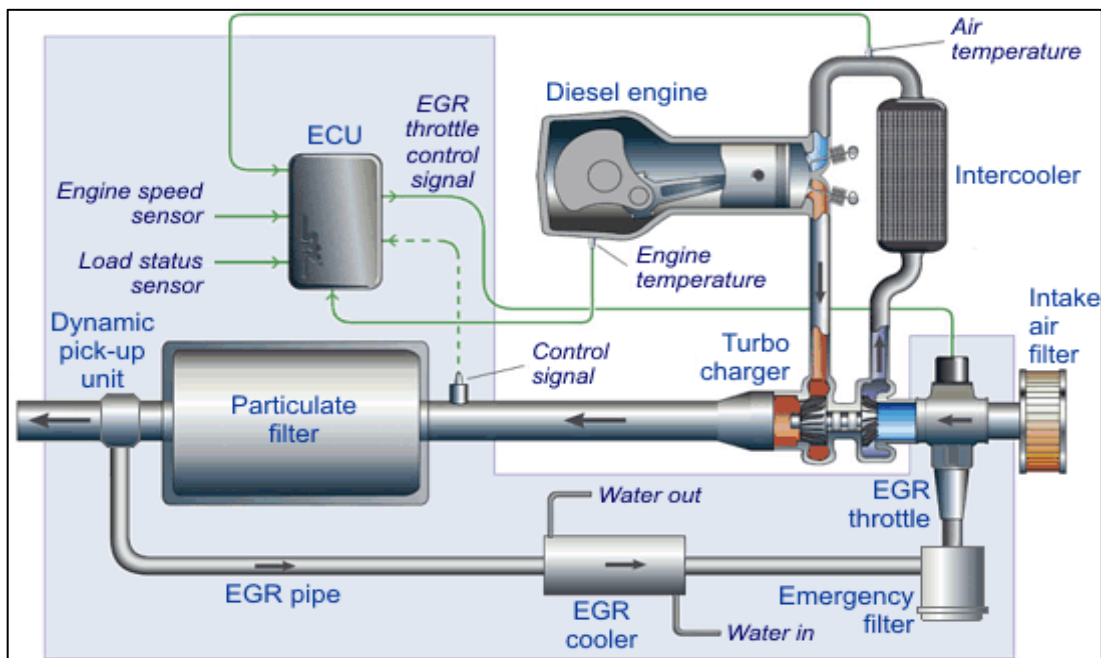


Figure 1. 8- EGR systems in a turbocharged engine [133].

1.5. EMISSIONS AND REGULATIONS

Human activities, in particular the burning of fossil fuels, have contributed to the increase in natural greenhouse gases [134,135]. Greenhouse gases in the atmosphere cause climate change. The main greenhouse gases emitted into the atmosphere are carbon dioxide, methane, nitrous oxide and fluorinated gases (hydrofluorocarbons, perfluorocarbons and, sulfur hexafluoride) [136,137]. Carbon dioxide (CO₂) is the main cause of global warming. The global emission of carbon dioxide reached 34 billion tonnes with an increase of 3% in 2011 [138]. In addition to global warming, the increase in the concentration of (CO₂) in the atmosphere leads to the acidification of the oceans by dissolution.

Diesel engines are used extensively compared to gasoline engines due to their low operating costs, energy efficiency, high durability and reliability. These important characteristics make them the most preferred engines, especially for heavy vehicles. As well as they have many advantages, but they have a significant impact on the problems of environmental pollution worldwide. Studies have shown that exposure to diesel exhaust is the cause of various problems that negatively affect human health [139].

Inside an engine, the complete combustion of the motor fuels composed exclusively of carbon and hydrogen would only generate CO₂ and H₂O, to the exclusion of any other harmful product [140]. However, the very short time allowed for chemical oxidation processes integration in combustion chambers, the lack of homogeneity in the carburetted mixtures, and the heterogeneity and rapid variations in the temperature do not allow for the state of ideal thermodynamic equilibrium to be reached. Thus, the incomplete combustion of hydrocarbon results in the formation of a wide range of organic and inorganic compounds distributed among the gaseous, semi-volatile and particulate phases [141] as is schematized in table 1. 3. The gaseous phase contains CO, CO₂, NO_x, SO_x, NH₃, water vapors, volatile organic compounds (VOC), hydrocarbons (UHC), polycyclic aromatic hydrocarbon (PAH), organic/inorganic acids, halogenated organic compounds, dioxins, etc [12].

Today, environmental protection has evolved to become a subject of concern. Many agencies and organizations are trying to prevent damage to the environment and human health from greenhouse gases and pollutant emissions. This is why many regions of the world, such as the European Union, are setting standards to reduce the emission of polluting gases from vehicles and car manufacturers are forced to produce cleaner cars and trucks. The “Euro” standards set the limits for emissions of air pollutants (nitrogen oxides, carbon monoxide, fine particles, hydrocarbons, etc.) not to be exceeded for new vehicles. Euro 6 (light vehicles) and

Euro VI (heavy vehicles) standards should however lead to further significant reductions. The higher the standard, the more recent it will be.

Table 1. 3- Typical diesel exhaust composition [12]

Component	Concentration
CO	100-10000 ppm
UHC	50-500 ppm
NO _x	30-1000 ppm
SO _x	Proportional to fuel S content
DPM	20-200mg/m ³
CO ₂	2-12 vol%
Ammonia	2.0 mg/mile
Cyanides	1.0 mg/mile
Benzene	6.0 mg/mile
Toluene	2.0 mg/mile
PAH	0.3 mg/mile
Aldehydes	0.0 mg/mile

1.5.1. Heavy-duty vehicles

Table 1. 5 summarizes heavy-duty vehicle emission standards introduced in the last two decades in Europe and table 1. 4 for selected years in the United States (US). The biggest improvement has been achieved for emissions of NO_x and PM in both US and Europe. Emission limits are not directly comparable, because they are set for different driving cycles, but US emissions are generally more stringent than European. EURO VI introduced in 2014 is said to be comparable with US 2010 standards [142], which were phased between 2007–2010 [143]. EUROVI additionally incorporates ammonia slip and particle number limits. CO₂ emissions are not regulated in heavy-duty vehicles.

Table 1. 4- US EPA Heavy duty diesel emissions standards

Level	CO	UHC	NO _x	PM	
				general	buses
US 1991	15.5	1.3	6	0.25	
US 1994	15.5	1.3	5	0.1	0.07
US 1998	15.5	1.3	4	0.1	0.05
US 2004	15.5	2.4		0.1	0.05
US 2010*	15.5	0.14	0.2	0.1	0.05

EPA- Environmental Protection Agency.

Table 1. 5- EU Heavy duty diesel emission standards in g/kWh

Tier	Year	Op. conditions	CO	UHC	NO _x	PM
EURO I	1992	Steady state	4.5	1.1	8	
EURO II	1998	Steady state	4	1.1	7	
EURO III	2000	Steady state	2.1	0.66	5	
		Transient	5.45	-	5	
EURO IV	2005	Steady state	1.5	0.46	3.5	0.8
		Transient	4	-	3.5	
EURO V	2008	Steady state	1.5	0.46	2	0.5
		Transient	4	-	2	
EURO VI	2014	Steady state	1.5	0.13	0.4	8x10 ¹¹
		Transient	4	-	0.46	6x10 ¹¹

1.5.2. Light-duty vehicles

European Union (EU) issued their first Euro 1 standard in 1992. The latest Euro 6 came into force in 2014 for new models and from September 2015 for all cars sold. See table 1. 6 for the summary. As of January 2015, any subsequent standards have not been proposed yet, but can be expected around 2020 [144].

Table 1. 6- EU emission limits for private vehicles in g.km⁻¹[145]

Standards	Year (NT)	CO	UHC+ NO _x	NO _x	Particles
Euro 1	1992	2.7220	0.970	-	0.140
Euro2- IDI	1996	1.000	0.700	-	0.080
Euro 2- DI	1999	1.000	0.900	-	0.100
Euro 3	01/2000	0.640	0.560	0.500	0.050
Euro 4	01/2005	0.500	0.300	0.250	0.025
Euro 5	09/2009	0.500	0.230	0.180	0.005
Euro 6	09/2014	0.500	0.170	0.080	0.005

NT- New types of model must comply with regulations in force as at the date of entry into force

CO- Carbon monoxide; UHC- unburned hydrocarbons; NO_x- Nitrogen oxides.

Reducing the pollution emitted by vehicles certainly requires further study. In this context, we then present a review of catalysts and their processes in diesel engines. Catalytic converters, also called catalysts, are exhaust pipes whose role is to ensure the transformation of polluting gases into harmless gas for gasoline and diesel vehicles. They are placed inside the exhaust pipe and consist of a stainless steel casing [146]. The envelope contains a ceramic

block ("honeycomb") inside which we find noble precious metals (palladium, rhodium, platinum, ...) which promote chemical reactions inside the catalyst.

1.6. POST-TREATMENT OF POLLUTING EMISSIONS FROM INTERNAL COMBUSTION THERMAL ENGINES

Diesel engines have high efficiency, reliability and durability. This is because diesel engines are specially used for heavy vehicles. Diesel engines are considered the main contributor to environmental contamination today. They contribute significantly to global warming through emissions of particles, hydrocarbons (UHC), nitrogen oxides (NO_x) and carbon oxides (CO_2). Their presence causes several health problems. Various effective techniques are currently available to reduce these emissions. Numerous policies have been imposed to reduce the negative health and environmental effects of diesel engine emissions, as well as much research, has been done on the reduction of exhaust pollutant emissions from diesel engines and emission control technologies [147].

There are different methods to reduce pollutants from the exhaust gases of an engine such as improving combustion in engines (reducing displacement, injection system and cooling the intake air) and reformulation of fuels. In this work, we were presented different post-treatment of polluting emissions in internal combustion engines mainly in diesel engines. This work reviews pollutant emission control technologies with standards and regulations. It can be said that emissions of pollutants such as CO and UHC are emitted due to incomplete combustion, and emissions of NO_x are due to high combustion temperatures in vehicles. Consequently, emission control systems are of the utmost importance where there are vehicles.

1.6.1. Exhaust gas recirculation (EGR)

As mentioned previously, exhaust gas recirculation (EGR) is another technique to reduce NO_x emissions. It makes it possible to slow down the combustion by injection of a gas containing little oxygen and replacing the air which causes the temperatures to drop. In systems (EGR), part of the exhaust gas returns to the engine to cool it and reduce peak temperatures and combustion pressures, thereby reducing production by NO_x . This process dilutes the oxygen in the incoming air stream and incorporates inert gases into the combustion, which absorb heat to reduce maximum temperatures in the cylinders. Exhaust gas recirculation (EGR) is commonly used by engine manufacturers as this method complies with new engine emission control standards. In addition, due to the reduced temperature in the cylinder, this technology generates increased emissions of UHC and CO [148].

1.6.2. NO_x trap type catalysts

The technology (LNT) also known as the NO_x trap is made of a filter, placed between the engine block and the particle filter, made of noble metals, which captures these gases and accumulates them in a "store". Once the stock is full, the system performs a regeneration which allows them to be burned by going back into the engine mixed with the fuel.

This technology was developed to reduce emissions by NO_x, and more specifically the elimination of nitrogen oxides present in diesel exhaust gases. In the first phase, there is oxidation in a poor medium (poor phases) of (NO) to (NO₂) as well as storage of these (NO₂) newly formed on platinum. Then comes the second phase where the fuel mixture becomes temporarily rich. There is then desorption and reduction of the nitrates thanks to the rhodium leading to the formation of nitrogen (N₂). The use of such technology achieves an elimination rate of NO_x of more than 90 % [149].

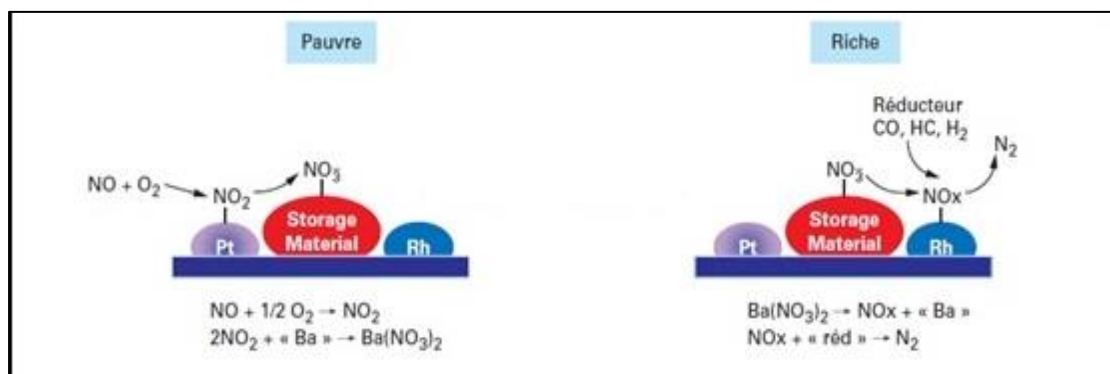


Figure 1. 9- Operation of a NO_x trap [150].

1.6.3. Diesel oxidation catalyst (DOC)

The diesel oxidation catalyst (DOC) was introduced in the 1970s to clean up vehicles. The catalysts (DOC) consist of monolithic support, generally cylindrical, provided with a multitude of small parallel channels with porous walls. The diesel oxidation catalyst has several roles. The main function of diesel oxidation catalysts (DOCs) is to promote the oxidation of hydrocarbons (UHC) (to form carbon dioxide CO₂ and water H₂O) and carbon monoxide CO (to form CO₂). The oxidation of (CO) and (UHC) emissions generates heat. This heat is used to increase the temperature of the exhaust gases. This exhaust gas temperature can rise approximately above 90°C for every 1% of oxidation of (CO).

Catalysts (DOCs) play a role in reducing the mass of diesel particle emissions by oxidizing part of the hydrocarbons which are adsorbed [151,152]. Catalysts (DOC) are inexpensive, maintenance-free and suitable for diesel engines [153]. Diesel oxidation catalysts (DOC) can also be used in conjunction with catalysts selective catalytic reduction (SCR).

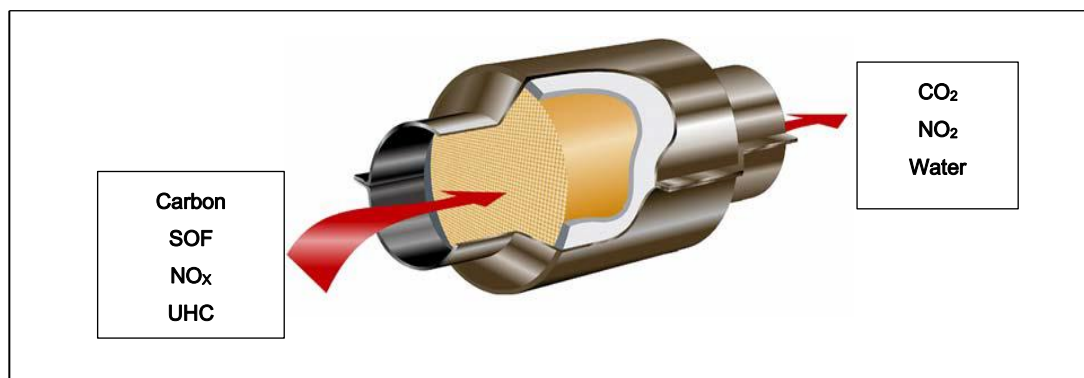


Figure 1. 10- Flow-through diesel oxidation catalyst [12].

1.6.4. Diesel particulate filters (DPFs)

To meet the emissions legislation the most widely used approach is to trap DPM in porous wall-flow diesel particulate filters, usually made of cordierite ($2\text{MgO}\cdot 2\text{Al}_2\text{O}_3\cdot 5\text{SiO}_2$) [154] or silicon carbide (SiC) [155] honeycomb structure monolith (figure 1. 11). The adjacent channels of the honeycomb are alternatively plugged at each end in order to force the diesel aerosol through the porous substrate walls, which act as a mechanical filter.

The filter walls are designed to have an optimum porosity, enabling the exhaust gases to pass through their walls without much hindrance, whilst being sufficiently impervious to collect the particulate species. These filters have PM trapping efficiencies of almost 100%, making it possible to remove the particulate species from the exhaust stream [156]. As the filters accumulate DPM, it builds up backpressure that has many negative effects such as decreased fuel economy and possible engine and/or filter failure [157]. To prevent these negative effects, the DPF has to be regenerated by oxidizing (i.e. burning) trapped PM. Filter control capabilities: DPM 80% to 90% reduction, CO > 75% and UHCs > 85%.



Figure 1. 11- Ceramic monolith [12].

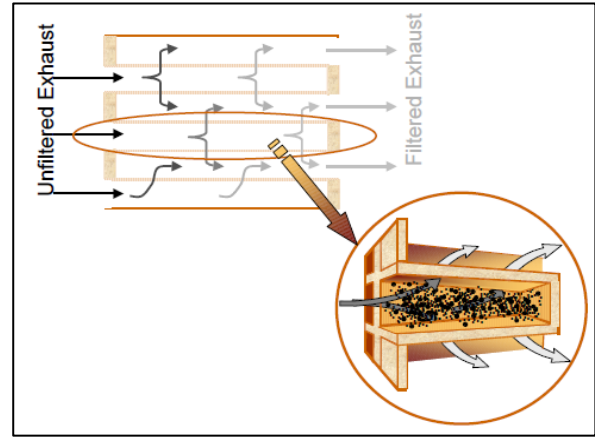


Figure 1. 12- Schematic representation of wall flow DPF [158].

1.6.5. Selective catalytic reduction (SCR)

SCR was the main technology used by the European automotive industry to meet the requirements of the more stringent emission standards (Euro 4 and Euro 5) for heavy diesel engines between 2005 and 2008, and in recent years some manufacturers have announced it for light applications in the United States and more recently in Europe [159].

The selective catalytic reduction system (SCR) is a technique used to reduce emissions of nitrogen oxides (NO_x). An injection of AdBlue liquid, composed of a mixture of water and urea in the exhaust gas line upstream of the (SCR) will react with the exhaust gases to produce ammonia (NH_3) in gaseous form and it will be the latter which will react in the catalyst with the NO_x in order to treat them. AdBlue converts NO_x from diesel vehicle exhaust to environmentally friendly nitrogen (N_2) and water vapor (H_2O).

The SCR is used to minimize the emissions of NO_x in the exhaust gases in order to use ammonia (NH_3) as a reducing agent [160]. The systems (SCR) require periodic refilling with AdBlue. Systems (SCR) are commonly used with a diesel oxidation catalyst (DOC) to reduce the emission of fine particles. Because of the new standards on (NO_x), most road diesel engines manufactured since 2010 are equipped with a system (SCR).

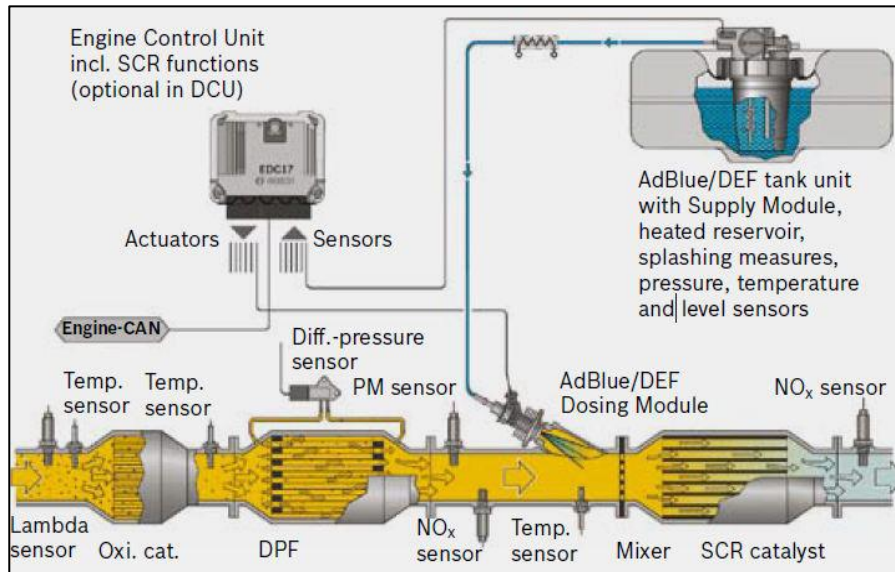


Figure 1. 13- SCR layout in a heavy duty vehicle. Consists of the DOC (Diesel oxidation catalyst), DPF(Diesel particulate filter), Urea injector, SCR [161].

1.7. CONCLUSION

To control the pollutant emissions as desired, it is only possible with after-treatment systems, which are used to remove the main pollutant emissions from the exhaust gases. These diesel exhaust gas after-treatment systems include the diesel oxidation catalyst (DOC), diesel particulate filter (DPF), NO_x trap type catalysts (LNT) and selective catalytic reduction (SCR) system. Catalysts (DOCs) play a role in reducing the mass of diesel particulate emissions, CO and UHC emissions. Diesel particulate filters (DPF) are typically used with diesel oxidation catalyst (DOC) which converts (NO) to (NO₂) to increase systems conversion efficiency (SCR).

AdBlue (urea + water) is a simple product, not dangerous. However, there are some clear rules of use to follow as it is used with a catalyst (SCR). Catalysts based on (Pt) and (Pd) are the most commonly used catalysts for diesel oxidation catalyst (DOC) and selective catalytic reduction (SCR) system.

Interestingly, in recent years the researchers are focusing on alternative combustion modes such as homogeneous charge compression ignition (HCCI). This is a promising concept, as it has the potential to combine the best spark ignition (SI) and compression ignition (CI) engines. HCCI is a state-of-the-art engine technology that has the potential to overcome the current fundamental NO_x and particulate emissions of compression ignition engines maintaining its efficiency and fuel economy.

CHAPTER 2- MODELING AND SIMULATION OF HETEROGENEOUS AND HOMOGENEOUS COMBUSTION

2.1. INTRODUCTION

Diesel engines operate with excess air. The diesel fuel is injected under pressure into a mass of previously compressed air. Combustion is initiated by self-ignition (compression ignition). Combustion is said to be stratified or heterogeneous because it takes place in an environment made up of both areas very rich in fuel (located in particular near the injector nose) and very poor areas (near the cylinder wall) [162].

Generally, the Homogeneous Charge Compression Ignition (HCCI) engines present superior fuel economy and ultra-low NO_x and particle matter emissions compared with the traditional combustion engine. However, the HCCI engine is essentially decoupled from the spark plug and fuel injection. That means the HCCI engines have no direct control mechanism for the auto-ignition timing and subsequent combustion phase [15]. Where combustion begins in multiple spots when the homogeneous charge mixtures reach chemical activation energy. The combustion process results in an increase in pressure and temperature as the energy stored in the fuel is released, with the exhaust gases are produced. Some of the energy is radiated and convected to the cylinder walls, cylinder head, piston and valves then wasted. Most of the energy goes to the power stroke, as the exhaust gases expand to push the piston to the bottom position.

Currently, the research centers of internal combustion engines in the world have focused on research and development of software to solve simulation problems and complete the working cycle to solve problems related to the logical organization of the mixture generation process and combustion in diesel engines [163]. Numerical simulation can be carried out in an internal combustion engine by different resolution software such as Diesel-RK, KIVA, Open FOAM, etc. Diesel-RK is a software for calculating internal combustion engines developed by the Bauman Technical University (Russian Federation) experts. It has been used by many facilities specializing in research, development and production.

NO_x emissions have been the subject of several studies with the Diesel-RK software. Among these studies, we can cite the study carried out by AL-Dawody and Bhatti [164] on the combustion, performance and emission parameters of a single-cylinder, four-stroke, and constant-speed diesel engine running on diesel and different mixtures. In the same context, Mater [165] conducted a study using Diesel-RK software to find solutions to reduce fuel consumption and the concentrations of NO_x emissions in combustion products. This research includes the mechanism of NO_x formation and techniques for their reduction. Using Diesel-RK software, Hamdan et al. [166] carried out theoretical research concerning the performance of a four-stroke compression engine, which is powered by alternative fuels in the form of mixtures diesel-ethanol and diesel-ether. Several parameters were calculated as follows: the engine torque, the mean effective pressure, power, fuel specific consumption and thermal efficiency. The RK model makes it possible to determine the soot and NO emissions according to the formation of the mixture and the combustion conditions. The software makes it possible to find the optimal shape of the piston bowl, the directions of fuel spraying, the diameters and number of nozzles, the shape of the injection profile,....., etc. Kuleshov [167] critically examined the performance and emission characteristics of the diesel engine when it was simulated through Diesel-RK simulation software at standard operating conditions. Also, they reported that this software was one of the efficient tools for optimization of engine operating parameters such as piston bowl geometry, exhaust gas recirculation, fuel injection and several nozzles. Venu et al. [168] investigated the influence of combustion chamber geometry on the performance, combustion and emission characteristics of the diesel engine experimentally as well as engine simulation through Diesel-RK software at similar operating conditions.

At present, there are still several challenges that must be addressed before HCCI can go into production, but this is a promising concept [47]. HCCI combustion is the topic of this thesis and this chapter will discuss it in detail.

2.2. COMBUSTION MODELLING

Numerical simulations were carried out to study heterogeneous and homogeneous combustion models. The comparison between them was carried out using Diesel-RK and ANSYS CHEMKIN-Pro software, respectively.

2.2.1. Heterogeneous combustion

2.2.1.1. Diesel-RK engine simulation software

In the first part (Section 2.2.1); simulation has been carried out using the commercial software Diesel-RK. Before the simulation, the engine model has to be chosen and incorporated into the software. The engine that has been considered in the work is the F8L413 type Deutz engine equipping the TB230 truck, manufactured by the National Company of Industrial Vehicles (SNVI) of Rouiba (Algeria), whose cavity shape is cylindro-spherical. The details of the engine are given in table 2. 2. The simulation has been performed over the speed range of (1200 rpm to 2650 rpm) and fuel injection timing values ranging from 26 deg to 32 deg before TDC at a constant compression ratio of 18:1. In order to predict the different performance and emission parameters, different fuels were used. To understand the behavior, certain parameters were also studied. These parameters were; indicated mean effective pressure (IMEP), specific fuel consumption (SFC), Bosch smoke number (BSN), specific carbon dioxide emission (S-CO₂),....., etc.

The combustion chamber of the engine is to a large extent integrated into the piston, as shown in figure 2. 1. The F8L413 has a bore of 120 mm, a stroke of 125 mm, and develops an output of 169 kW (230 HP) at 2650 rpm, which corresponds to a brake mean effective pressure of 6.7 bars.

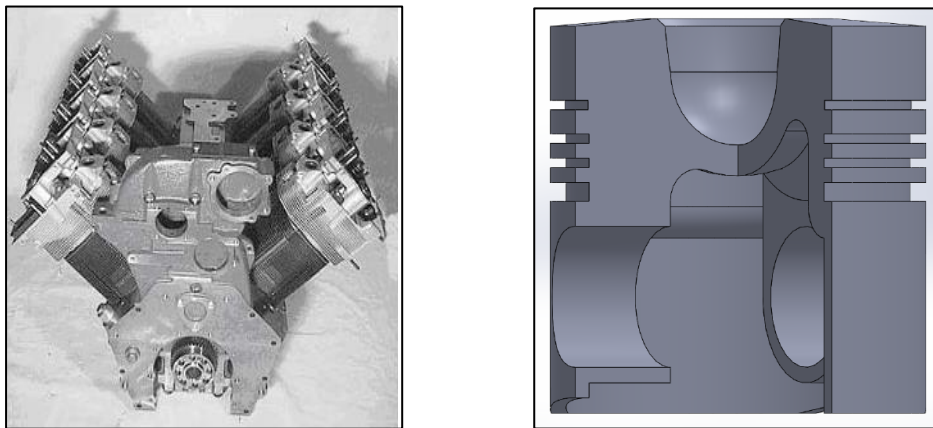


Figure 2. 1- Photo of an F8L413 diesel engine and its cross-section piston.

The combustion chamber and the position of the injection jets are shown in figure 2. 2. This direct injection system with mixing taking place near the piston bowl wall is very favorable concerning acoustics due to combustion with a slow rate of pressure rise [169].

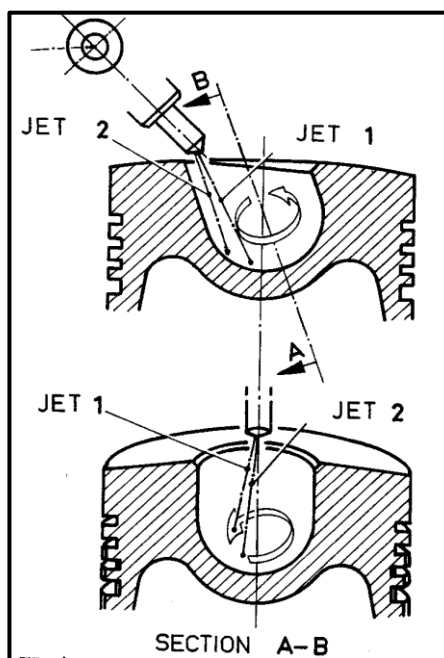


Figure 2. 2- FL413 F combustion chamber and position of the injection jets [169].

The fuel properties used are listed in table 2. 1. It can be seen that the low heating value (LHV) of Hexadecane fuel is 43.947 MJ/kg, which is much higher than of other fuels. Furthermore, the density of Heavy diesel fuel is higher than n-Hexadecane and Diesel No. 2 fuels. The properties for Diesel No. 2 and Heavy diesel fuel are incorporated in the Diesel-RK fuel library.

Table 2. 1-Properties of n-Hexadecane, Diesel No. 2 and Heavy diesel fuels

Properties		n-Hexadecane (C ₁₆ H ₃₄)	Diesel No. 2	Heavy fuel
Composition	C	0.848658	0.87	0.87
	H	0.15134	0,126	0,13
	O	0	0,004	0
Density of fuel (kg/m ³) at 323 K		770	830	981
Cetane number		100	48	48
Lower heating value (MJ/kg)		43.947	42.5	40.6
Molaire mass (g/mol)		226.44	190	190
Dynamic viscosity (Pa.s)		0.003	0.003	0.003

Table 2. 2-Simulated engine specifications

General parameters and specifications				
Type		4-Stroke / Diesel Engine		
Engine design		V-Engine		
Combustion system		Naturally aspirated		
Max. Power		169 KW @ 2650 rpm		
Max. Torque		671 Nm @ 1600 rpm		
No. of injector's nozzle hole/Injector		2		
Number of cylinders		8		
Number of valves		2 valves per cylinder		
Compression ratio		18: 1		
Connecting rod length		238 mm		
Valve timing		Exhaust valve open (EVO)	67 deg bBDC	
		Exhaust valve close (EVC)	27 deg aTDC	
		Intake valve open (IVO)	22 deg bTDC	
		Intake valve close (IVC)	52 deg aBDC	
Injection pressure		175 bars		
Angle Spray		Nozzle hole 1	10 deg	
		Nozzle hole 2	18 deg	
Cooling System		Air cooling		
Fuel injection timing (Start of injection)		with injection advance up to 2650 rpm		
		without injection advance	from 1200 to 1799 rpm	28 deg bTDC
			from 1800 to 2299 rpm	30 deg bTDC
			from 2300 to 2650 rpm	32 deg bTDC

A numerical simulation is a tool for optimizing and improving the performance of the internal combustion engine, which requires having to manufacture new prototypes and test them each time. Diesel-RK software is considered to be a very good open-source software for research students, as it is free and able to simulate the combustion and thermodynamics of diesel engines very well. Diesel-RK software is primarily designed for simulating the actual operating conditions of a diesel engine. It is also one of the best software for optimizing engine parameters. The main applications of this software are the prediction of engine performance, combustion and emission characteristics of a diesel engine running on diesel or with various raw materials such as biodiesel. It is also an excellent tool for optimizing the shape of the piston bowl according to the specific design. In addition, it allows the visualization of fuel dispersion to

the walls of the combustion chamber and the movement of the air vortex in visual animation format. Diesel engine characteristics such as thermal efficiency, specific fuel consumption, pressure and temperature cylinder, heat release rate, ignition delay, carbon monoxide, hydrocarbons, nitrogen oxides and soot concentrations can be analyzed.

- **Engine parameter test in DIESEL-RK**

When the Diesel-RK software is opened, a wizard for creating a new project is displayed to help create a model and a data file to analyze and optimize the engine considered as shown in figure 2. 3.

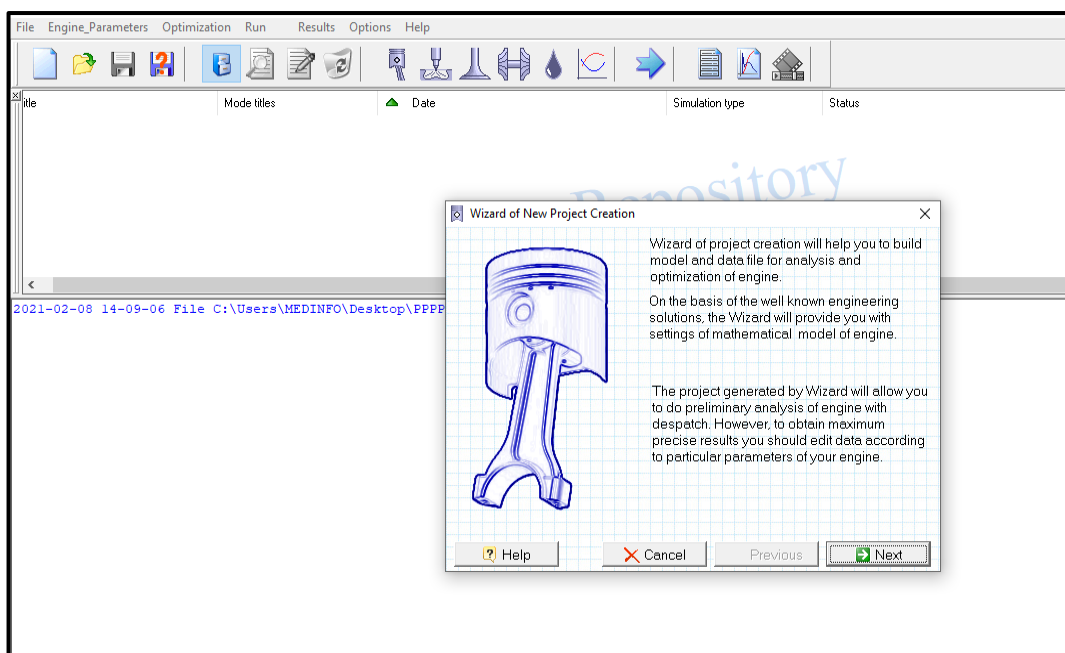


Figure 2. 3- Show the cylinder shape.

By selecting next, the window is shown in figure 2. 4. We select the name of an engine (a project name), then we determine the type of work cycle to choose (Four-stroke cycle). After which we choose the fuel and the ignition method (DI Diesel) then we validate by pressing NEXT.

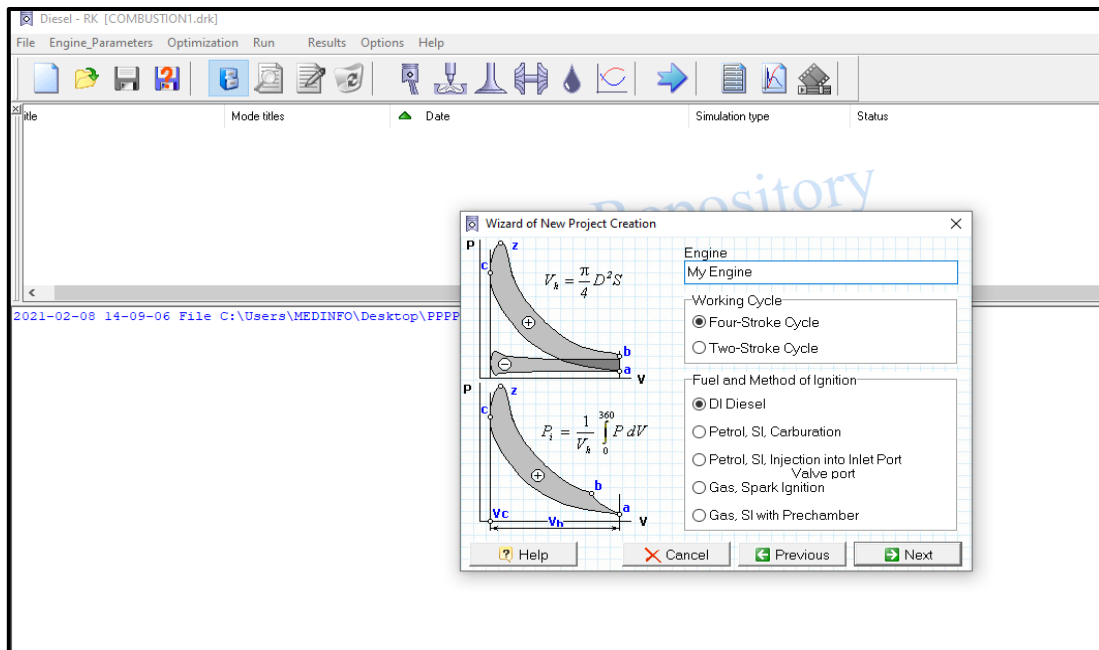


Figure 2. 4- The selection of engine cycle, fuel, and method of ignition.

In the new window, we define the type of basic engine design we choose (V-Engine), then we determine the number of cylinders (8) and the cooling system (air cooling) then we validate by pressing NEXT as shown in figure 2. 5.

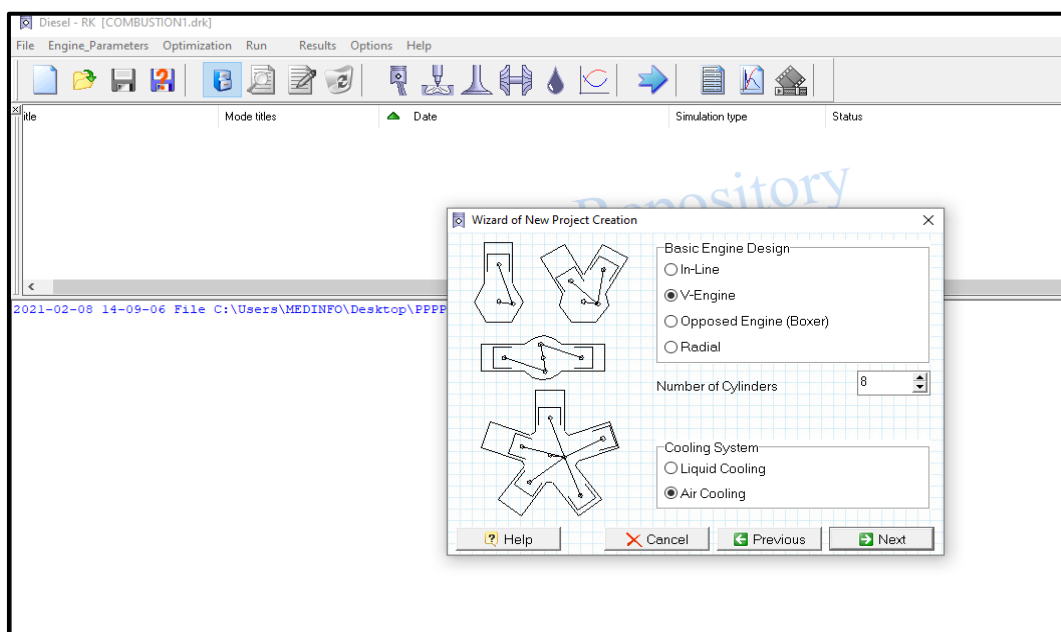


Figure 2. 5- Selection of the basic engine design, number of cylinders, and type of cooling system.

In the new window, we determine the cylinder bore (120 mm), the piston stroke (125 mm), the nominal engine speed (2650 rpm) and compression ratio (18), then press (NEXT) as shown in figure 2. 6.

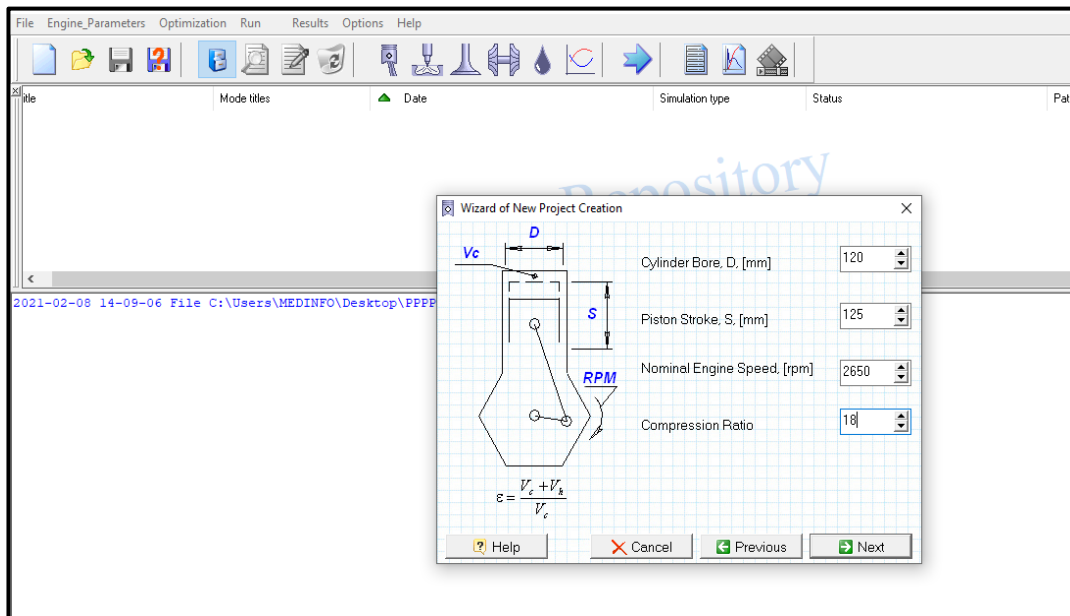


Figure 2. 6- Engine geometrical dimensions (cylinder bore, stroke, engine speed and compression ratio).

The ambient parameter of the sea level window appears, then choose the pressure value (1 bar), temperature value (295 K) and determine the application type so we choose (Overland and on the sea), then press (NEXT) as shown in figure 2. 7.

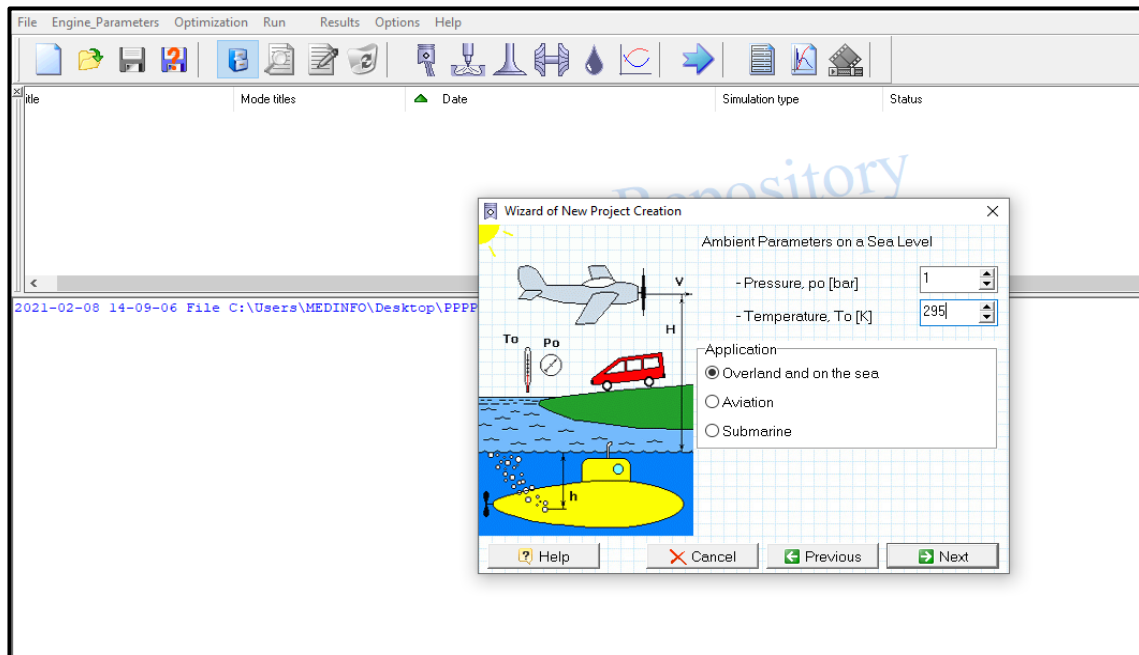


Figure 2. 7- Options that selected ambient parameters (pressure and temperature) and engine application.

In the new window we choose delete super – or turbocharged engine, according to cylinder head design we determine the number of valves we choose (two valves), then choose the range of injection pressure (Less than 500 bars), then press (Done) as shown in figure 2. 8.

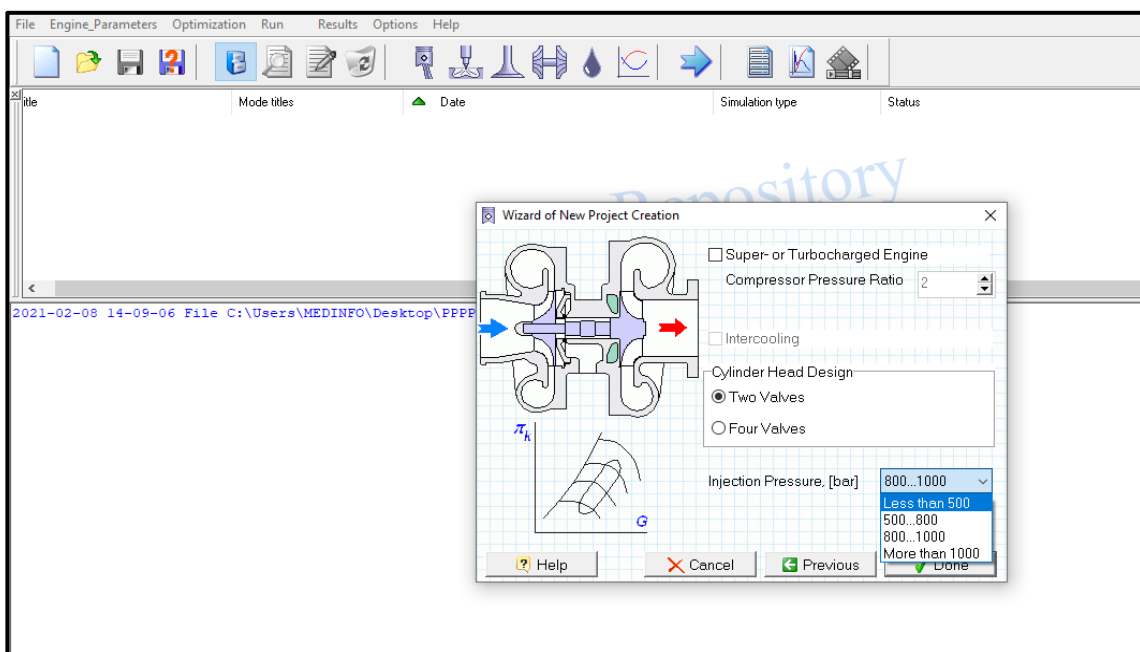


Figure 2. 8- Options selected for compressor pressure ratio and the number of valves per cylinder.

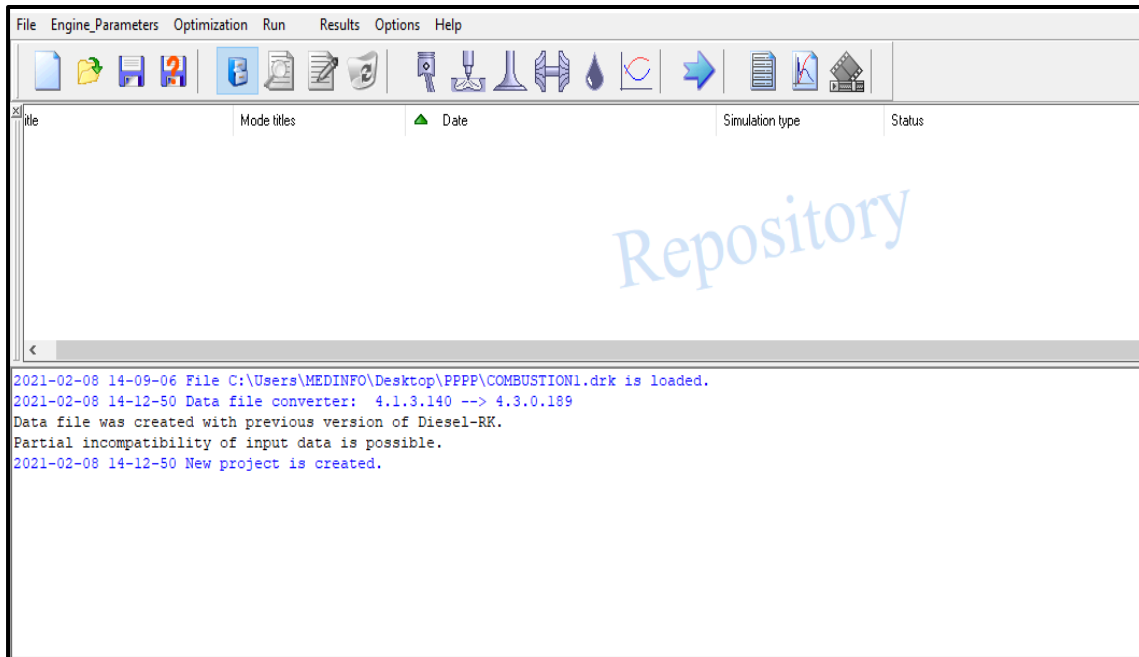


Figure 2. 9- Shows how to save the result file.

In the window of figures 2. 10 and 2. 11 we define the basic parameters of the charging/ discharging system: the opening and closing time of the valves

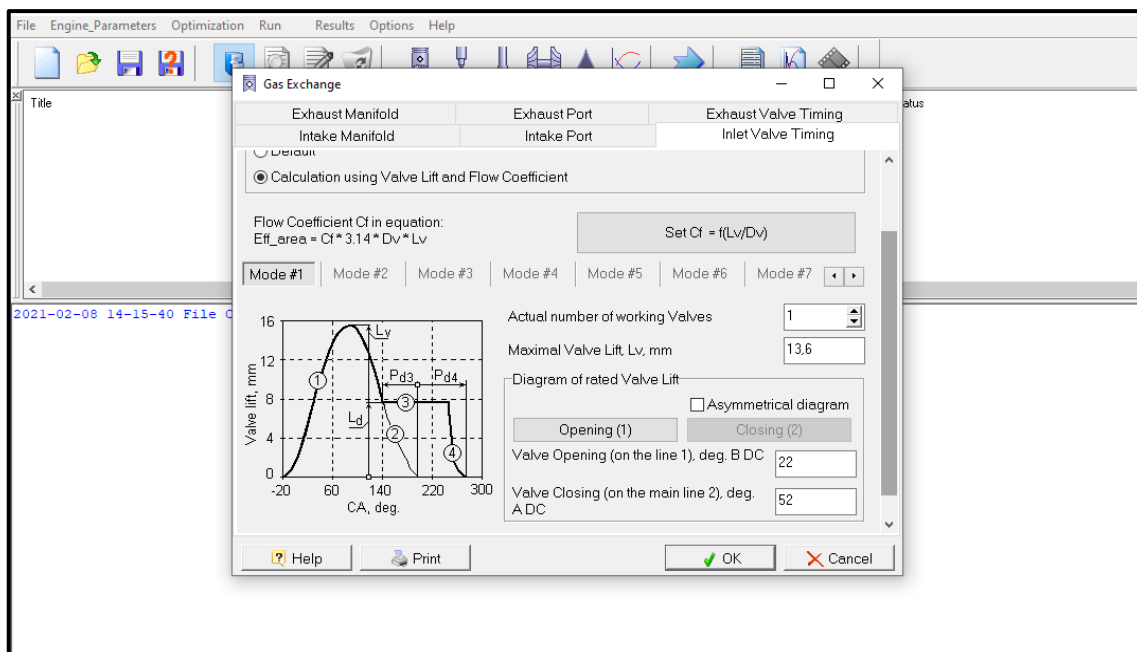


Figure 2. 10- Inlet valve timing parameters.

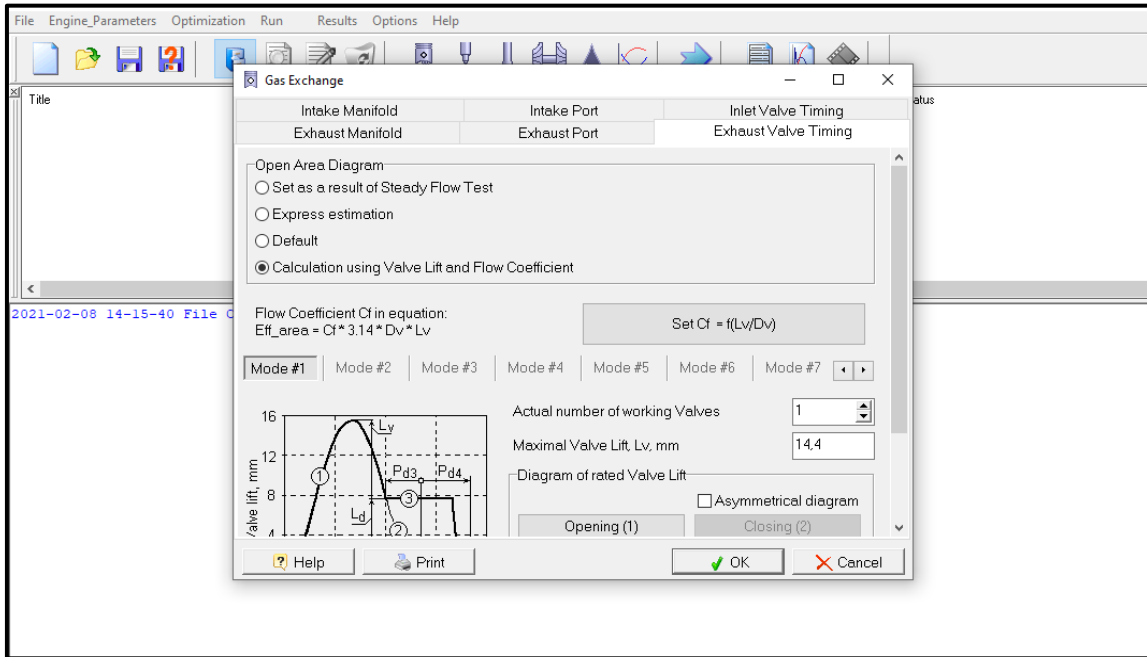


Figure 2. 11- Exhaust valve timing parameters.

The window in figure 2. 12 contains a set of fuel parameters making it possible to choose and its specifications that will be used, and we will use Hexadecane (Cetane).

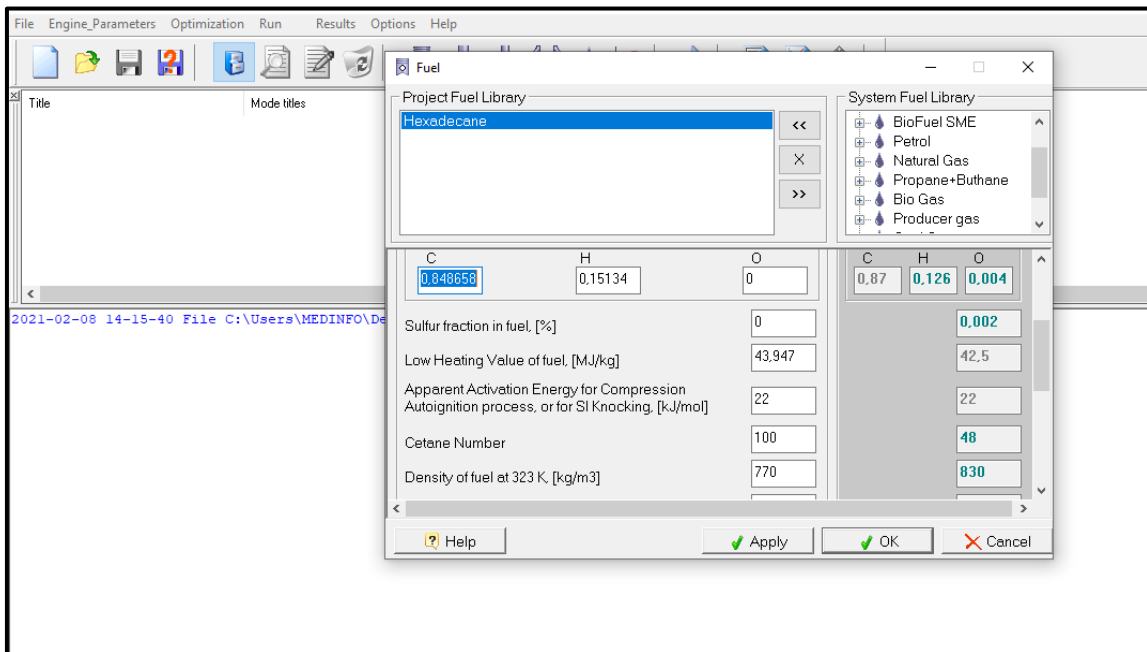


Figure 2. 12- Fuel type and properties (Hexadecane).

The window in figure 2. 13, shows the interface for declaring the structural parameters of the piston bowl design.

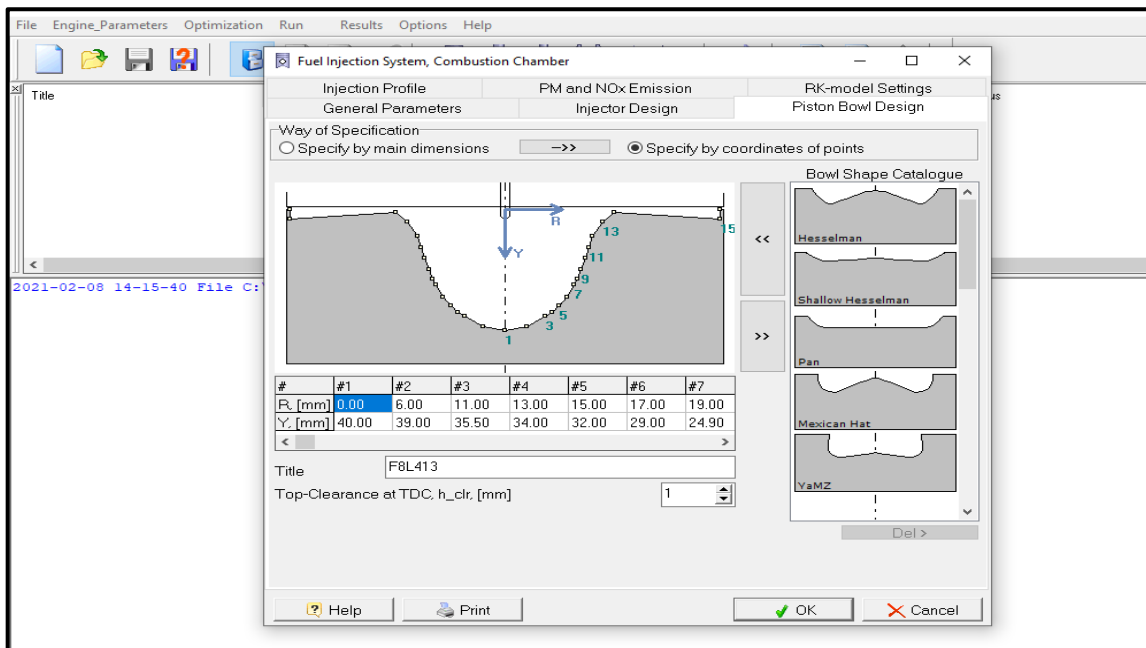


Figure 2. 13- Design of the piston bowl (geometry of F8L413 engine).

The window in figure 2. 14 shows the interface of the module which allows declaring the operating mode parameters such as engine speed, air-fuel equivalence ratio, injection timing, ambient pressure and ambient temperature.

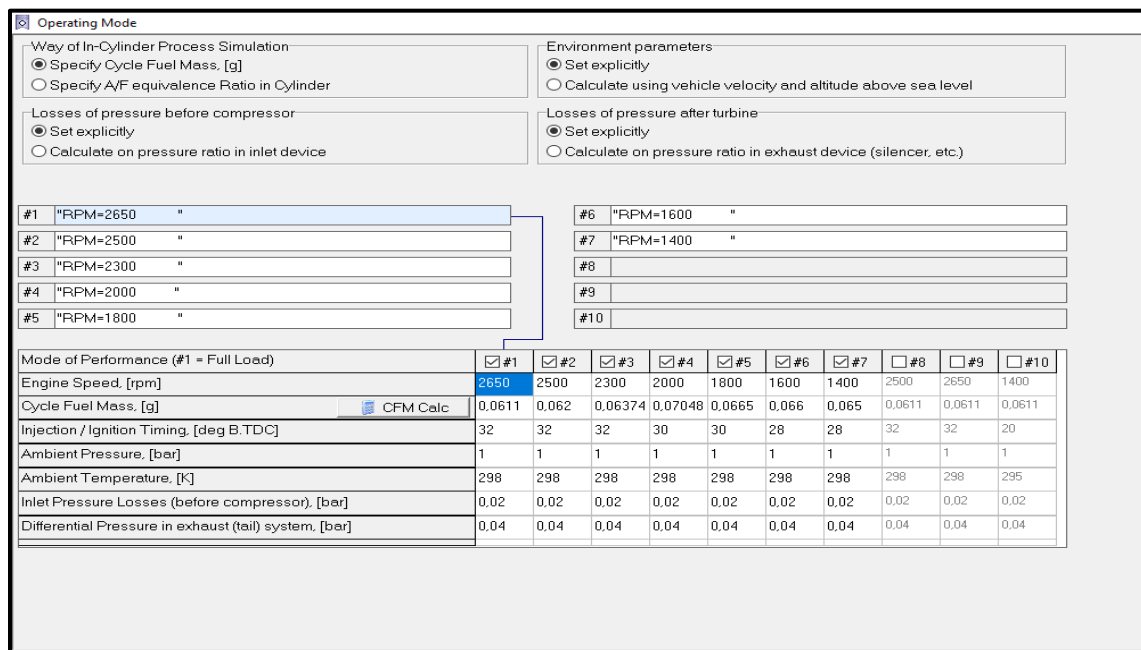


Figure 2. 14- Operating mode table.

- **Cycle fuel mass**

The following points refer to several parameters that were calculated for every regime. Notice that the fluctuations of cycle fuel mass values are expected in order to find the best combination.

$$m_f = \frac{SFC \text{ Power}}{N i_{cycl} 30} \quad (2-1)$$

m_f – Cycle fuel mass, g;

SFC – Specific fuel consumption, usually for Heavy-duty diesel engine (HDDE) ranges between 225–230, g/kWh;

$Power$ – Engine power corresponding to the rpm;

i_{cycl} – Number of cylinders (in this case, $i_{cycl} = 8$).

In this step, we will enter the parameters of the injector, as this step is the most important in this research as we change these variables in order to obtain lower emissions and higher efficiency.

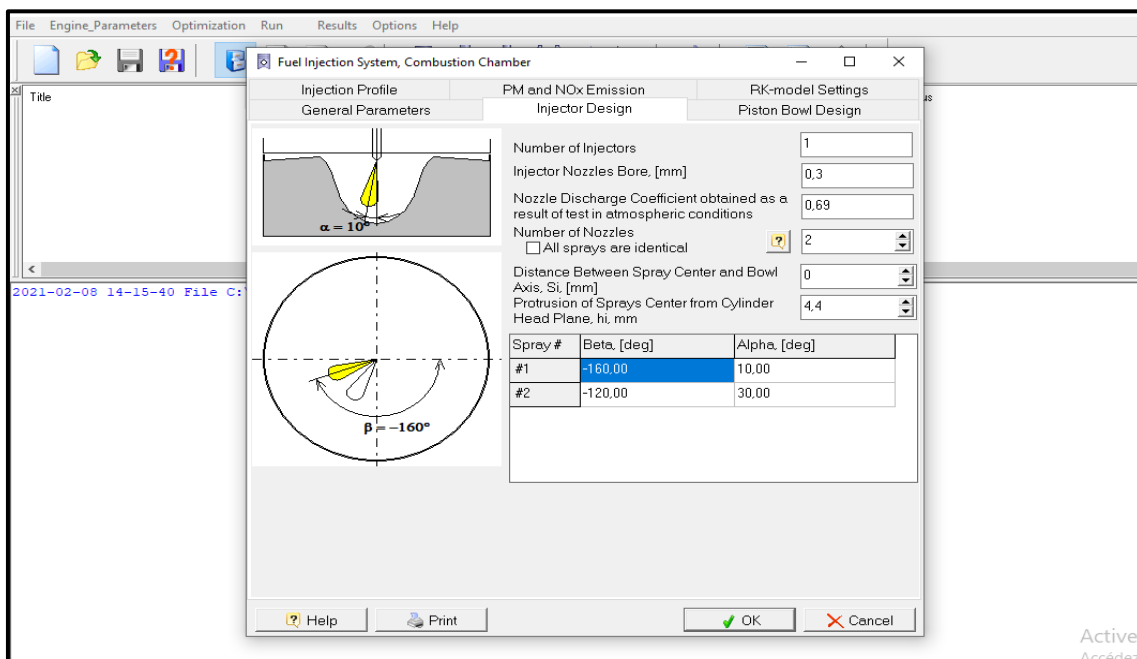


Figure 2. 15- Design of injector, orientation, and diameter of holes.

- **Number of injectors:** here we enter the number of injectors that each cylinder contains;

- **Injector nozzles bore (mm):** here we enter the diameter of the injector nozzle in millimeters;
- **Nozzles discharge coefficient:** is the ratio of the mass flow rate at the discharge end of the nozzle to that of an ideal nozzle which expands an identical working fluid from the same initial conditions to the same exit pressures is the ratio of the actual discharge to the theoretical discharge, it is entered as a fraction and ranges from 0 to 0.9.

The window in figure 2. 16 shows the mode of the specification of the injection profile in the combustion chamber.

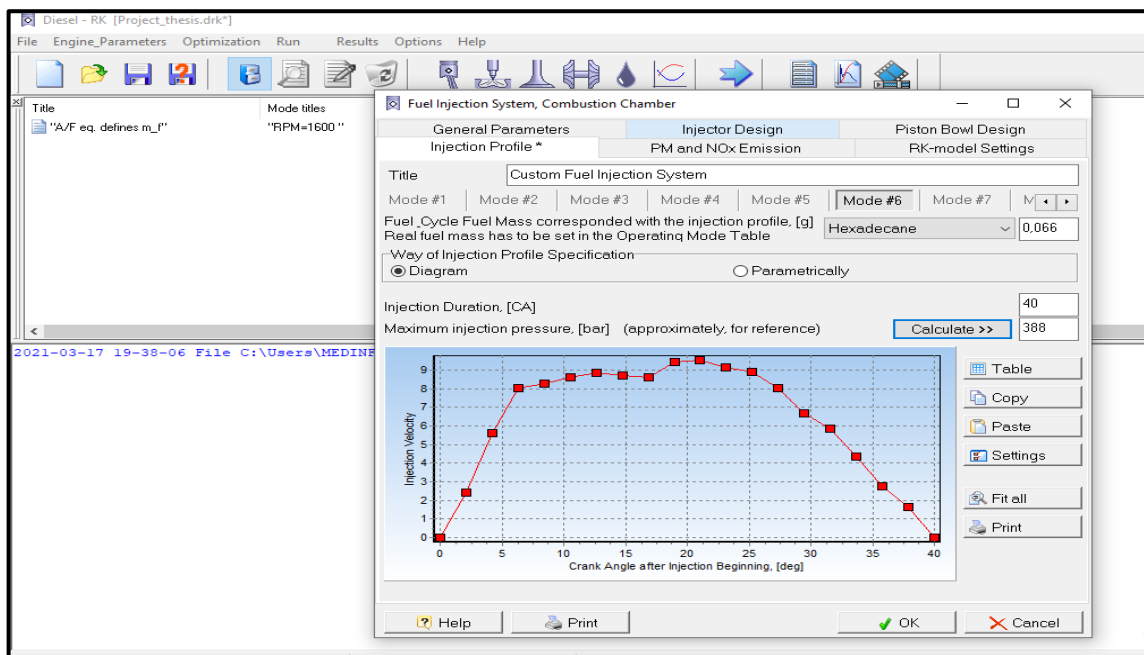


Figure 2. 16- Input injection profile.

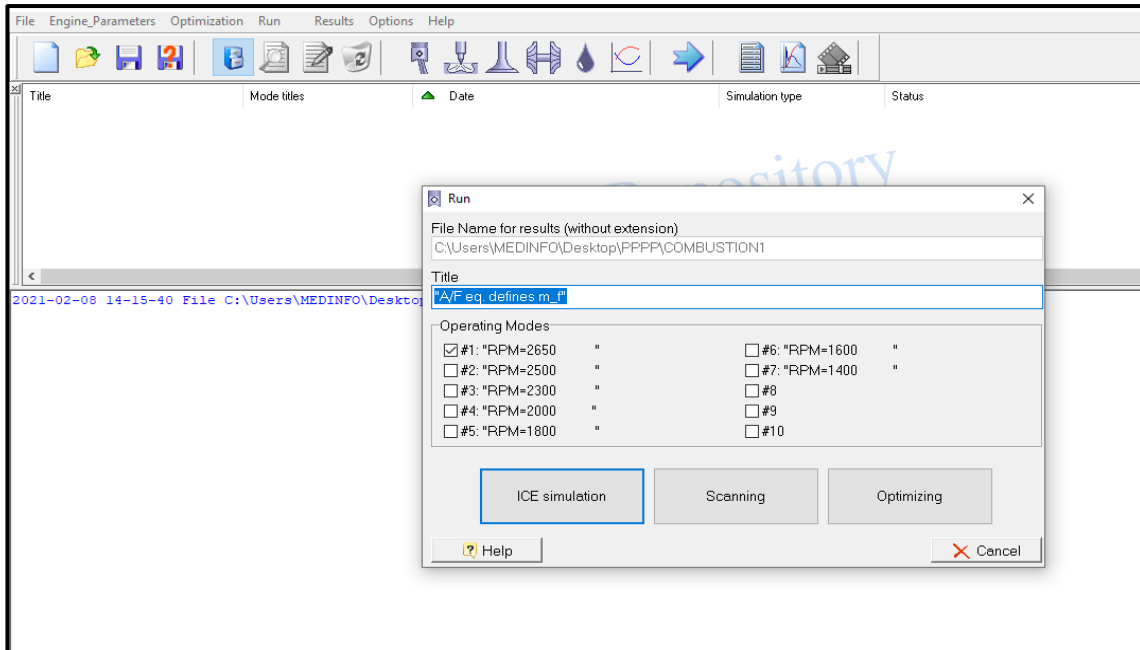


Figure 2. 17- Run the program.

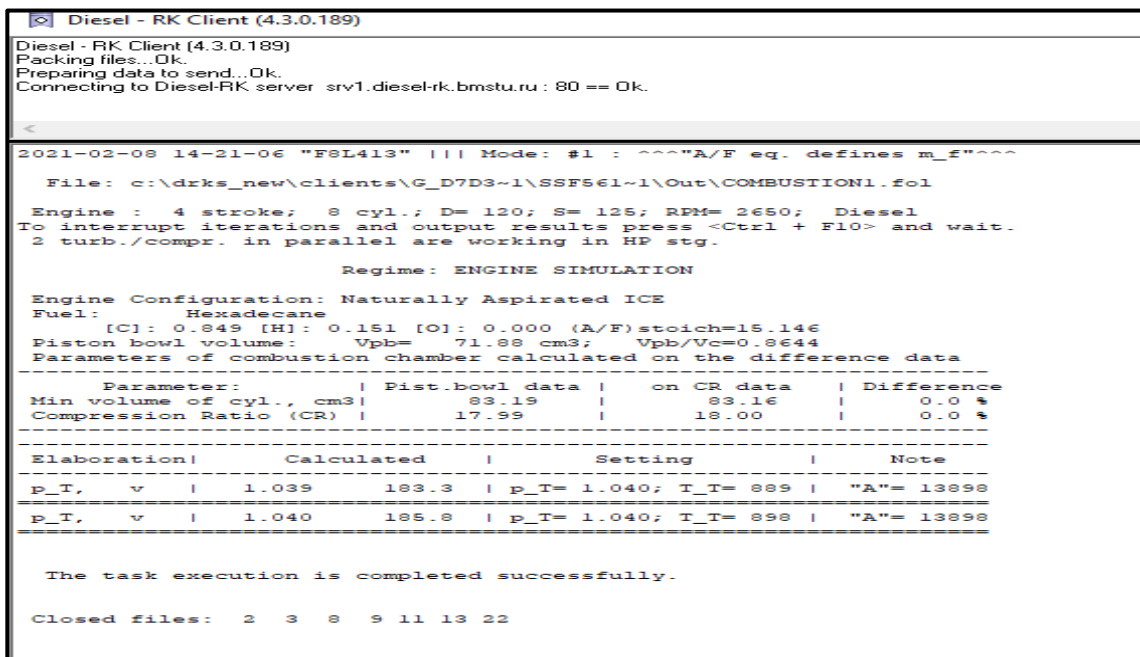


Figure 2. 18- Shows a run of the program.

2.2.1.2. Model equations

The main equations of the model are as follows [164,170,171]:

a. Mass conservation

The rate of mass change in an open system is the net mass flow through the boundaries of the system and can be expressed mathematically as follows:

$$\frac{dm}{dt} = \sum_j \dot{m}_j \quad (2-2)$$

With,

m – Total mass in the cylinder;

\dot{m}_j – Mass flow rate of the j^{th} species.

b. Species conservation

The equations of the evolution of species in the combustion chamber will be developed based on the mass fraction.

$$\dot{Y}_i = \sum_j \left(\frac{\dot{m}_j}{m} \right) (Y_i^r - Y_i^p) + \frac{\Omega_i W_{mw}}{\rho} \quad (2-3)$$

With

Y_i^r, Y_i^p – Represent the stoichiometric coefficients;

Ω_i – Molar rate of production;

ρ – Density;

W_{mw} – Molecular weight.

c. Energy conservation

The generalized energy equation for an open thermodynamic system can be written:

$$\frac{d(mu)}{dt} = -P \frac{dV}{dt} + \frac{dQ_{ht}}{dt} + \sum_j \dot{m}_j h_j \quad (2-4)$$

With

$P \frac{dV}{dt}$ – Displacement work;

$\frac{dQ_{ht}}{dt}$ – Heat transfer;

$\sum_j \dot{m}_j h_j$ – Enthalpy flux.

d. Heat release simulation

At simulation, the assumption is made that the heat release process consists of four main phases. They differ by physical and chemical peculiarities and factors limiting the rate of the process:

- Ignition delay period.
- Premixed combustion phase.
- Mixing-controlled combustion phase.
- Late combustion phase after the ending of fuel injection.

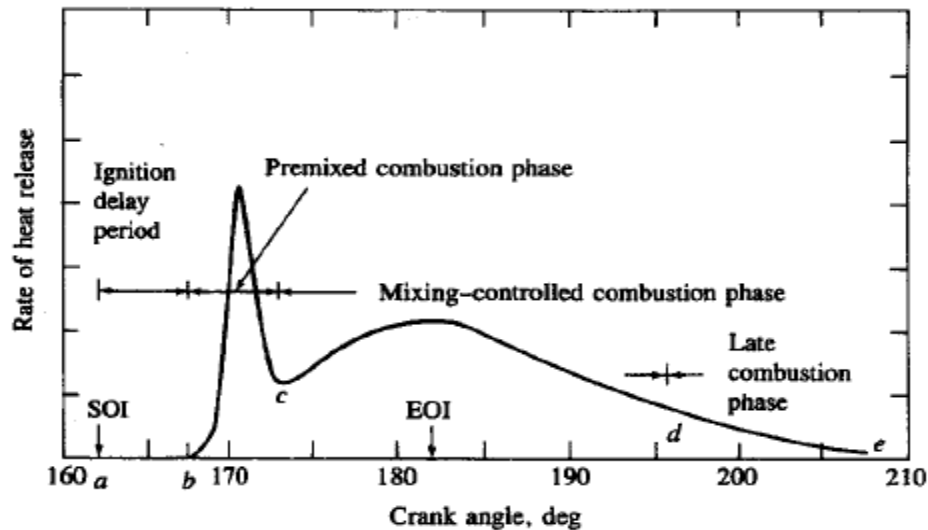


Figure 2. 19- Identification of the phases of the combustion, from heat release rate [8]

⇒ Ignition delay period

The auto-ignition delay period is the first phase of heat release, and is calculated using the Tolstov equation modified as follows:

$$\tau = 3.8 \cdot 10^{-6} \left(1 - 1.6 \cdot 10^{-4} N\right) \sqrt{\frac{T}{P}} \exp\left(\frac{E_A}{8.12T} - \frac{70}{CN + 25}\right) \quad (2-5)$$

With

CN – Cetane number of fuel;

E_A – Apparent activation energy for the auto-ignition process 23000–28000 kJ/kmole;

T and P are current in-cylinder temperature and pressure.

➤ Premixed combustion phase

During premixed combustion phase the heat release rate is given by:

$$\frac{dx}{d\tau} = \varphi_0 \left(A_0 \left(\frac{m_f}{V_i} \right) (\sigma_{ud} - x_0)(0.1\sigma_{ud} + x_0) \right) + \varphi_1 \left(\frac{d\sigma_u}{d\tau} \right) \quad (2-6)$$

Where

$\frac{dx}{d\tau}$ – Heat release rate, 1/s;

φ_0, φ_1 – Function for description of the completion of combustion;

m_f – Fuel mass;

A_0 – Empirical factor;

x_0 – Fraction of burnt fuel during ignition delay;

σ_{ud} and σ_u – are fuel fractions evaporated during the ignition delay period and up to the current moment, respectively.

➤ Mixing controlled combustion phase

In the mixing controlled combustion period the heat release rate can be determined as;

$$\frac{dx}{d\tau} = \varphi_1 \left(\frac{d\sigma_u}{d\tau} \right) + \varphi_2 \left(A_2 \left(\frac{m_f}{V} \right) (\sigma_u - x)(\lambda - x) \right) \quad (2-7)$$

Where

λ – The air-fuel equivalence ratio;

x – Fraction of fuel burnt.

➤ Late combustion phase

In this phase the heat release rate is:

$$\frac{dx}{d\tau} = \varphi_3 A_3 K_T (1-x)(\xi_a \lambda - x) \quad (2-8)$$

Where

K_T – Evaporation constant;

ξ_a – Efficiency of air used.

In these equations it is assumed that $\varphi_0 = \varphi_1 = \varphi_2 = \varphi$ which is function describing completeness of fuel vapor combustion in the zones.

$$\varphi = 1 - \frac{A_1}{\xi_b \lambda - x} \left(r_V + \sum_{i=1}^{mW} \left(300 r_{Wi} \exp\left(\frac{-16000}{2500 + T_{Wi}} \right) \right) \right) \frac{dx}{d\tau} \quad (2-9)$$

r_V – Relative evaporation rate in the zones of environment and front;

r_{Wi} – Relative evaporation rate in the different zones of WSF.

During the simulation process, the heat transfer in the cylinder is taken into account and heat transfer coefficients for its different zones are calculated using heat transfer coefficients [172]:

- Woschni's formula (original);
- Woschni's formula (modified for HCCI by Assanis);
- Hohenberg's formula;
- Eichelberg's formula;
- Woschni's formula (modified).

e. Modeling of NO_x formation

The emission parameters that are evaluated by this software use some basic equations derived by different researchers. NO formation modeling was described by Kuleshov [173]. Usually, nitric oxide (NO) and nitrogen dioxide (NO₂) are grouped and known as NO_x. Out of these oxides of nitrogen, NO is predominant in diesel engines [8] and hence only NO formation is considered in this simulation work. The simulation model used here for NO_x formation is based on Thermal Zeldovich's Mechanism. Thermal NO is calculated using the chain Zeldovich mechanism and the basic reactions for NO formation are as follows:



The volume concentration of NO in combustion products formed in a current calculation step is obtained from the following equation:

$$\frac{d[NO]}{d\theta} = \frac{2.33310^7 P \exp^{\frac{-38020}{T_z}} [N_2]_e [O]_e \left(1 - \left(\frac{[NO]}{[NO]_e}\right)^2\right)}{RT_Z \left(1 + \frac{2365}{T_Z} \exp^{\frac{3365}{T_z}} \frac{[NO]}{[O_2]_e}\right)} \frac{1}{\omega} \quad (2-13)$$

Where

P – Cylinder pressure, Pa;

T_z – Temperature in a burnt gas zone, K;

R – Ideal gas constant, J/ mole⁻¹. K⁻¹;

ω – Angular velocity, 1/sec.

NO concentration in a cylinder is given by, $r_{NO_c} = r_{NO} r_{bc}$, r_{bc} being the burnt gas fraction. NO concentration in “dry” burnt gas within the cylinder is obtained as follows, $r_{NO_{dry}} = r_{NO} / (1 - r_{H_2O})$ where, r_{H_2O} is a volume fraction of water vapor in a combustion chamber.

Specific NO emission in g/kWh unit is defined as:

$$e_{NO} = \frac{30 r_{NO} M_{bg}}{L_C \eta_M} \quad (2-14)$$

Where

M_{bg} – Mass of burnt gas in a cylinder at the end of combustion, kmol;

L_C – Working cycle work, kJ;

η_M – The mechanical efficiency of the engine;

$[NO]_e$ – Equilibrium concentrations of oxide of nitrogen;

$[N_2]_e$ – Equilibrium concentrations of molecular nitrogen;

$[O_2]_e$ – Equilibrium concentrations of molecular oxygen;

$[O]_e$ – Equilibrium concentrations of atomic oxygen.

f. The soot concentration model

Soot particle forms and oxidize due to chemical reactions occurring through combustion. It has a deep impact on the pollution of the environment the concentration of soot particles is calculated [174].

$$\left(\frac{d[C]}{d\tau}\right)_k = 0.004 \frac{q_c}{V} \frac{dx}{dt} \quad (2-15)$$

q_c –Cycle fuel mass, kg;

V – Current volume of the cylinder;

$\frac{dx}{dt}$ – Heat release rate, J/deg.

The Bosch smoke number (BSN) was obtained from the Hartidge smoke equation given below [175]:

$$Hartidge = 100[1 - 0.9545 \exp(-24226[C])] \quad (2-16)$$

The PM emissions (are obtained from [175]):

$$[PM] = 565 \left[\ln \frac{10}{10 - Bosch} \right]^{1.206} \quad (2-17)$$

g. Basic equations of performance

The main equations of performance are as follows [176,177,178]:

Brake power (BP) – The brake power of an engine is the actual power delivered by the crankshaft and is measured by the means of an electric dynamometer. It is an important factor for calculating the mechanical efficiency of an engine [177].

$$BP = \frac{2\pi NT}{60} \quad (2-18)$$

Where

T – Brake torque, N.m;

N – Speed of the engine, rpm.

Mean effective pressure (MEP) – The mean effective pressure is the hypothetical pressure that is assumed to be acting on the piston during the power stroke.

Indicated power (IP) – The indicated power of an engine is the actual power developed within the cylinder during the combustion process. It is always greater than the brake power. The sum of brake power and friction power gives the indicated power. The indicated power of a single-cylinder engine is determined by using the following formulae,

$$IP = \frac{IMEP S A N}{60} \quad (2-19)$$

Where,

IMEP – Indicated mean effective pressure, N/m² or Pa;

S – Length of stroke, m;

A – Area of the cylinder, m²;

N – Number of working strokes per minute.

Friction power (FP) – Friction power is the power that is required to overcome the loss of power due to friction in an engine. Friction power increases in relation to the engine speed and it is calculated by subtracting the brake power from the indicated power.

$$FP = IP - BP \quad (2-20)$$

Specific fuel consumption (SFC) – It is defined as the amount of fuel consumed per unit of power developed per hour.

Brake specific fuel consumption (BSFC) – It is a measure of the fuel efficiency of an engine that burns fuel and develops power. It is obtained by using the formula,

$$BSFC = \frac{\dot{m}_f}{BP} \quad (2-21)$$

Where,

\dot{m}_f – Mass flow of fuel in the engine, g/s;

BP – The power produced, Watts.

Indicated specific fuel consumption (ISFC) – It is the ratio of the amount of fuel used by an engine to the indicated power of an engine. It is obtained by using the formula,

$$ISFC = \frac{m_f}{IP} \quad (2-22)$$

Brake thermal efficiency (BTE) – It is used to evaluate how well an engine converts the heat energy produced from the combustion of fuel to useful mechanical energy. It is obtained by using the formula,

$$BTE = BP \frac{3600}{m_f LHV} \quad (2-23)$$

Mechanical efficiency (ME) – It is a relationship between the power delivered and the power that would be available. It is used to evaluate the effectiveness of the engine in converting the energy produced by the combustion of fuel into useful work.

$$ME = \frac{BP}{IP} \quad (2-24)$$

Exhaust gas temperature– It is the temperature at which the exhaust gas comes out from the exhaust system of the engine.

For engines where a fuel is burned there are two types of thermal efficiency: indicated thermal efficiency and brake thermal efficiency:

Indicated thermal efficiency (ITE) – The ratio between the indicated power output of an engine and the rate of supply of energy in form of combustion of fuel. It is obtained by using the formula,

$$ITE = IP \frac{3600}{m_f LHV} \quad (2-25)$$

Brake thermal efficiency (BTE) - It is defined as the brake power of a heat engine as a function of the thermal input from the fuel. It is used to evaluate how well an engine converts the heat from fuel to mechanical energy.

$$\eta_b = \frac{BP}{m_f LHV} 100\% \quad (2-26)$$

m_f – Fuel flow, kg/s.

2.2.2. Homogeneous combustion

2.2.2.1. CHEMKIN-Pro simulation software

CHEMKIN is a set of calculation programs that allow the resolution of problems relating to several disciplines such as chemistry, energy... etc. In this case, we are interested in studying the single-zone model of combustion HCCI. The main objective is to present a general description of the mathematical simulation models used in the analysis of flow and combustion in HCCI engines. The HCCI single-zone combustion model allows detailed modeling of chemical kinetics for single fuels by assuming that the gas distribution in the combustion chamber is homogeneous, with uniform temperature, pressure and gas composition. A single-zone model can adequately predict auto-ignition. The model uses the library of CHEMKIN-Pro software for determining chemical production rates.

2.2.2.2. CHEMKIN Set Up

The package used for the combustion model and chemical kinetics of the HCCI combustion is called CHEMKIN. This software is one of the most known packages for solving complex chemical kinetics problems and allows the user to calculate species concentrations, heat release rate, temperature and pressure history of the combustion [179].

CHEMKIN is a set of software tools, written in FORTRAN, to solve complex problems in gas-phase chemical kinetics. Thermochemical data for each species in the chemical kinetic mechanism is used by CHEMKIN to calculate thermodynamic properties, heat transfer properties and reaction equilibrium constants. Its structure is made up of four parts: the interpreter, the thermodynamic and transfer databases, the link files and the library of gas-phase kinetic calculation subroutines. A simulation calculation corresponds to two very distinct steps: the interpretation of the thermokinetic data by the chemical interpreter and the resolution of the problem by the code (figure 2. 20).

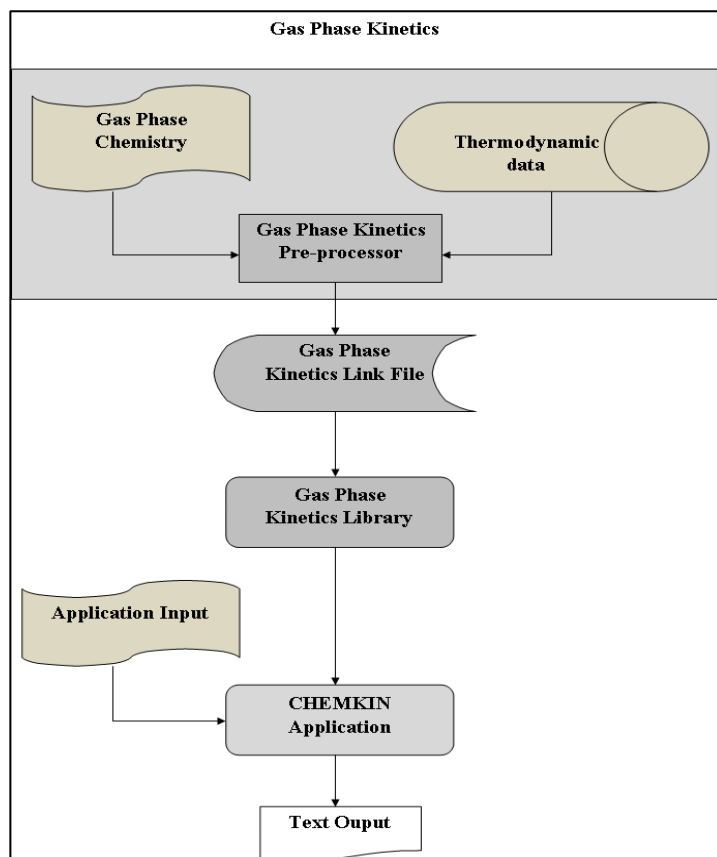


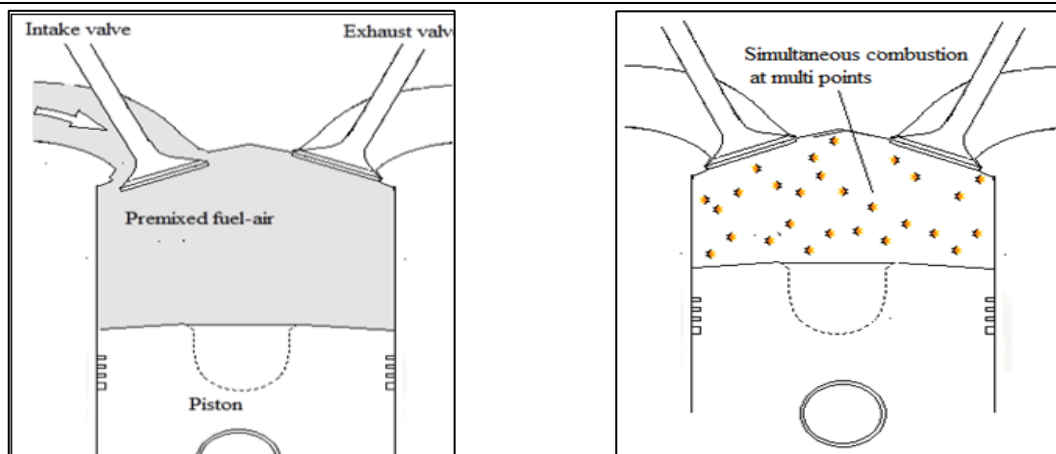
Figure 2. 20- Structure of CHEMKIN.

The next stage of the modeling process is where a specific reactor is selected to cope with the demands of the desired simulation.

The CHEMKIN input for the simulation was based on the HCCI model that the package from Reaction Design, already includes.

2.2.2.3. Model description

Figure 2. 21 shows typical HCCI combustion where the fuel-air charge is fully premixed in order to make it sufficiently homogeneous during the inlet phase the HCCI engine involves a type of internal combustion in which the mixture of fuel takes place in the most homogeneous way possible (as in gasoline engines), and is compressed strongly enough to reach the point of self-ignition where it ignites automatically. In phase combustion, the mixture starts rapidly and simultaneously at multi-points whenever heat and pressure are high enough (figure 2. 21b). In this study, this typical combustion HCCI is applied to a direct injection diesel F8L413 engine in order to reduce emissions and protect the environment.



(a) Premixed fuel

(b) Homogeneous charge compression ignition

Figure 2. 21- Typical HCCI with premixed fuel-air for F8L413 engine.

2.2.2.4. Charge compression ignition (HCCI) model (CHEMKIN-Pro Set-Up)

In the second part of the work (Section 2.2.2), a simulation in the "IC Engine" module from ANSYS CHEMKIN-Pro software [180] was carried out. ANSYS CHEMKIN-Pro uses to perform thermodynamic and chemical kinetics analysis [181]. In this part, the equivalence ratio (ϕ) varied from 0.3 to 0.6 and the intake temperature of the mixture (T_{IVC}) is fixed at 450 K, 500 K and 550 K. The engine parameters are specified by the user directly in the CHEMKIN Interface for the internal combustion HCCI engine reactor model [181]. Heywood [8] provides equations that describe the volume (to first order) as a function of time, based on engine parameters, and the specifications of the single-cylinder HCCI engine are illustrated in table 2. 2. The calculation starts with an intake valve close (IVC) value of 52 deg aBDC and ended at an exhaust valve open (EVO) value of 67 deg bBDC. The single-zone model allows relatively short computational. Methane is the main component of natural gas thus; the mechanism we have selected is the GRI-Mech 3.0 (325 reactions, 53 species) to describe the combustion process [182]. The heat transfer correlation has as parameters: $a = 0.035$, $m = 0.7$, $c = 0.0$; the temperature of the wall was taken equal to 400 K; the Woschni correlation of average cylinder gas velocity has as parameters: $C_{11} = 2.28$, $C_{12} = 0.308$, $C_2 = 3.24 \times 10^{-3}$ and finally the swirl speed ratio was taken equal to 0.0.

The zero-dimensional single-zone HCCI thermodynamic simulation model used in this part is based on the following assumptions:

- Whole combustion chamber is considered a volume control;
- Only the closed cycle from IVC to EVO was taken into account in the model;

- Temperature and pressure have a uniform distribution;
- The heat exchange is done with the walls and is taken into account by the modified Woschni model [183];
- The fuel is premixed with air before entering the cylinder and is compressed during the compression stroke;
- The mixture ignites automatically by auto-ignition;
- Mixing in the cylinder was considered an ideal gas.

2.2.2.5. Structure of the calculation program (CHEMKIN-Pro)

- ↳ **Choice of reactor:** in our case, it is an engine using a single-zone model (IC HCCI Engine).

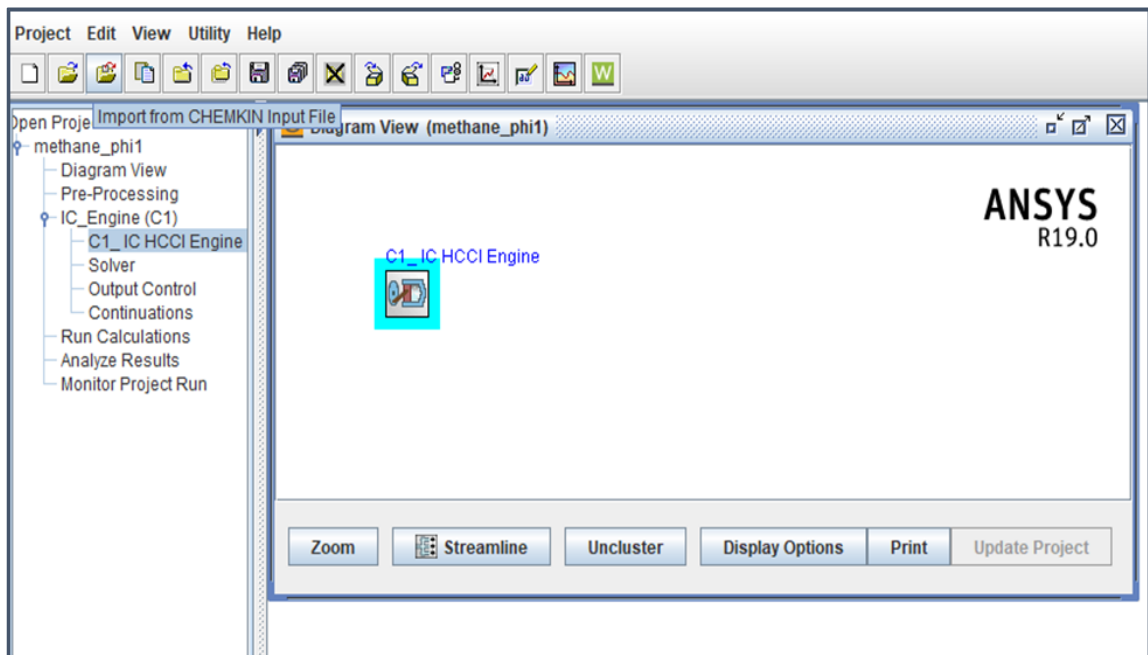


Figure 2. 22- Choice of the reactor.

- ↳ **Choice of the reaction mechanism with the thermodynamic and transport data file:**

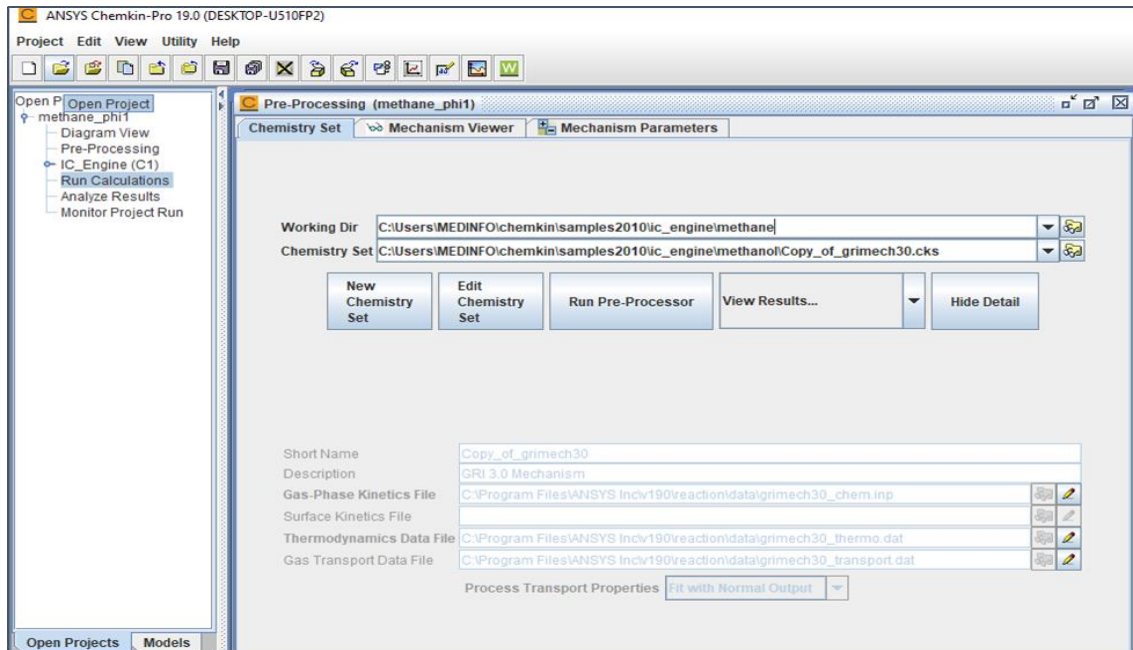


Figure 2. 23- Chemistry set of Gas-Phase Kinetics file and Thermodynamics date file.

↪ Engine parameters:

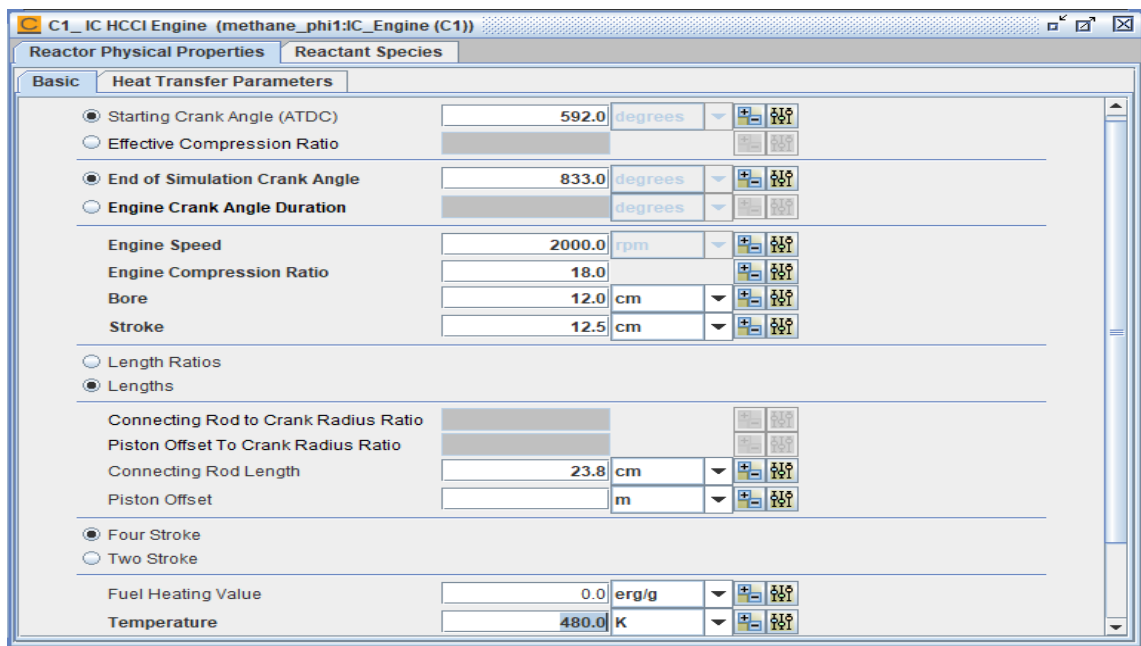


Figure 2. 24- Engine basic and heat transfer parameters.

↪ Heat exchanger:

There are two different approaches to defining the heat loss through a cylinder wall. One approach assumes the cylinder is adiabatic and the other considers heat loss through the cylinder wall. Figure 2. 25 shows reactor physical property for the Woschni heat loss model.

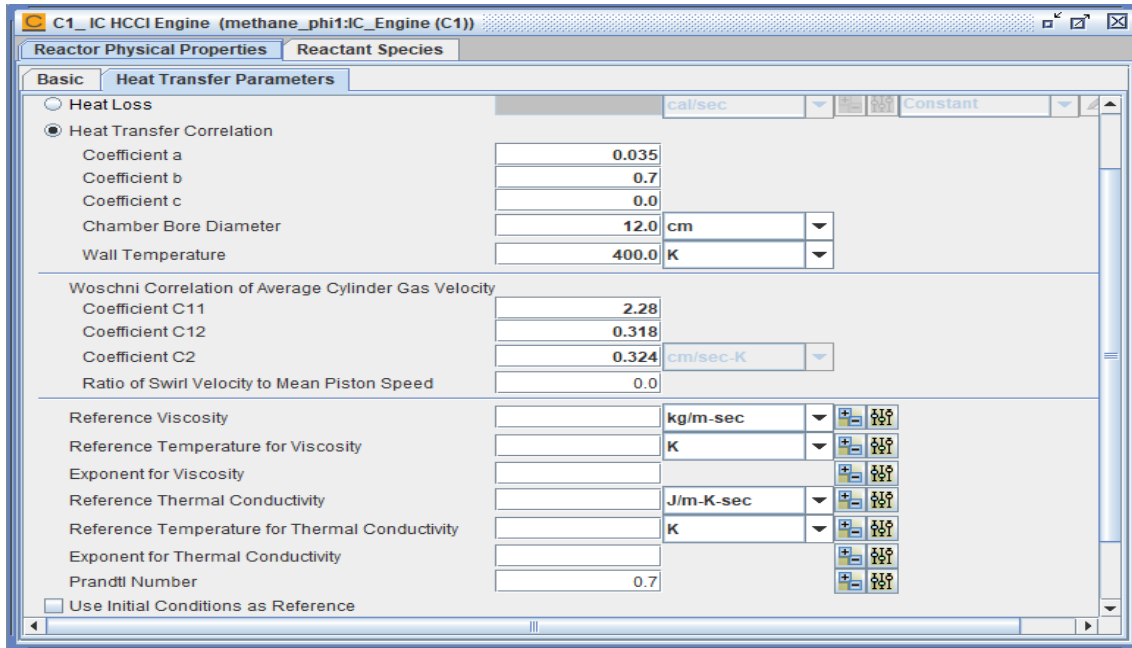


Figure 2. 25- Reactor Physical Property for Woschni heat loss model.

Reactant species

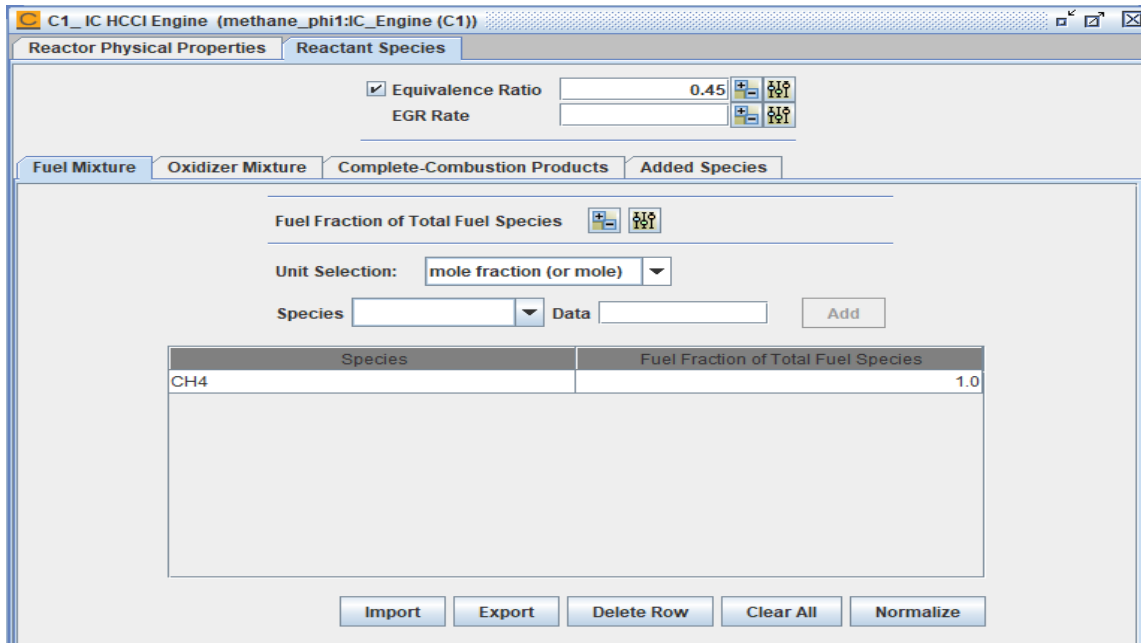
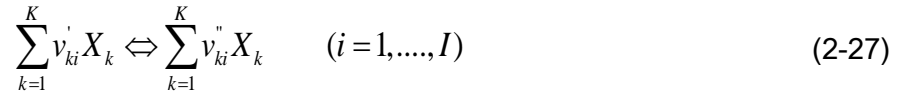


Figure 2. 26- Reactant species.

2.2.2.6. Chemical kinetics model

The CHEMKIN-Pro software is designed for modeling different chemically reacting flow configurations [184]. Therefore, CHEMKIN-Pro was used as the calculation solver.

The I reversible (or irreversible) surface reactions involve K chemical species and can be represented in the general form [185]:



$$\dot{\omega}_k = \sum_{i=1}^I (v_{ki}'' - v_{ki}') q_i \quad (k = 1, \dots, K) \quad (2-28)$$

$$q_i = k_{fi} \prod_{k=1}^K [X_k]^{v_{ki}'} - k_{ri} \prod_{k=1}^K [X_k]^{v_{ki}''} \quad (2-29)$$

Where

K – Number of chemical species, dimensionless;

X_k – Molar concentration of the k_{th} species, mole/cm³;

$\dot{\omega}_k$ – The chemical production rate of the k_{th} species due to gas-phase reactions, mole/cm³/sec;

q_i – Rate-of-progress variable, mole/cm³/sec;

v_{ki}' and v_{ki}'' represent the stoichiometric coefficients of the k_{th} reactant species and product species in the i_{th} reaction, respectively.

The forward k_{fi} and reverse rate k_{ri} constants and for the I reactions are expressed by:

$$k_{fi} = A_i T^{\beta_i} \exp\left(\frac{-E_i}{R_c T}\right) \quad (2-30)$$

$$k_{ri} = \frac{k_{fi}}{K_{ci}} \quad (2-31)$$

Where

A_i – Pre-exponential factor;

β_i – Temperature exponent;

E_i – Activation energy for the reaction;

R_c – Universal gas constant;

K_{ci} –Equilibrium constant in concentration units for the i_{th} reaction.

2.2.2.7. Governing equations

The governing equations for temperature and species as follows [186]:

- Internal Energy/Temperature:

$$\rho C_v \frac{dT}{dt} = - \sum_{k=1}^{kgas} \dot{\omega}_k W_k u_k - \frac{P}{V} \frac{dV}{dt} - \frac{h_g (T - T_w) A_w}{V} \quad (2-32)$$

- Species conservation equation:

$$\rho \frac{dY_k}{dt} = \dot{\omega}_k W_k \quad (2-33)$$

With

Y_k – Mass fraction of the k_{th} species, dimensionless;

C_v – Constant-volume specific heat capacity of the mixture, J/kg/ K;

T – Temperature, K;

ρ – Mass density of a gas mixture, kg/m³;

u_k – Specific internal energy of the k_{th} species, J/kg;

W_k – Molecular weight of the k_{th} species, kg/mole;

h_g – Heat transfer coefficient, W/m²/K;

A_w – Surface area, m².

2.2.2.8. Heat-transfer options for the IC-HCCI engine model

a. Woschni correlation for engine heat transfer

Heat transfer data can be correlated with the thermal conditions of the engine using two dimensionless parameters: the Nusselt number (Nu) and the Reynolds number (Re).

Several correlations used to calculate the thermal transfer coefficient in engines have been published in the literature. These include the Woschni, Annand and Hohenberg correlations, which are widely used to model engine heat transfers.

Woschni arrives at equation (2-34), which he will later use to determine the heat transfer coefficients for the various parts of the piston in a diesel engine [172].

$$h_g = 3.26 B^{-0.2} P^{0.8} T^{-0.55} w^{0.8} \quad (2-34)$$

And

$$w = \left[C_1 \bar{U}_p + C_2 \frac{V_d T_r}{P_r V_r} (P - P_m) \right] \quad (2-35)$$

Where

h_g – Heat transfer coefficient, W.m⁻².K⁻¹;

B – Cylinder bore, m;

w – Gas velocity;

\bar{U}_p – Mean piston speed (m/s), and is given by $2NS/60$;

V_d – Swept volume, m³;

P_m – The instantaneous motored cylinder pressure. It is given by the following equation:

$$P_m = P_r \left(\frac{V_r}{V} \right)^\gamma \quad (2-36)$$

Where

γ – Specific heat ratio (equal to 1.3 for a direct injection);

P – Instantaneous cylinder pressure, kPa;

P_r, V_r and T_r – Pressure, volume and temperature of the gas at a reference point, respectively.

Constants C_1 and C_2 given in table 2. 3 are determined using empirical research.

Table 2. 3-Coefficients C_1 and C_2 for Woschni correlation [172]

Phase	C_1 (-)	C_2 (m.s ⁻¹ . K ⁻¹)
Intake-exhaust	6.18	0
Compression	2.28	0
Combustion- expansion	2.28	3.24×10^{-3}

b. Correlation Woschni modified

Woschni correlation, modified for the HCCI engine, has been suggested by Chang et al. [183]. The correlation can be used to calculate a new heat transfer coefficient as follows:

$$h_{g,n} = 3.4 B^{-0.2} P^{0.8} T^{-0.73} w_{tuned}^{0.8} \quad (2-37)$$

And

$$w_{tuned} = \left[C_1 \bar{U}_p + \frac{C_2 V_d T_r}{6 P_r V_r} P - P_m \right] \quad (2-38)$$

With

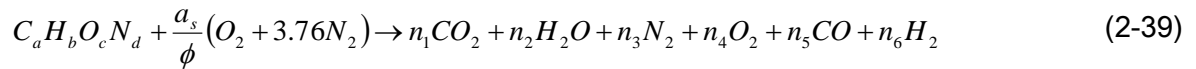
$$C_1 = C_{11} + C_{12} \frac{v_{swirl}}{\bar{U}_p} ;$$

v_{swirl} – Swirl velocity;

C_{11} and C_{12} – Constants.

2.2.2.9. Combustion reactions

At low temperatures ($T < 1000$ K, such as in the product gases in the exhaust stream) and carbon to oxygen ratios less than one, the overall combustion reaction for any equivalence ratio can be written as [187].



For lean ($\phi < 1$) combustion products at low temperature, we will assume no product CO and H_2 , i.e., $n_5 = n_6 = 0$. In this case, atomic species balance equations are sufficient to determine the product composition, since there are four equations and four unknowns [187].

Table 2. 4-Low-temperature ($T < 1000$ K) combustion products [187]

Species	The number of moles- n_i	$\phi \leq 1$	$\phi > 1$
CO ₂	n_1	a	n_1
H ₂ O	n_2	$b/2$	$b/2 - d_1 + n_5$
N ₂	n_3	$d/2 + 3.76 a_s / \phi$	$d/2 + 3.76 a_s / \phi$
O ₂	n_4	$a_s (1/\phi - 1)$	0
CO	n_5	0	n_5
H ₂	n_6	0	$d_1 - n_5$

Where the a_1 , b_1 , and c_1 coefficients are given by:

$$a_1 = 1 - K$$

$$b_1 = \frac{b}{2} + Ka - d_1(1 - K)$$

$$c_1 = -a d_1 K$$

$$d_1 = 2a_s \left(1 - \frac{1}{\phi} \right)$$

With

$$a_{st} = x + \frac{y}{4};$$

ϕ – Equivalence ratio.

2.2.3. Thermodynamic analysis

This part provided a mathematical model for theoretical predictions of the combustion characteristics of a direct injection diesel engine.

2.2.3.1. Governing equations

The zero-dimensional model is based on the first law of thermodynamics was elaborated to predict diesel engine performance.

- The 1st law of thermodynamics

The thermodynamic calculation of the combustion process is done differently depending on the type of engine and the method of creating the air-fuel mixture. However, all calculations are made according to the first law of thermodynamics and the ideal gas equation.

Therefore, for the time step dt , the first law of thermodynamics for a closed volume, connecting heat Q , mechanical work W , and absolute internal energy U , becomes

$$dU = dQ_H - dQ_W - PdV \quad (2-40)$$

Where

dU – Internal energy of gases, kJ/kg fuel;

dQ_H – Heat released by combustion, kJ/kg fuel;

dQ_W – Heat dissipated by cooling, kJ/kg fuel;

PdV – The work of the action of the piston, kJ/kg fuel.

- Ideal gas equation

$$P = \frac{R_m M T}{V} \quad (2-41)$$

The amount of heat released is found with the following expression [188]

$$dQ_H = \xi_d LHV g_c dx \quad (2-42)$$

Where

- ξ_d – Coefficient considering dissociation of combustion products;
 g_c – The amount of fuel in one cycle, kg;
 dx – The mass fraction burned calculated from Wiebe law.

A function form often used to represent the mass fraction burned versus crank angle curve is the Wiebe function:

$$x_b(\theta) = 1 - \exp\left[-6.908\left(\frac{\theta}{t_z}\right)^{m+1}\right] \quad (2-43)$$

Where $x_b(\theta)$ is the fraction of the heat release, θ refers to crank angle and t_z is the duration of heat release.

If the valves are closed according to the above equations, the average temperature in the cylinder is calculated as follows.

$$dT = \frac{dU}{(mC_v)_{t_0}^t M} \quad (2-44)$$

Where

- M – The amount of gas, kmol / kg fuel;
 $(mC_v)_{t_0}^t$ – Molar mean specific heat, kJ/kmol°C.

$$M = M_a [1 + (\mu - 1)] \quad (2-45)$$

Therefore, it is possible to calculate the parameter $(dQ_w + PdV)$ in Equation 2. 40 (total heat of compression and expansion processes in the heat transfer medium to the cooling system) with a small error for the diesel engine to be modeled mathematically with Equation (2-46), such as the heat of polytropic processes.

$$dQ_w + PdV = P_j V_j \frac{\left[1 - \left(\frac{V_j}{V_{j+1}}\right)^{n-1}\right]}{n-1} \quad (2-46)$$

In the formula; n-is the polytropic exponent in compression ($n_1=1.36$) and expansion ($n_2=1.26$).

Table 2. 5- Engine parameters

Diesel engine	ΔT	η_v	$Pa(MPa)$	λ	ξ_d
Parameters	10...20	0.75...0.92	(0.80÷1.05) P_0	1.4...2.2	0.8

Only air (in diesel engines) as work gases in cylinders in suction and compression processes; combustion product compositions are used in combustion, expansion, and exhaust processes.

- **Air quantity**

The theoretical amount of air required for the complete combustion of 1kg of fuel is calculated as in Equation (2-47) and Equation (2-48) in terms of volume and mass respectively.

$$L_0 = \frac{1}{0.208} \left(\frac{C}{12} + \frac{H}{4} - \frac{O}{32} \right) \quad [Kmoles/kgfuel] \quad (2-47)$$

L_0 – is the number of moles of air required for stoichiometric combustion of 1 kg of fuel.

C, H, O – is the fuel composition percent by mass of C, H₂, and O₂.

$$l_0 = \frac{1}{0.23} \left(8 \frac{C}{3} + 8H - O \right) \quad (2-48)$$

The molar mass of air:

$$\mu_a = \frac{l_0}{L_0} \quad (2-49)$$

The amount of fresh air taken into the cylinder; $L = L_0 \lambda$

$$l = l_0 \lambda \quad (2-50)$$

The coefficient of variation theoretical molar:

$$\mu_0 = \frac{M_2}{M_1} \quad (2-51)$$

$$M_1 = \frac{1}{m_y} + L \quad (2-52)$$

(m_y – The molar mass of fuel. For diesel (n-Hexadecane) $m_y = 226.43$ kg/kmol)

$$\mu_0 = 1 + \frac{\frac{H}{4} + \frac{O}{32} - \frac{1}{m_y}}{\lambda L_0 + \frac{1}{m_y}} \quad (2-53)$$

$$\mu = \frac{\mu_0 + \gamma_r}{1 + \gamma_r} \quad (2-54)$$

With V the instantaneous cylinder volume given by:

In-cylinder volume at any crank angle θ is calculated using the following equation:

$$V(\theta) = \left[1 + \frac{1}{2}(CR - 1) \left(\left(\frac{1}{\lambda_s} + 1 - \cos(\theta) \right) - \sqrt{\left(\left(\frac{1}{\lambda_s} \right)^2 - \sin^2(\theta) \right)} \right) \right] V \quad (2-55)$$

$$V_s = \frac{\pi}{4} B^2 S \quad (2-56)$$

$$V_c = \frac{V_s}{(CR - 1)} \quad (2-57)$$

Where

V_s – Swept volume;

V_c – Clearance volume;

$\lambda_s = \frac{r}{l}$ – Where l – Connecting rod length and r – Crank radius.

- Ignition delay model

A number of research studies have been carried out to predict ignition delay (the time between the start of the fuel injection and the start of combustion) in a diesel engine [8]. Here, we have used the empirical formula (equation (2-58)) provided by Hardenberg et al. [8] to predict the ignition delay of our engine. This ignition time τ_{id} is calculated in crank angle degrees (deg). The ignition delay is dependent on the fuel properties along with the mixture pressure, temperature, ..., etc.

During this delay both physical and chemical processes take place, preparing the fuel for combustion. The physical processes include:

- Atomization of the liquid fuel jet.
- Vaporization of the fuel droplets.
- Mixing the fuel vapor with the surrounding air.

$$\tau_{id}(\text{deg}) = \left(0.36 + 0.22\bar{U}_P\right) \exp \left[E_A \left(\frac{1}{RT} - \frac{1}{17190} \right) \left(\frac{21.2}{P-12.4} \right)^{0.63} \right] \quad (2-58)$$

Where

P and T are pressure and temperature of the gas mixture, respectively at the time of fuel injection;

R – Is the universal gas constant (8.314 J. mol⁻¹. K⁻¹).

The energy is calculated using the equation:

$$E_A = \frac{618840}{CN + 25} \quad (2-59)$$

Ignition delay τ_{id} (ms) is obtained using the following equation:

$$\tau_{id}(ms) = \frac{\tau_{id}(\text{deg})}{0.006N} \quad (2-60)$$

- Model algorithm

All these steps are represented in the following flowchart (see figure 2. 27). The main program was developed in MATLAB language.

A MATLAB-based calculation program has been developed to determine the evolution of various parameters such as pressure, temperature and ignition delay period. The MATLAB code involved in this effort can accept basic input parameters such as bore, stroke, compression ratio, boundary conditions, rpm, air/fuel equivalence ratio and volumetric efficiency; and the output parameters including in-cylinder pressure, in-cylinder temperature and mass fraction burned using the Wiebe function.

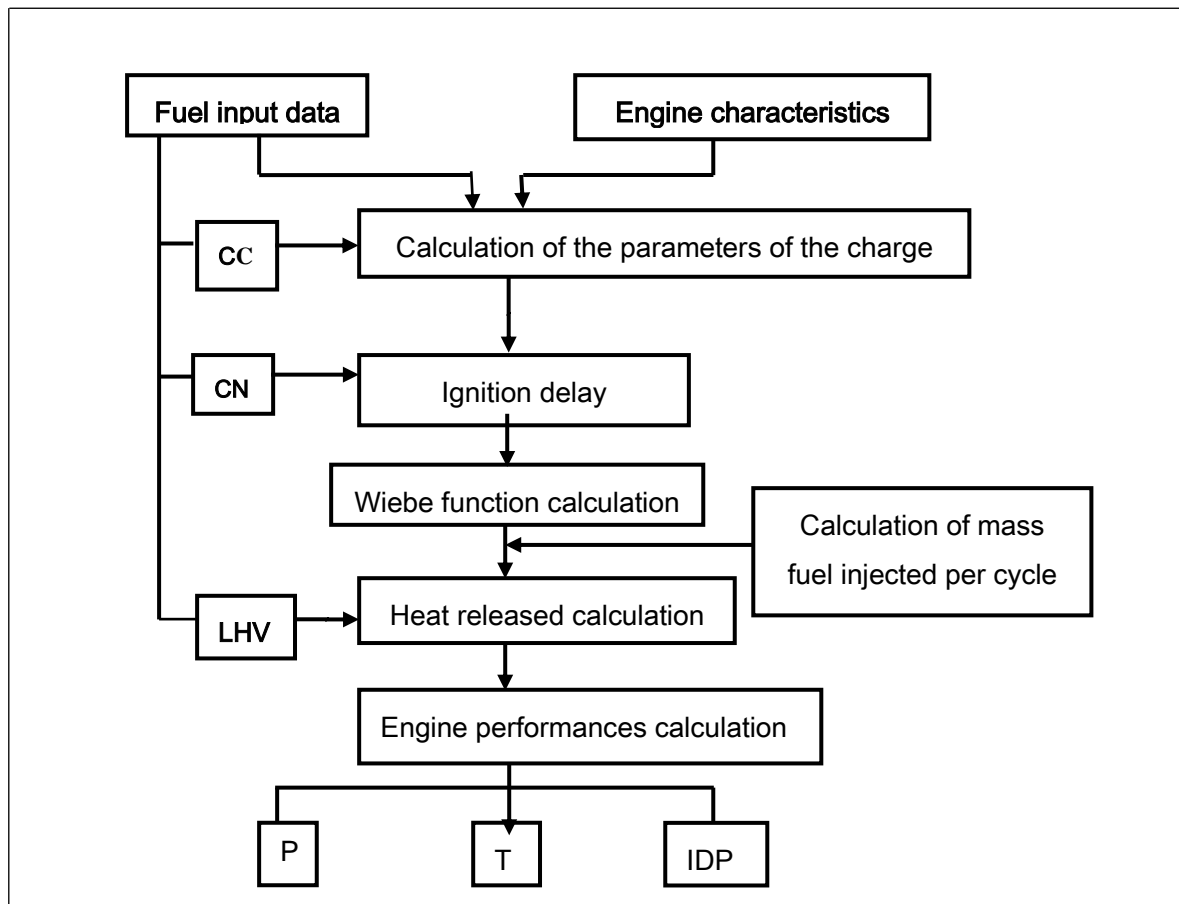


Figure 2. 27- Model algorithm; CN—Cetane number; CC—Chemical composition; P—Pressure; T—Temperature; LHV—Lower heating value; IDP— Ignition delay period.

2.3. CONCLUSION

Although HCCI proves to have good characteristics regarding emissions levels and efficiency, there are some drawbacks to using this concept. There is the inability to control the initiation and the rate of combustion over the required speed and load range of the engine, and due to very rapid energy release during combustion, HCCI is restricted to very lean mixtures, resulting in low power density. Also, the formation of carbon monoxide (CO) and unburned hydrocarbons (UHC) tend to be rather high. These factors, presently, are limiting the commercialization of the HCCI concept, and many of these issues are associated with the fact that HCCI combustion is mainly chemically controlled.

CHAPTER 3- RESULTS AND DISCUSSION

3.1. INTRODUCTION

The main interest of this study is the comparison between three different diesel fuels. The tests are performed on thermodynamic software: "Diesel-RK" and are intended for calculation and optimization of exhaust products. On the other hand, this study investigated the mechanisms of auto-ignition reactivity under operation parameters fueled with natural gas using CHEMKIN-Pro software. Therefore, it is important to understand how these parameters (ϕ , T_{IVC} , P_{IVC} , CR) influence the auto-ignition process of a homogeneous charge compression ignition (HCCI) engine under IC engine conditions on the one hand and the other hand, the amount of gas due to the EGR introduced into the simulation by CHEMKIN consists of CO₂, H₂O, N₂ and O₂. Its quantity varied from 0% to 60%.

Mixture air-fuel enters the cylinder at an intake charge temperature (T_{IVC}) and intake charge pressure (P_{IVC}). In the compression stroke, the volume of the chamber reduces because the piston moves from BDC to TDC. Furthermore, the mixture is compressed, so the pressure and temperature of the fuel-air mixture gradually increase, leading to ignition. The effect of ϕ , T_{IVC} , P_{IVC} , CR and EGR ratios on the performance characteristics of an internal combustion engine (ICE) was carried out.

3.2. SIMULATION RESULTS (DIESEL-RK SOFTWARE)

3.2.1. Combustion parameters effect

3.2.1.1. Cylinder pressure evolution

Cylinder pressure curves for various crank angles for different fuels (Hexadecane, Heavy fuel and Diesel No. 2) are shown in figure 3. 1a. The cylinder pressure gradually raises from the start of the compression stroke. At the end of the compression stroke, fuel is injected and this results in a slight decrease in temperature and pressure of the cylinder. The fuel vaporizes into droplets and combustion starts and hence a large increase in pressure is observed [189]. The figure displays that increasing the lower heating value of fuel in the engine increased the cylinder peak pressure. The highest cylinder peak pressure (CPP) was obtained to baseline fuel while the lowest values were recorded with heavy fuel. It was observed that the

graph cylinder pressure at Heavy diesel fuel lies close to Diesel No.2 fuel. At a crank angle of 724 deg, the value of Heavy diesel fuel was 90.43 bars while that of Diesel No.2 was 91.9 bars. The CPP of Heavy fuel is lower than the baseline diesel fuel. The lower heating value is the predominant factor in influencing the pressure rise of the cylinder.

3.2.1.2. Cylinder temperature evolution

The temperature inside an engine has a great impact on the emissions and knocking characteristics of an engine. The distribution of cylinder temperature for different test fuels is shown in figure 3. 1b. As we can see from the graph, the temperature of the cylinder slowly increases as a result of the compression stroke of the engine. There was a slight change in the temperature of the engine cylinder during the injection of fuel, as some of the heat is being absorbed for vaporization of the fuel droplets at the end of the compression stroke. The temperature rose to a peak during the combustion of fuel as a large amount of heat is being released. Then the temperature slowly declines in the expansion stroke and throughout the exhaust phase [189].

3.2.1.3. Ignition delay

The ignition delay time is related to the cetane number of the fuel. The higher the cetane number, the shorter is the ignition delay or vice versa [190,191]. The ignition delay in a direct injection diesel engine is of great interest due to its direct impact on the heat release as well as its indirect effect on the formation of pollutants and engine noise. The ignition delay period is composed of a physical delay, including atomization, vaporization and mixing, coupled with a chemical delay.

3.2.2. Performance parameters

3.2.2.1. Indicated thermal efficiency (ITE)

The indicated thermal efficiency (ITE) is the ratio of the indicated work per cycle with the amount of fuel energy supplied per cycle [192]. Table 3. 1 shows the performance parameter for the three different fuels tested. It can be seen that the Heavy diesel fuel has a higher indicated thermal efficiency (ITE) than those of baseline fuel and Diesel No. 2. The ITE was obtained at 46.26% for Heavy diesel fuel, 43.95% for baseline fuel and 44.46% for Diesel No.2.

3.2.2.2. Brake torque

Figure 3. 2 shows the variation in brake torque at full-load for Heavy diesel fuel. It can be seen clearly that, when the engine speed increases the brake torque will increase continuously and up to 1400 rpm. The brake torque begins to decrease from a speed higher than 1400 rpm.

3.2.2.3. Brake mean effective pressure (BMEP)

In our numerical study, the diagram of figure 3. 3 shows the relation between engine speed and brake mean effective pressure. This graph shows that the BMEP gradually decreases as the engine speed increases.

3.2.3. Emission parameters

3.2.3.1. NO_x emissions

Various factors impact NO_x emissions such as combustion chamber pressure, temperature, oxygen contents, homogeneity of the mixture and density of the mixture. NO_x emissions are also affected by stoichiometry, flame temperatures, ignition delay, chain length and fatty acids of fuel, heat removal rate, premixed combustion time, cetane number, injection timing and fuel properties [193-195]. According to calculations conducted by Diesel-RK software, figure 3. 1d shows the existence of variation in NO_x emissions from the three different fuels tested. The NO_x emission values are higher for baseline fuel (Hexadecane diesel fuel) compared to Diesel No.2 and Heavy diesel fuels. Heavy fuel delivers a significant dropping in NO_x emissions due to less calorific value and combustion temperature. There is 50.53% and 5.9% lesser in NO_x emission for Heavy diesel fuel and Diesel No.2 compared to baseline fuel. The temperature rise during combustion is maximum with baseline fuel, which enhances the NO_x formation. However, in some reports, it was found that the high cetane number of the Hexadecane resulted in a lower ignition delay period. Moreover, the oxygen content in Diesel No. 2 is responsible for higher NO_x emissions.

3.2.3.2. Specific carbon dioxide emissions

It is well-known that complete combustion in the combustion chamber helps to increase CO₂ emissions. Specific CO₂ emissions can be defined as the amount of CO₂ formed during the fuel combustion to produce unit power. Average CO₂ emission rates were increased by 4% and 4.6% for Diesel No. 2 and Heavy fuels, respectively, compared to base fuel (table 3. 1). The

CO₂ emissions from the engine show the level of combustion rate. Also, the increase in CO₂ emissions shows the complete combustion in the combustion chamber [176,189].

3.2.3.3. Specific particulate matter (PM) emissions

From the present numerical investigation, it can be concluded that from table 3. 1 the highest PM emissions are observed for Diesel No.2, followed by Heavy fuel and lastly by Hexadecane fuel. Generally, smoke and particulate matter (PM) formations are interrelated. Particulate matters (PM) are formed due to improper combustion and burning of lubricating oil. Smoke is formed in the fuel-rich zone at high temperature and high pressure due to incomplete combustion.

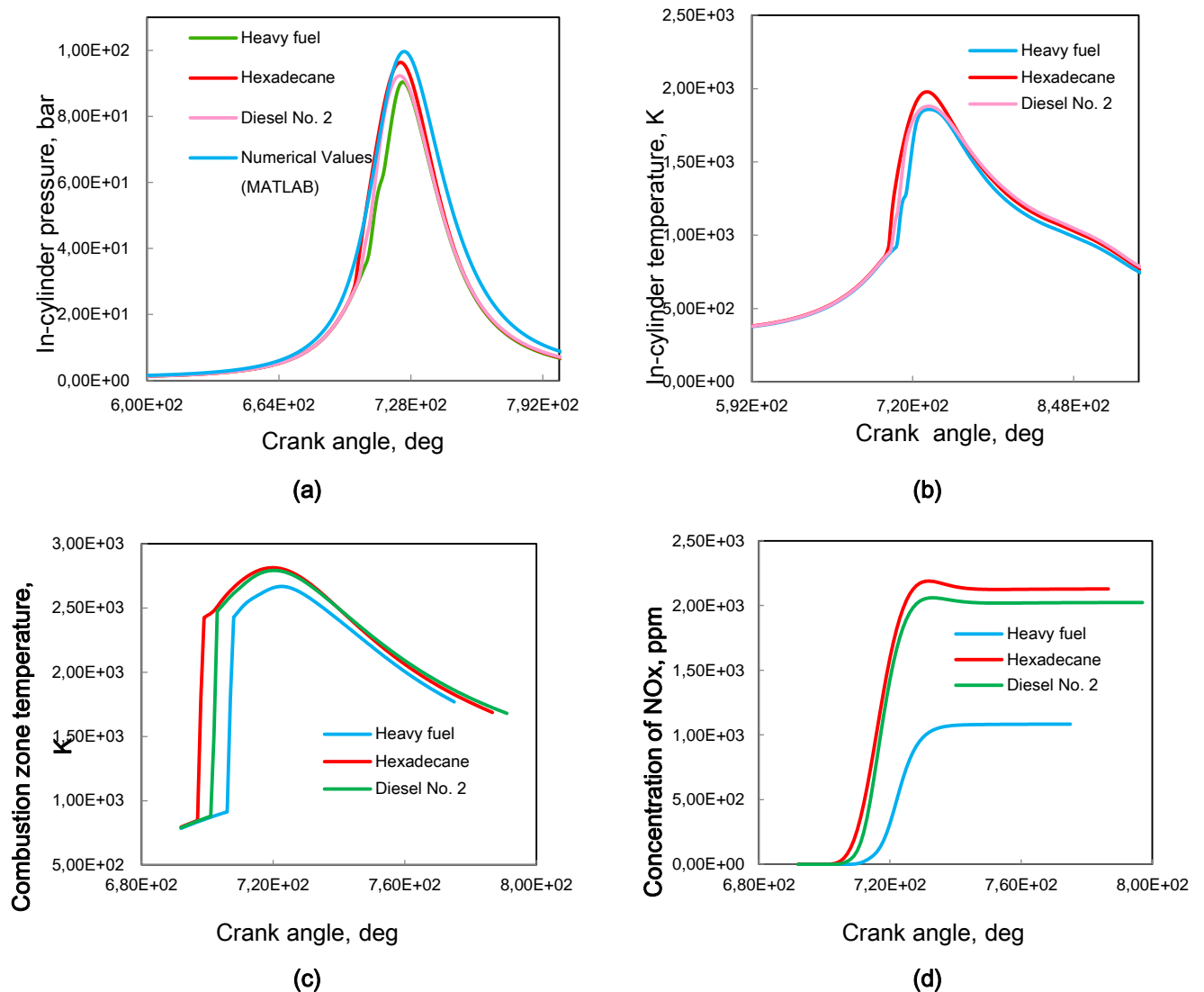


Figure 3. 1- Variation of (a) cylinder pressure,(b) cylinder temperature, (c) combustion zone temperature and (d) concentration NO with crank angle according to the fuel type (engine speed=1600 rpm).

Table 3. 1- Summary of relative change in engine parameters to the base fuel parameters

Performance parameters	At 1600 rpm		
	Fuels		
	Baseline fuel-Hexadecane	Diesel No. 2	Heavy fuel
P_eng, kW	95.618	98.718	97.992
IMEP, bar	7.2188	7.4021	7.3373
SFC, kg/kWh	0.22099	0.22437	0.22544
Brake Torque, N.m	570.72	589.22	584.89
Indicated Efficiency	0.43958	0.44467	0.46260
IDP, deg	8.4361	15.326	21.876
T_max, K	1958.7	1879.8	1859.4
P_max, bar	95.311	92.289	90.636
BSN	2.1450	2.5515	2.2703
Hartridge	21.617	27.136	23.132
S-CO ₂ , g/kWh (CO ₂)	694.62	722.95	726.43
S-PM, g/kWh (PM)	0.54300	0.67054	0.57757

IMEP– Indicated Mean Effective Pressure; SFC– Specific Fuel Consumption; BSN– Bosch Smoke Number; S-CO₂– Specific Carbon dioxide emission; S-PM– Specific Particulate Matter emission; IDP– Ignition Delay Period; P_eng– Piston Engine Power.

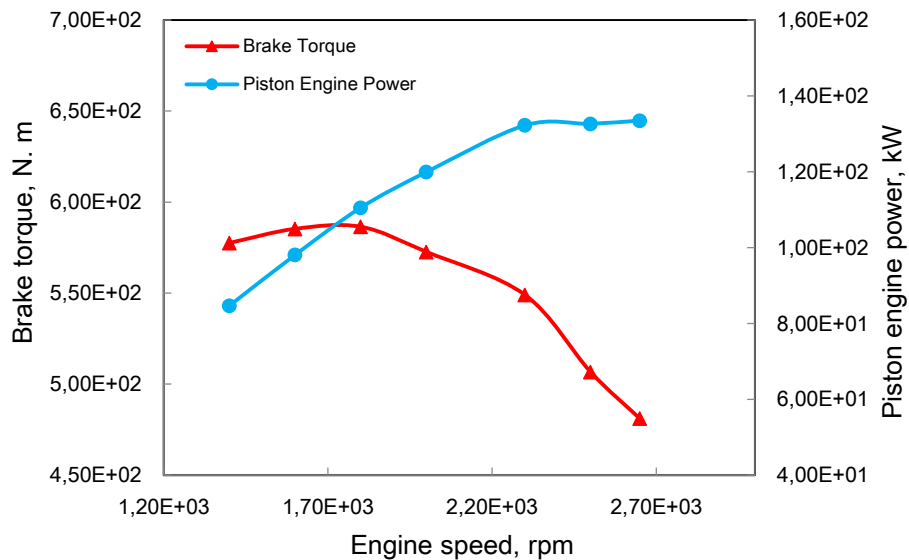


Figure 3. 2- Results of engine torque and piston engine power.

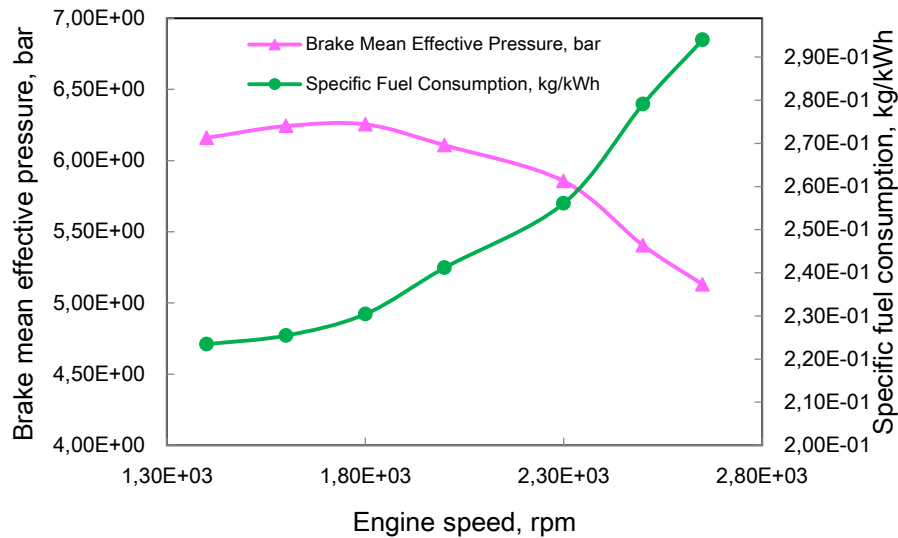


Figure 3. 3- Results of brake mean effective pressure and specific fuel consumption.

3.3. VALIDATION MODEL

Simulation results obtained from the Diesel-RK software were compared with those obtained from MATLAB code in order to compare and validate the study conducted on a single-cylinder diesel engine (The model equations are presented in detail in Chapter 2) for the same operating conditions. By the way, the Hexadecane diesel fuel was used for model validation (base fuel).

The validation model has been used to predict and analyze the cylinder temperature, cylinder pressure, and ignition delay period. From figure 3. 1a, a slight difference is recorded between the curve values obtained through Diesel-RK software simulation and those obtained with the programming languages MATLAB, indicating the reasonable and acceptable accuracy of the present work. It has been observed that the peak pressure value obtained through Diesel-RK software simulation is 95.311 bars while that obtained through MATLAB code is 99.6 bars. As well, the peak temperature obtained through Diesel-RK software simulation is 1958.7 K and the temperature obtained through MATLAB code is 2102.24 K as presented in table 3. 2. The maximum deviation was found to be 3.53% for cylinder temperature, 2.20% for cylinder pressure and 8.94% for the ignition delay period.

Table 3. 2- Comparison of the results between Diesel-RK software and MATLAB code at 1600 rpm

Performance parameters	Diesel-RK simulation software results	MATLAB simulation code	Error
T_max, K	1958.7	2102.24	±3.53 %
P_max, bar	95.311	99.6	±2.20 %
IDP, deg	8.43	7.046	±8.94 %

3.4. SIMULATION RESULTS (ANSYS CHEMKIN-PRO)

The results of the work carried out on CHEMKIN-Pro were compared to those found in the literature (Ennetta et al. 2012) [196] to verify the model performance. Figures (3. 4a) and (3. 4b) show the cylinder pressure and temperature evolution, respectively. We can see that the trend of the simulated curve has a similar shape to the Ennetta curve. The main difference between the curves is that Ennetta et al. used stoichiometric mixtures ($\phi = 1$) while the homogeneous model used in the presented work is based on lean mixtures ($\phi < 1$).

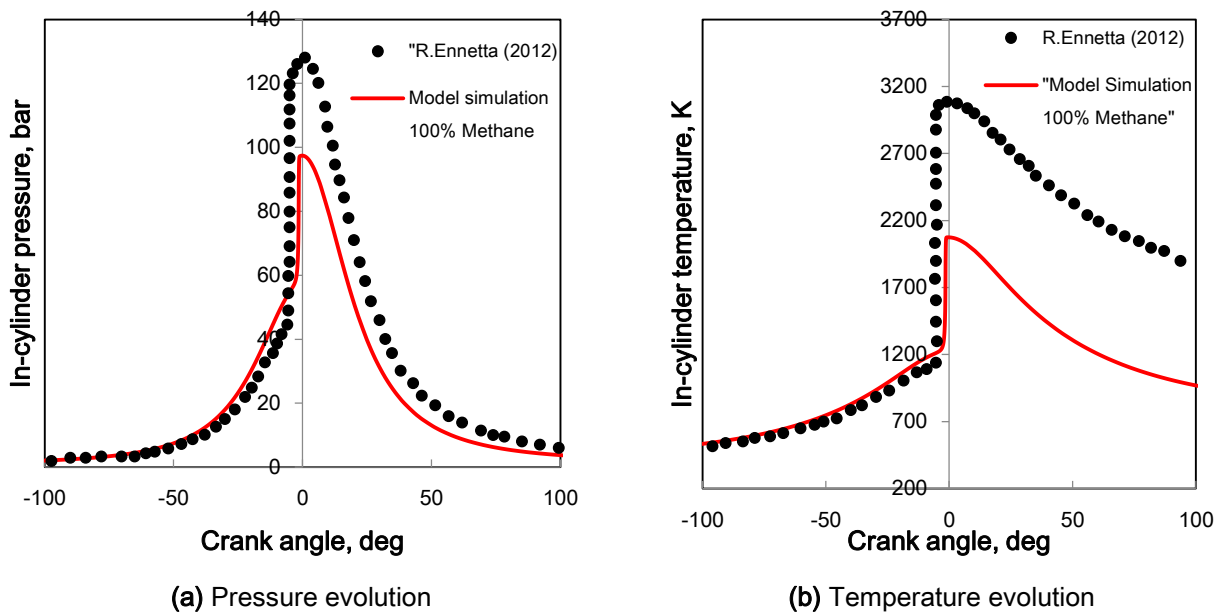


Figure 3. 4- Comparison between model simulation results with those found in the literature [196].

3.4.1. Combustion parameters effect

3.4.1.1. Cylinder temperature evolution

Figures (3. 5, 3. 6, 3. 7) show the temperature curves obtained versus crank angle position for different engine operating conditions. Figure 3. 5 shows the effect of equivalent ratios ($\phi = 0.3, 0.45, 0.5, 0.6$) on cylinder temperature using ANSYS CHEMKIN-Pro software. It can be seen that an increase ϕ led to increasing values of in-cylinder temperature. According to the $\phi = 0.3$ to 0.6 , predicted peak in-cylinder temperatures range from 2107.61 K to 2693.70 K.

Figure 3. 7 shows the effect of temperature T_{IVC} on cylinder temperature. Advances in auto-ignition timing lead to increased peak values of the cylinder temperature after compression. This phenomenon is due to the progressive diffusion combustion that occurs at an early stage before TDC for a higher intake charge temperature. This can be explained that by increasing the temperature T_{IVC} enhances to the advance of the ignition because it leads to an increase in the mean mixture temperature. Whereas the decreasing in temperature T_{IVC} reduces the reaction rate and thus the ignition is delayed [197].

From figure 3. 6 it can be noticed that when the compression ratio increases, the cylinder temperature evolution rate will advance. As it will advance around 1.41 deg bTDC for CR = 18 and reach a higher peak value of 2426.68 K, while it advances around 10.78 deg aTDC for CR = 14 and reached 2306.59 K. El-Kassaby et al. demonstrated that the increasing of compression ratio increases the air temperature inside the cylinder, helping for early combustion which reduced the ignition timing [198].

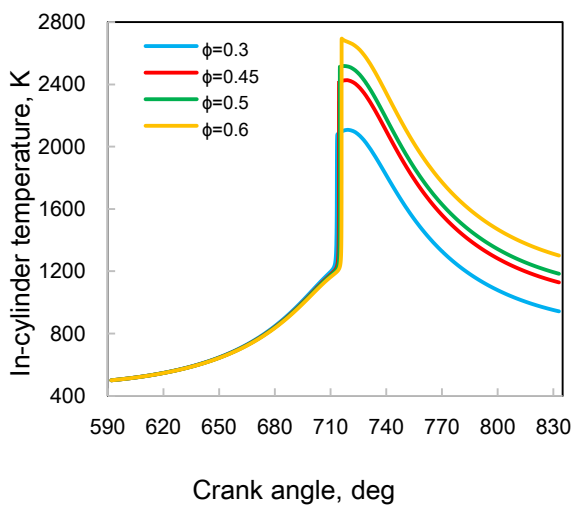


Figure 3. 5- Variation of cylinder temperature with crank angle according to the equivalence ratios ϕ ($P_{IVC} = 1.8\text{bar}$, $T_{IVC} = 500\text{K}$, $N = 2000\text{rpm}$).

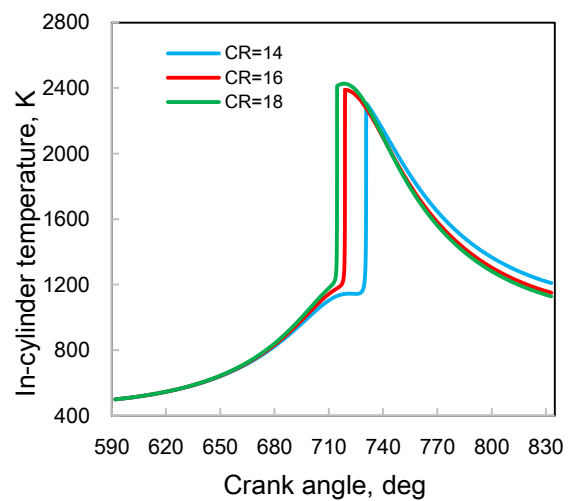


Figure 3. 6- Variation of cylinder temperature with crank angle according to the compression ratio ($P_{IVC} = 1.8\text{bar}$, $T_{IVC} = 500\text{K}$, $\phi = 0.45$, $N = 2000\text{rpm}$).

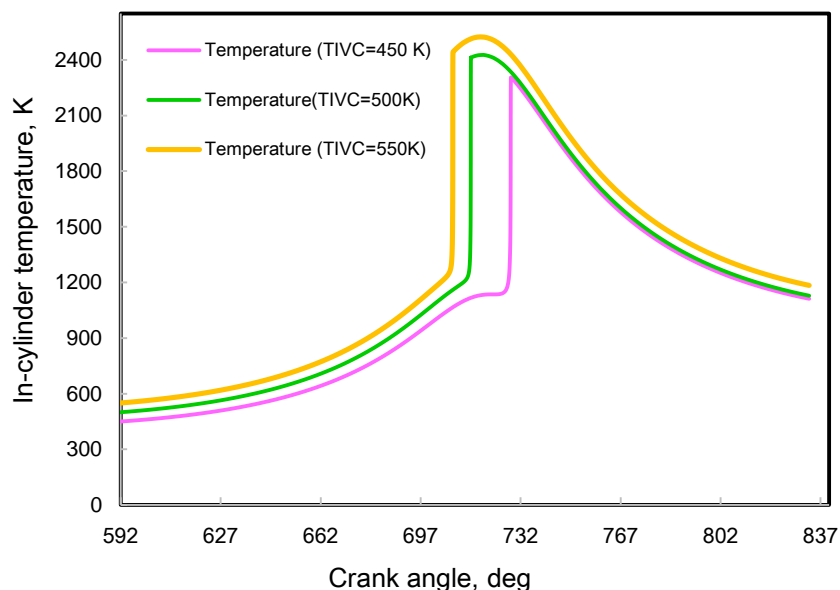


Figure 3. 7- Variation of cylinder temperature according to the intake charge temperature. Intake conditions ($P_{IVC}= 1.8\text{bar}$, $\phi= 0.45$, $CR= 18$, engine speed= 2000rpm).

3.4.1.2. Cylinder pressure evolution

The maximum pressure rise rate leads to making the engine noise. Figures (3. 8, 3. 9, 3. 10 and 3. 11) show the pressure curves obtained versus crank angle position for different engine operating conditions. It can be concluded from figure 3. 8, that with a higher of ϕ , more heat is released which in turn leads to an increase in-cylinder pressure [199].

As shown in figure 3. 9, increasing the temperature T_{IVC} significantly advances the auto-ignition timing and produces a shorter delay start of combustion, but the combustion is not so efficient, and by decreasing the temperature, the ignition would be retarded. Also by decreasing the intake charge temperature, the maximum cylinder pressure decreases and the ignition timing would be so retarded that causes some misfiring [200]. Higher pressure rise rate creates a rapid heat release rate (figure 3. 13), after which a decrease in-cylinder pressure should be avoided to limit the knocking phenomena that deteriorate the HCCI combustion [201,202].

Figure 3. 10 shows the cylinder pressure trace in an engine running at 2000 rpm with various compression ratios ranging from 14:1 to 18:1. That shows the sensitivity of the pressure to the compression ratio (CR) where the curves vary significantly. The peak in-cylinder pressure increased with the increase of the compression ratio [203]. It can explain that the increase of the compression ratio increased the in-cylinder temperature, thus contributing to early combustion,

which reduced the ignition time [204]. In addition, increasing the CR leads to an increase in the mean temperature of the mixture [197].

The in-cylinder pressure is presented and plotted in figure 3. 11, the intake charge pressure has been increased from 1.8-2.2 bars. The cylinder pressure increases, the charge density increases, and the corresponding charge temperatures would also increase, making promising conditions for fuel combustion [199]. It is widely accepted that increasing the intake charge pressure P_{IVC} increases the auto-ignition temperature in HCCI operation and the increase of the temperature leads to increases in the burning rate.

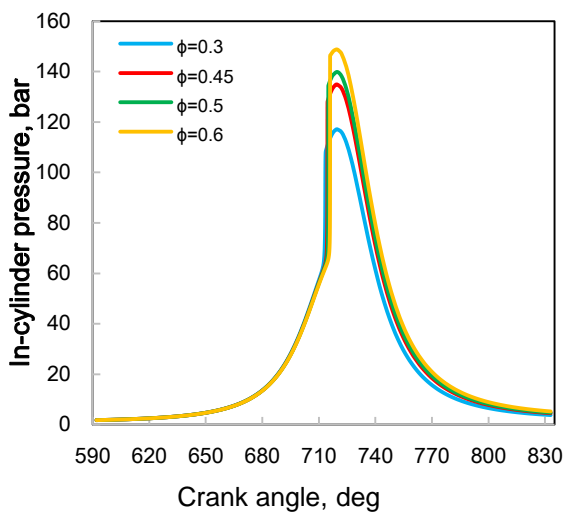


Figure 3. 8- Variation of cylinder pressure with crank angle according to the equivalence ratios ϕ ($P_{IVC}=1.8\text{bar}$, $T_{IVC}=500\text{K}$, $N=2000\text{rpm}$).

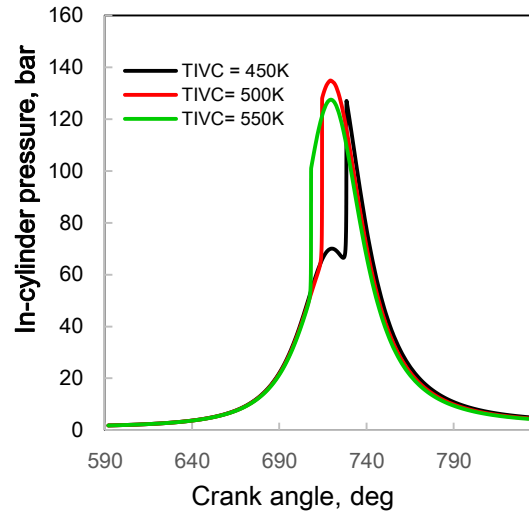


Figure 3. 9- Variation of cylinder pressure with crank angle according to the intake charge temperature ($P_{IVC}=1.8\text{bar}$, $\phi=0.45$, $N=2000\text{rpm}$).

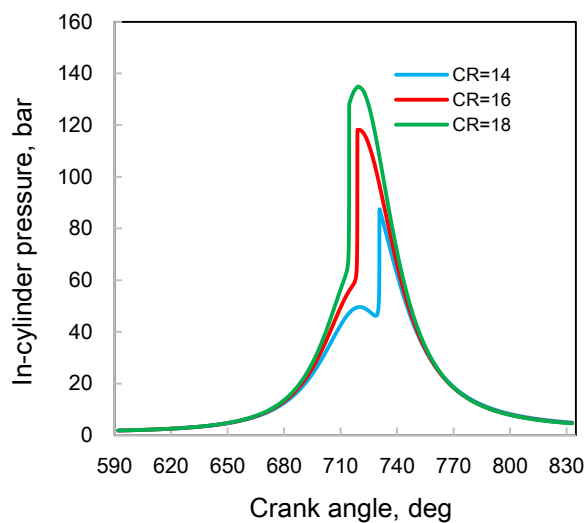


Figure 3. 10- Variation of cylinder pressure with crank angle according to the compression ratio. Intake conditions ($P_{IVC}=1.8\text{bar}$, $T_{IVC}=500\text{K}$, $\phi=0.45$, engine speed= 2000rpm).

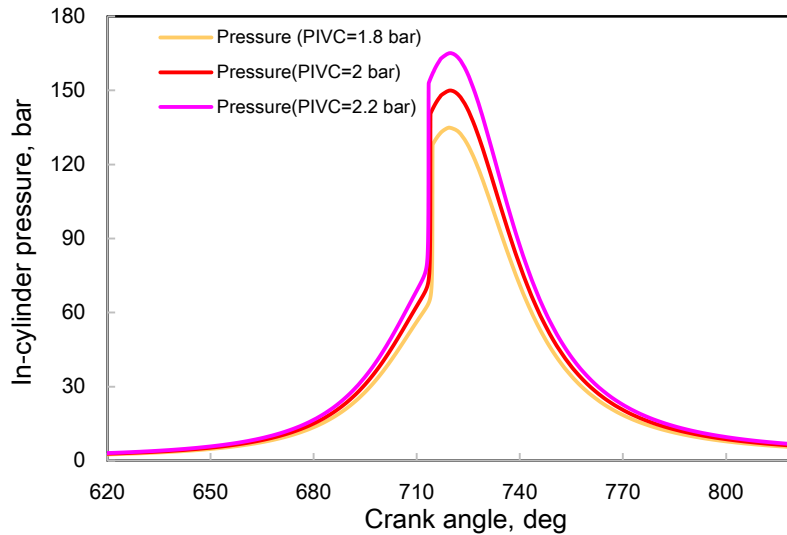


Figure 3. 11- Variation of cylinder pressure with crank angle according to the pressure inlet. Intake conditions ($T_{IVC} = 500$ K, $CR = 18$, $\phi = 0.45$, engine speed = 2000 rpm)

3.4.1.3. Net heat release rate (NHRR) evolution

Figure 3. 12 shows the net heat release rate (NHRR) profiles per crank angle (CA) for various equivalence ratios (ϕ) at $T_{IVC} = 500$ K. It can be observed that the peak of the NHRR per CA increases rapidly when the ϕ goes from 0.3 to 0.6. These results are in agreement with those found in the literature. It can be seen that the NHRRs have a smaller peak value for $\phi = 0.3$ (~ 6.57deg bTDC), while the peak NHRRs occur at a higher value for $\phi = 0.6$ (~4deg bTDC). Furthermore, growing the ϕ causes the combustion to start later, which hence increases the temperature and pressure of the cylinder (figs. 3. 5 & 3. 8). These figures also show how the NHRR is extremely advanced so that the pressure peak occurs around the TDC position [205]. The explanation is that for a higher ϕ more fuel is burned in the cylinder and therefore more heat is released, which leads to higher gas temperatures and pressures [199].

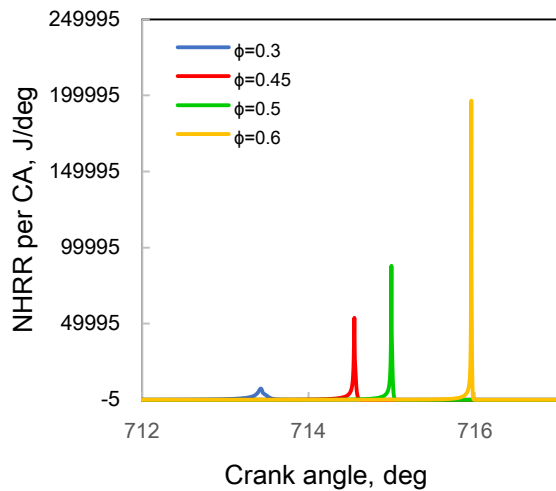


Figure 3. 12- Variation of net heat release with crank angle according to the equivalence ratios ϕ ($P_{IVC}= 1.8\text{bar}$, $T_{IVC}= 500\text{K}$, $N= 2000\text{rpm}$).

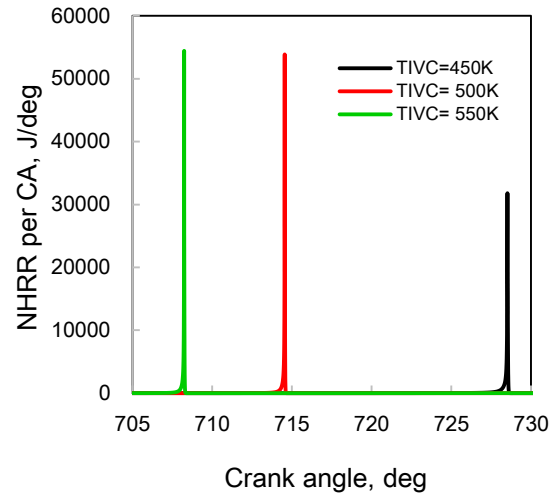


Figure 3. 13- Variation of net heat release rate according to the intake charge temperature ($P_{IVC}= 1.8\text{bar}$, $\phi= 0.45$, $N= 2000\text{rpm}$).

3.4.2. Engine performance parameters

Figures (3. 14 and 3. 15) illustrate a representation of the results obtained in terms of performance (IMEP, ISFC, T_q , ITE, W_i and IP). It was observed that the IMEP, ISFC, IP, W_i , T_q and indicated thermal efficiency (ITE) related to the evaluated intake charge conditions. The increase in the intake charge temperature caused the value of peak pressure to decrease. This makes a reduction in the IMEP, W_i and IP [206] (figure 3. 14b & 3. 14c). While the ITE decreased with increasing T_{IVC} (figure 3. 14a). In addition, from figure 3. 14b a higher T_{IVC} caused an increase in ISFC which led to an advance in the ignition. Thus, increasing the T_{IVC} advances the combustion, but decreases engine performance parameters [197].

Furthermore, the higher the equivalence ratio (ϕ) leads to an increase in the indicated specific fuel consumption (ISFC) and IMEP because more fuel quantity is injected thus burning rates are higher, leading to a decrease in the ITE. The explanation is that for higher equivalence ratios, the heat losses are higher, thereby decreasing the thermal efficiency. It was concluded that increasing the equivalence ratio (ϕ) takes a toll on the thermal efficiency of the engine [199].

At the levels of intake charge pressure and intake charge temperature evaluated here, the first parameter had a more important effect on IMEP [207]. Increasing the pressure P_{IVC} from 2 bars to 2.2 bars led to an increase of 0.804 bars in IMEP. While increasing the temperature T_{IVC} from 450 K to 550 K led to a decrease of 2.286 bars in IMEP. Moreover,

thermal efficiency decreases by intake charge pressure and intake charge temperature (figure 3. 14a).

In addition, IMEP, ITE and T_q were increased with increasing the compression ratio (CR) and reached the maximum value for CR near 16 (figure 3. 15b). This is because there are chemical reactions that occur during the compression stroke which depend on the in-cylinder pressure and temperature [202], in order to start decreasing again with an increase of CR. While, the specific fuel consumption decreases and reached the minimal value for CR near 17, in order to start raising again with an increase of CR [208] (figure 3. 15a). Increasing the CR improved the performance of the engine [209,198] (figure 3 .15).

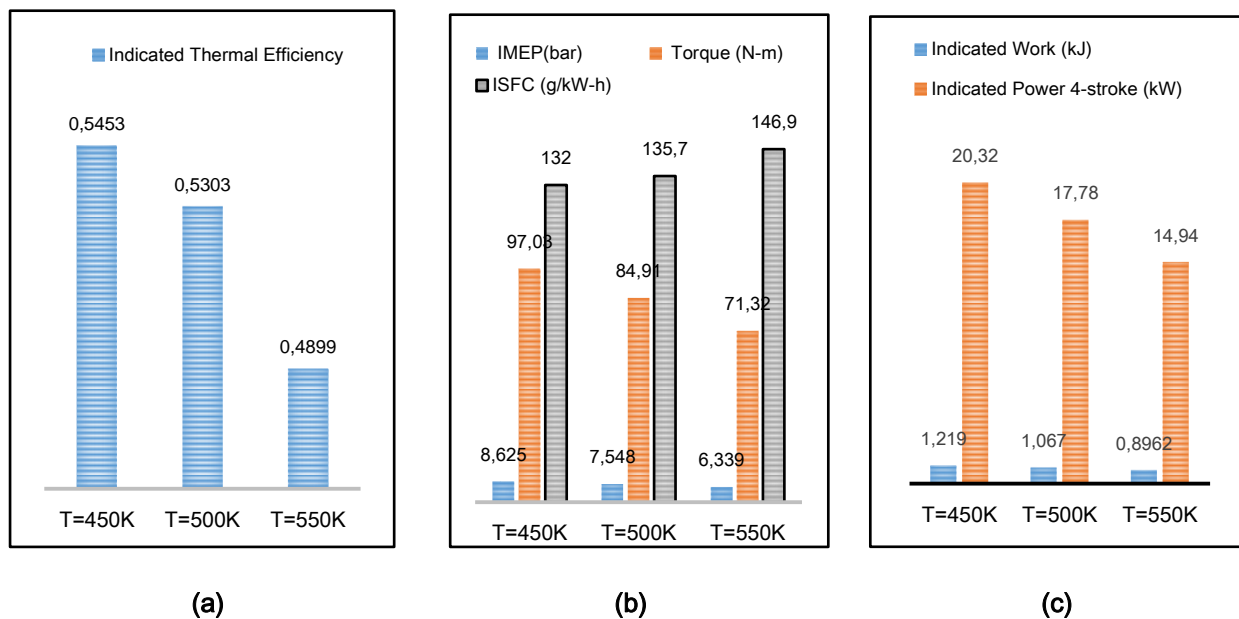


Figure 3. 14- Engine performance parameters (cycle) according to the intake temperatures.

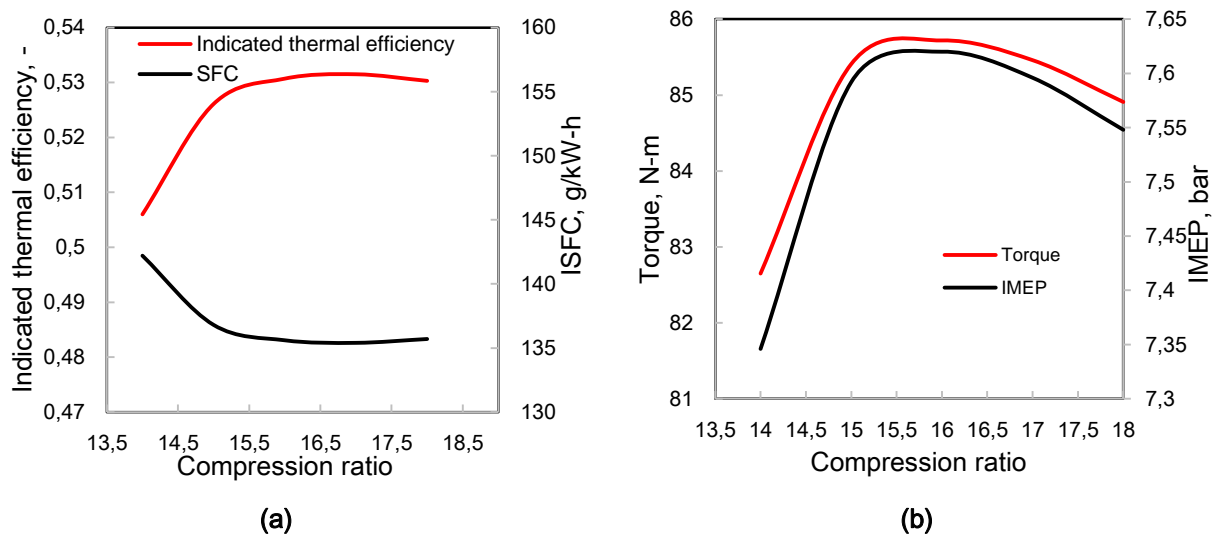


Figure 3. 15- Engine performance parameters (cycle) according to the compression ratios.

3.4.3. Emissions evolution

Equivalence ratios $\phi = 0.3, 0.45, 0.5$ and 0.6 were chosen and the predicted CO, UHC and NO_x levels are shown and presented in figures (3. 16, 3. 18 and 3. 20), respectively. The upward trend in NO_x levels can clearly be seen as the ϕ is increased. The CO, UHC and NO_x emissions for various temperatures T_{IVC} in the same engine for $P_{IVC} = 1.8$ bars and $\phi = 0.45$ were represented in figures (3. 17, 3. 19 and 3. 21), respectively. By decreasing the temperature, the CO molar fraction and NO_x emissions have decreased significantly. Also, as demonstrated in figure 3. 17, the trend of emissions at temperature T_{IVC} of 550 K has more advanced than other intake charge temperatures used and NO_x emissions were at the highest levels (figure 3. 21). It is clear that the cylinder temperature difference increased about 217.6 K when the temperature goes from 450 K to 550 K and that this increase is sufficient to raise the NO_x rate to its highest level since it reaches 13826.75 ppm for $T_{IVC} = 550$ K, while it reaches 558.81 ppm for $T_{IVC}=450$ K.

NO_x emissions are seen as an emission polluting the air environment, so the results obtained from figure 3. 23 are very significant. The NO_x emission rate increases significantly as the CR increases because it is a consequence of increased combustion temperature while the carbon monoxide rate (figure 3. 22) did not change with CR but has more advanced at CR = 18 than other compression ratios used.

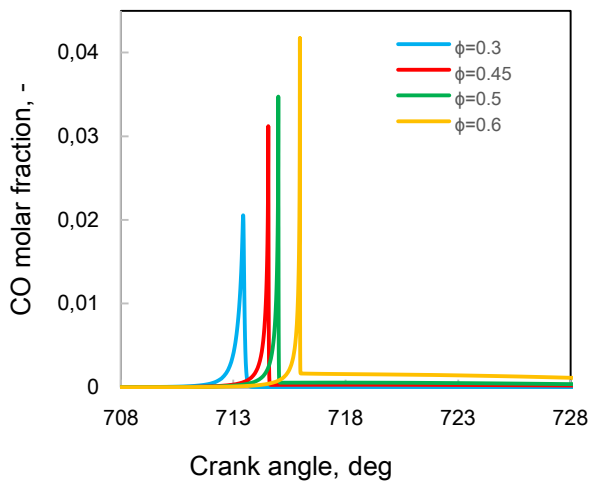


Figure 3. 16- Variation of CO molar fraction with crank angle according to the equivalence ratios ϕ ($P_{IVC} = 1.8$ bar, $T_{IVC} = 500$ K, $N = 2000$ rpm).

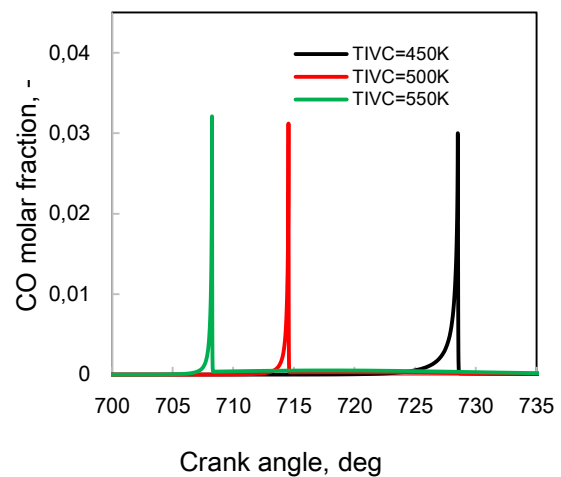


Figure 3. 17- Variation of CO molar fraction with crank angle according to the intake charge temperature ($P_{IVC} = 1.8$ bar, $\phi = 0.45$, $N = 2000$ rpm).

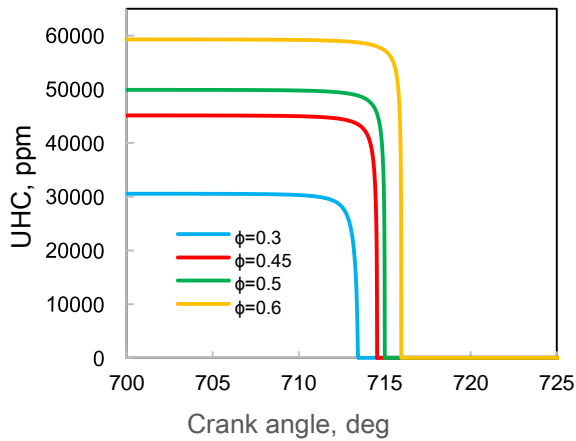


Figure 3. 18- Variation of unburned hydrocarbons with crank angle according to the equivalence ratios ϕ ($P_{IVC}= 1.8$ bar, $T_{IVC}= 500$ K, $N= 2000$ rpm).

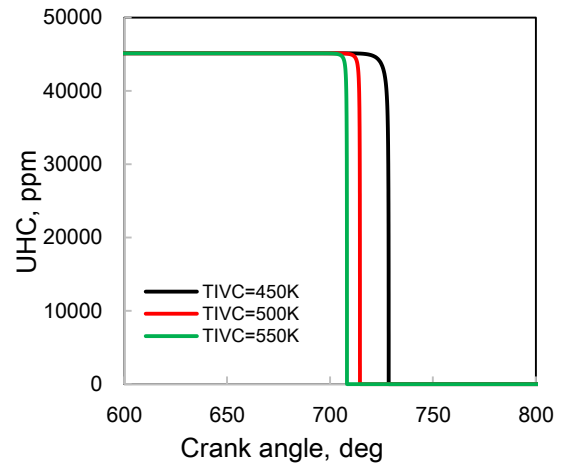


Figure 3. 19- Variation of unburned hydrocarbons with crank angle according to the intake charge temperature ($P_{IVC}= 1.8$ bar, $\phi= 0.45$, $N= 2000$ rpm).

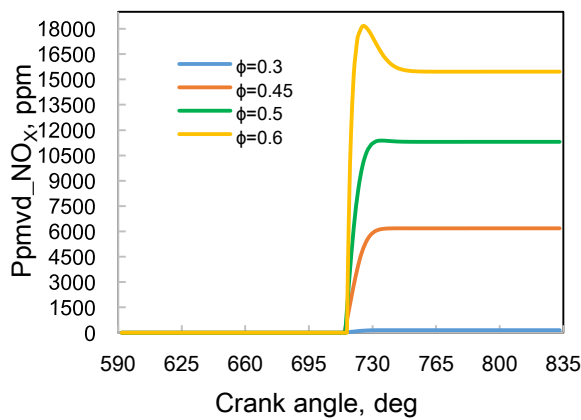


Figure 3. 20- Variation of NO_x emissions with crank angle according to the equivalence ratios ϕ ($P_{IVC}= 1.8$ bar, $T_{IVC}= 500$ K, $N= 2000$ rpm).

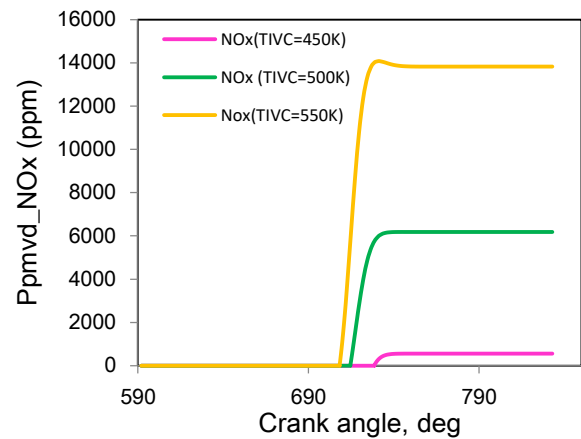


Figure 3. 21- Variation of NO_x emissions with crank angle according to the intake charge temperature ($P_{IVC}= 1.8$ bar, $\phi= 0.45$, $N= 2000$ rpm).

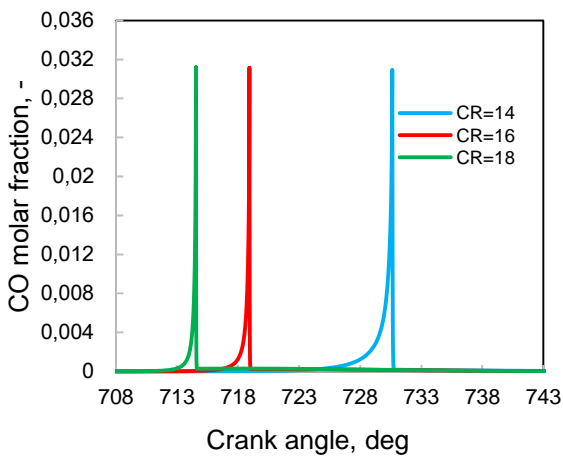


Figure 3. 22- Variation of CO molar fraction with crank angle according to the compression ratio ($P_{IVC}= 1.8$ bar, $T_{IVC}= 500$ K, $\phi= 0.45$, $N= 2000$ rpm).

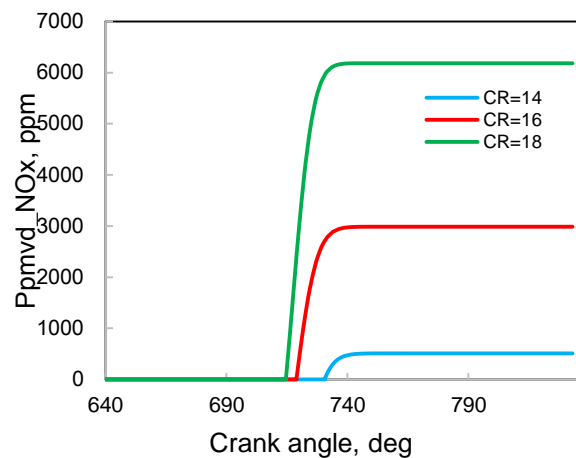


Figure 3. 23- Variation of NO_x emissions with crank angle according to the compression ratio ($P_{IVC}= 1.8$ bar, $T_{IVC}= 500$ K, $\phi= 0.45$, $N= 2000$ rpm).

3.4.4. EGR rate affect

The gas due to the EGR and introduced into the simulation by CHEMKIN consists of CO₂, H₂O, N₂ and O₂. Its quantity varies from 0% to 60%. The air-fuel mixture becomes more homogeneous than in the case of conventional diesel combustion, which makes it possible to maintain low emission rates of NO_x.

The input parameters used in this section are: the engine speed equal to 2600 rpm; the gas mixture pressure at IVC equal to 1.2 bar; the gas mixture temperature at IVC equal to 460 K; the equivalence ratio (ϕ) = 0.3. The EGRs are mainly composed of CO₂, H₂O, O₂ and N₂. Therefore, the increase of the recycled gases reduces the heat release rate, and thus lowers the maximum temperature of the cylinder due mainly to CO₂ and H₂O, which have higher specific calorific capacities [179]. The decrease in temperature and pressure of the gas in the cylinder with the increase in the EGR rate leads to the reduction, of the specific fuel consumption, torque, indicated work, and therefore an increase in thermal efficiency as shown in table 3. 3.

Figure 3. 25 shows the NO molar fraction versus crank angle with different EGR rates. It can be seen that with the increase in the rate of EGR, NO emissions are clearly reduced compared to those of combustion without EGR.

Table 3. 3- Engine performance parameters (cycle) with different EGR rates

Performance	0 %-EGR	5 %-EGR	10 %-EGR	30 %-EGR	50 %-EGR	60 %-EGR
Max-T, K	2216.0	2154.0	2103.0	1899.0	1698.0	1595.0
Max-P, bar	106.1	103.0	100.5	90.36	80.49	75.46
Work, kJ	0.6146	0.5816	0.5537	0.4395	0.3239	0.263
T _q , N.m	48.91	46.28	44.06	34.97	25.78	20.93
SFC, g/kWh	161.9	160.4	159.7	156.4	151.6	149.4
Thermal efficiency,-	0.5052	0.5101	0.5124	0.5232	0.5397	0.5478

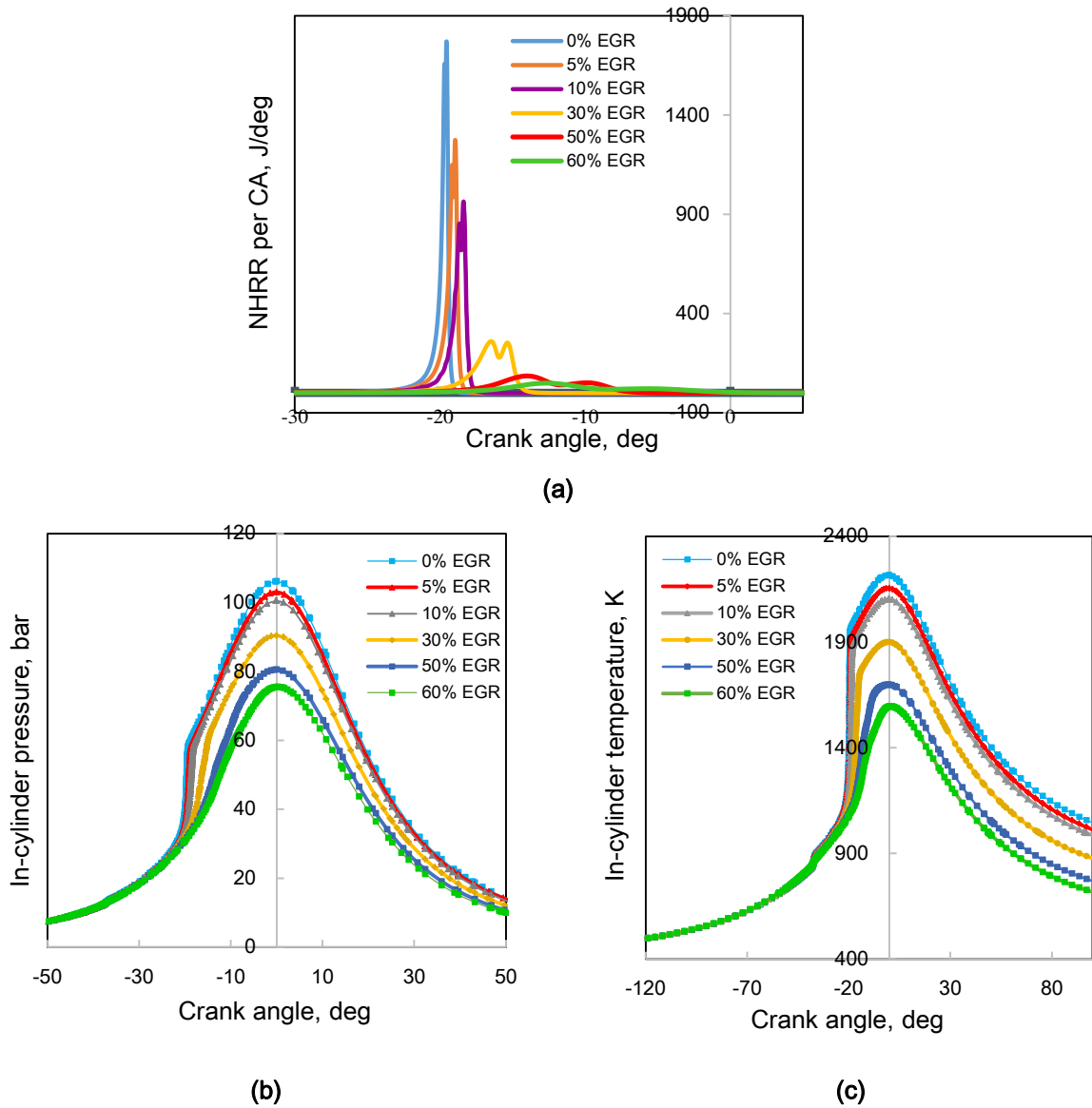


Figure 3. 24- Evolution of (a) NHRR, (b) pressure, and (c) temperature cylinder for $C_{16}H_{34}$ fuel for different EGR rates.

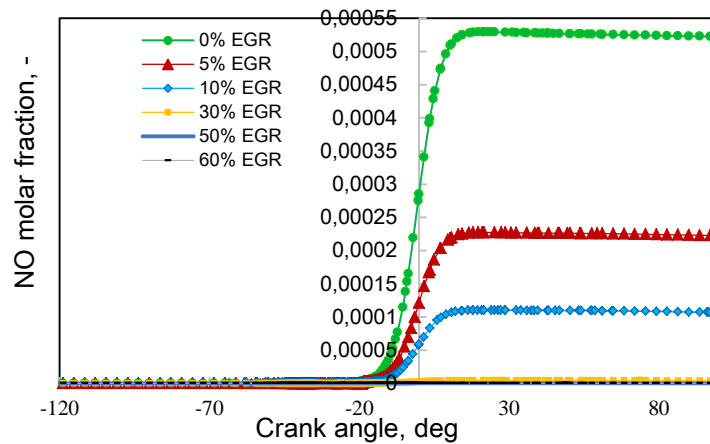


Figure 3. 25- NO molar fraction evolution for different EGR rates.

3.5. COMPARISON RESULTS (CHEMKIN-PRO/ DIESEL-RK SOFTWARE)

Table 3. 4 shows the important results obtained, which are compared numerically by using the CHEMKIN-Pro and Diesel-RK are the indicated mean effective pressure (IMEP), specific fuel consumption (SFC), indicated thermal efficiency, peak temperature in-cylinder and peak pressure in-cylinder. The simulation comparison was carried out between the HCCI model without EGR and the baseline diesel engine operating in conventional combustion mode. The input parameters used are the engine speed equal to 2600 rpm; the gas mixture pressure at intake valve close (IVC) equal to 1.2 bar; the gas mixture temperature at IVC equal to 460 K; the equivalence ratio (ϕ) equal to 0.3.

In the numerical simulation, the results obtained in the conventional as well as HCCI combustion modes are presented in table 3. 4. Results show that HCCI combustion mode delivers higher indicated thermal efficiency as compared to conventional diesel combustion. It happens mainly due to improved combustion of the relatively richer combustible mixture at a higher temperature in HCCI combustion mode. In addition, it can be noted that the external charge preparation technique gives improved homogeneity of the mixture as compared to the conventional method (heterogeneous), which improves the combustion results and delivers normal combustion events, thus avoiding higher fuel consumption. In the conventional combustion mode, the specific fuel consumption (SFC) is higher compared to the HCCI mode as shown in table 3. 4. It can be concluded that the HCCI combustion mode is more practical for a very lean mixture and ensures adequate combustion.

Table 3. 4- Comparison between CHEMKIN and Diesel-RK software results

Performance parameters	At 2600 rpm and $\phi= 0.3$	
	CHEMKIN software results (HCCI model)	Diesel-RK software results (Conventional mode)
IMEP, bar	4.348	3.0975
SFC, kg/kWh	0.1619	0.53801
Efficacité indiquée	0.5052	0.45445
T_max, K	2216	1614.4
P_max, bar	106.1	60
NO _x , ppm	243	408

GENERAL CONCLUSION

The truth is, conventional engines face their biggest challenge from their invention to the present day. Engineers and designers have gone to great lengths and companies have spent huge sums for decades on the continuous development of these engines to reduce fuel consumption and harmful emissions. In this thesis, the effect of EGR ratios on the HCCI combustion model has been investigated. These ratios can be used, to control the start of auto-ignition and/or to extend the load limits in which HCCI operation is possible. As part of this work, Methane was selected for HCCI engines as fuel. In order to study these effects on HCCI combustion mode, a detailed chemical mechanism of fuel oxidation was used. HCCI mode combustion simulations were performed using a single-zone zero-dimensional model. As well, in this work, the characteristics of HCCI are numerically investigated by ANSYS CHEMKIN-Pro software to allow the evaluation of the effects of different parameters (equivalence ratio, mixture temperature at IVC, mixture pressure at IVC, ..., etc.) on engine performance parameters.

The study yielded the following conclusions:

1. The use of Heavy fuel as a fuel has a significant effect on engine performance and emission characteristics. Only the specific carbon dioxide emissions(S-CO₂) show some negative impact. It can be concluded that the lower heating value is the predominant factor in influencing the pressure rise of the cylinder.
2. It is important to note that the pressure and temperature behavior in the combustion chamber are controlled by different intake charge conditions; the model predicts that, the peak in-cylinder temperature increases for a higher value of intake charge temperature. Additionally, increasing the overall gas temperature significantly advances the HCCI combustion timing and faster net heat release rates.
3. The quantity of NO_x increases with the intake charge temperature. In addition, the emissions of NO_x increase with the increase in the equivalence ratio (ϕ) due to the higher combustion chamber temperature.
4. The indicated work was reduced with a higher intake charge temperature in the HCCI mode.

5. The HCCI combustion is more practical for a very lean mixture. Further, it was found that the peak value in-cylinder pressure and temperature increase with the equivalence ratio variation, and the peak pressure occurs around the TDC position.
6. The reduction of the compression ratio decreases the in-cylinder temperatures; hence lowering flame temperatures during the combustion to reduce NO_x emissions. While increasing the compression ratio leads to an increase in the cylinder pressure. Thermal efficiency was increased by about 4.58% when compression ratios are between 14 and 18.
7. It is noted that a change in the compression ratio and the boundary conditions could be the source of the increase in NO_x emissions.
8. There is an optimum value of additive for each operating condition, resulting in higher engine power and less NO_x (increasing the amount of EGR from 5% to 10% reduces NO emissions up to 'at 52.42%).
9. Alternative fuel is promising green technologies for reducing engine emissions and therefore air pollution.
10. The external charge preparation technique gives improved homogeneity of the mixture as compared to the conventional method (heterogeneous).

HCCI mode is a combustion concept that is developed in response to the need of reducing NO_x emissions and increasing engine performance. The results obtained in the case of combustion in HCCI mode are very encouraging and this work deserves to be followed up.

Finally, as prospects as resulting from this work, we can predict that:

It is possible to study a multi-zone HCCI combustion model would also be extremely practical. Further increasing the zones number, when compared with the single-zone HCCI model used in this thesis, engendering some interaction between zones would be the way forward that would most probably lead to better simulation results while achieving higher efficiencies and low nitrogen oxides (NO_x) and particulate emissions (PM) on the one hand, and the other hand is adaptable to different kinds of fuels.

BIBLIOGRAPHY

- [1] H.-W. Wu, R.-H. Wang, D.-J. Ou, Y.-C. Chen, and T. Chen, 'Reduction of smoke and nitrogen oxides of a partial HCCI engine using premixed gasoline and ethanol with air', *Appl. Energy*, vol. 88, no. 11, pp. 3882–3890, 2011.
- [2] R. K. Pachauri and A. Reisinger, 'Bilan 2007 des changements climatiques: Rapport de synthèse'. GIEC, 2008.
- [3] K. Protocol, 'United Nations framework convention on climate change', *Kyoto Protoc. Kyoto*, vol. 19, p. 497, 1997.
- [4] M. D. Geller *et al.*, 'Physicochemical and redox characteristics of particulate matter (PM) emitted from gasoline and diesel passenger cars', *Atmos. Environ.*, vol. 40, no. 36, pp. 6988–7004, 2006.
- [5] D. T. Hountalas, R. G. Papagiannakis, G. Zovanos, and A. Antonopoulos, 'Comparative evaluation of various methodologies to account for the effect of load variation during cylinder pressure measurement of large scale two-stroke diesel engines', *Appl. Energy*, vol. 113, pp. 1027–1042, 2014.
- [6] H. Tse, C. W. Leung, and C. S. Cheung, 'Performances, emissions and soot properties from a diesel-biodiesel-ethanol blend fuelled engine', *Adv Automob Eng*, vol. 1, p. 005, 2016.
- [7] V. Praveena and M. L. J. Martin, 'A review on various after treatment techniques to reduce NOx emissions in a CI engine', *J. Energy Inst.*, vol. 91, no. 5, pp. 704–720, 2018.
- [8] J. Heywood, 'Internal Combustion Engine Fundamentals'. 1988.
- [9] İ. A. Reşitoğlu, K. Altinişik, and A. Keskin, 'The pollutant emissions from diesel-engine vehicles and exhaust aftertreatment systems', *Clean Technol. Environ. Policy*, vol. 17, no. 1, pp. 15–27, 2015.
- [10] S. I. Raptotasios, N. F. Sakellaris, R. G. Papagiannakis, and D. T. Hountalas, 'Application of a multi-zone combustion model to investigate the NOx reduction potential of two-stroke marine diesel engines using EGR', *Appl. Energy*, vol. 157, pp. 814–823, 2015.
- [11] B. V. V. S. U. Prasad, C. S. Sharma, T. N. C. Anand, and R. V. Ravikrishna, 'High swirl-inducing piston bowls in small diesel engines for emission reduction', *Appl. Energy*, vol. 88, no. 7, pp. 2355–2367, 2011.
- [12] R. Prasad and V. R. Bella, 'A review on diesel soot emission, its effect and control', *Bull. Chem. React. Eng. Catal.*, vol. 5, no. 2, p. 69, 2010.
- [13] H. Bendu and S. Murugan, 'Homogeneous charge compression ignition (HCCI) combustion: Mixture preparation and control strategies in diesel engines', *Renew. Sustain. Energy Rev.*, vol. 38, pp. 732–746, 2014.
- [14] X. Duan *et al.*, 'Experimental study the effects of various compression ratios and spark timing on performance and emission of a lean-burn heavy-duty spark ignition engine fueled with methane gas and hydrogen blends', *Energy*, vol. 169, pp. 558–571, 2019.

- [15] X. Duan, M.-C. Lai, M. Jansons, G. Guo, and J. Liu, 'A review of controlling strategies of the ignition timing and combustion phase in homogeneous charge compression ignition (HCCI) engine', *Fuel*, vol. 285, p. 119142, 2021.
- [16] H. Köten and M. Yılmaz, 'HCCI Engines New trends in automotive industry', Riga: LAMBERT Academic Publishing, 2017.
- [17] V. Soloiu *et al.*, 'LTC (low-temperature combustion) analysis of PCCI (premixed charge compression ignition) with n-butanol and cotton seed biodiesel versus combustion and emissions characteristics of their binary mixtures', *Renew. Energy*, vol. 123, pp. 323–333, 2018.
- [18] A. Jain, A. P. Singh, and A. K. Agarwal, 'Effect of fuel injection parameters on combustion stability and emissions of a mineral diesel fueled partially premixed charge compression ignition (PCCI) engine', *Appl. Energy*, vol. 190, pp. 658–669, 2017.
- [19] B. Wang, Z. Wang, S. Shuai, H. Yang, and J. Wang, 'Combustion and emission characteristics of multiple premixed compression ignition (MPCI) fuelled with naphtha and gasoline in wide load range', *Energy Convers. Manag.*, vol. 88, pp. 79–87, 2014.
- [20] V. Soloiu, M. Duggan, S. Harp, B. Vlack, and D. Williams, 'PFI (port fuel injection) of n-butanol and direct injection of biodiesel to attain LTC (low-temperature combustion) for low-emissions idling in a compression engine', *Energy*, vol. 52, pp. 143–154, 2013.
- [21] J. Li, W. Yang, and D. Zhou, 'Review on the management of RCCI engines', *Renew. Sustain. Energy Rev.*, vol. 69, pp. 65–79, 2017.
- [22] K. Epping, S. Aceves, R. Bechtold, and J. E. Dec, 'The potential of HCCI combustion for high efficiency and low emissions', 2002, pp. 2002-01–1923.
- [23] P. Kumar and A. Rehman, 'Bio-diesel in homogeneous charge compression ignition (HCCI) combustion', *Renew. Sustain. Energy Rev.*, vol. 56, pp. 536–550, 2016.
- [24] X. Duan *et al.*, 'Experimental investigation of the effects of injection strategies on cycle-to-cycle variations of a DISI engine fueled with ethanol and gasoline blend', *Energy*, vol. 165, pp. 455–470, 2018.
- [25] G. Guo, Z. He, Y. Jin, Z. Chen, X. Duan, and X. Leng, 'Visualization investigations of flow regimes in different sizes of diesel injector nozzles and their effects on spray', *At. Sprays*, vol. 28, no. 6, 2018.
- [26] I. E. Fox, 'Numerical evaluation of the potential for fuel economy improvement due to boundary friction reduction within heavy-duty diesel engines', *Tribol. Int.*, vol. 38, no. 3, pp. 265–275, 2005.
- [27] M. M. Hasan and M. M. Rahman, 'Homogeneous charge compression ignition combustion: Advantages over compression ignition combustion, challenges and solutions', *Renew. Sustain. Energy Rev.*, vol. 57, pp. 282–291, 2016.
- [28] K. Akihama, Y. Takatori, K. Inagaki, S. Sasaki, and A. M. Dean, 'Mechanism of the smokeless rich diesel combustion by reducing temperature', *Sae Trans.*, pp. 648–662, 2001.
- [29] G. D. Neely, S. Sasaki, Y. Huang, J. A. Leet, and D. W. Stewart, 'New diesel emission control strategy to meet US Tier 2 emissions regulations', *SAE Trans.*, pp. 512–524, 2005.

- [30] M. Chhiboo, '4842 Automotive Engines: how a four stroke engine works..', *4842 Automotive Engines*, Apr. 06, 2011. <http://minhazchhiboo.blogspot.com/2011/04/how-four-stroke-engine-works.html> (accessed Mar. 17, 2021).
- [31] xxx, 'Additional Aspects for a Proper Fuel Injection System', *Issuu*. https://issuu.com/starmotors/docs/additional_aspects_for_a_proper_fue (accessed Mar. 21, 2021).
- [32] V. Lazarev, G. Lomakin, and E. Lazarev, 'Modeling of injection parameters for diesel engine injector nozzles with the additional precision guiding interface', *Procedia Eng.*, vol. 150, pp. 52–60, 2016.
- [33] R. D. Reitz and F. B. Bracco, 'On the dependence of spray angle and other spray parameters on nozzle design and operating conditions', 1979, p. 790494.
- [34] M. J. Murphy, J. D. Taylor, and R. L. McCormick, 'Compendium of experimental cetane number data'. National Renewable Energy Laboratory Golden, CO, 2004.
- [35] B. Johansson, 'Homogeneous charge compression ignition: the future of IC engines?', *Int. J. Veh. Des.*, vol. 44, no. 1–2, pp. 1–19, 2007.
- [36] M. Jennische, 'Closed-loop control of start of combustion in a homogeneous charge compression Ignition engine', in *international congress and exposition*, 2003, vol. 1.
- [37] A. Hultqvist, U. Engdar, B. Johansson, and J. Klingmann, 'Reacting boundary layers in a homogeneous charge compression ignition (HCCI) engine', *SAE Trans.*, pp. 1086–1098, 2001.
- [38] A. Hultqvist *et al.*, 'The HCCI combustion process in a single cycle—high-speed fuel tracer LIF and chemiluminescence imaging', *SAE Trans.*, pp. 913–927, 2002.
- [39] S. M. Aceves *et al.*, 'HCCI combustion: analysis and experiments', Lawrence Berkeley National Lab., CA (US), 2001.
- [40] N. Milovanovic and R. Chen, 'A review of experimental and simulation studies on controlled auto-ignition combustion', 2001.
- [41] S. M. Aceves *et al.*, 'A multi-zone model for prediction of HCCI combustion and emissions', *SAE Trans.*, pp. 431–441, 2000.
- [42] J. Yang, T. Culp, and T. Kenney, 'Development of a gasoline engine system using HCCI technology—the concept and the test results', *SAE Trans.*, pp. 1841–1854, 2002.
- [43] T. W. Ryan III and A. C. Matheaus, 'Fuel requirements for HCCI engine operation', *SAE Trans.*, pp. 1143–1152, 2003.
- [44] J. Martinez-Frias, S. M. Aceves, D. Flowers, J. R. Smith, and R. Dibble, 'HCCI engine control by thermal management', *SAE Trans.*, pp. 2646–2655, 2000.
- [45] J. Martinez-Frias, S. M. Aceves, D. Flowers, J. R. Smith, and R. Dibble, 'Equivalence ratio-EGR control of HCCI engine operation and the potential for transition to spark-ignited operation', SAE Technical paper, 2001.
- [46] A. Bhave, M. Kraft, L. Montorsi, and F. Mauss, 'Sources of CO emissions in an HCCI engine: A numerical analysis', *Combust. Flame*, vol. 144, no. 3, pp. 634–637, 2006.
- [47] E. R. Correia, 'Computational studies on HCCI engines', Thesis, Cranfield University, 2010.
- [48] XXX, 'Hot-bulb engine - Wikipedia'. https://en.wikipedia.org/wiki/Hot_bulb_engine (accessed Apr. 05, 2021).

- [49] XXXX, 'A Brief History of the Diesel Engine'. <https://www.agdiesel.com/Blog/ID/153/A-Brief-History-of-the-Diesel-Engine> (accessed Apr. 08, 2021).
- [50] S. Onishi, S. H. Jo, K. Shoda, P. D. Jo, and S. Kato, 'Active thermo-atmosphere combustion (ATAC)—a new combustion process for internal combustion engines', *SAE Trans.*, pp. 1851–1860, 1979.
- [51] M. Noguchi, Y. Tanaka, T. Tanaka, and Y. Takeuchi, 'A study on gasoline engine combustion by observation of intermediate reactive products during combustion', *SAE Trans.*, pp. 2816–2828, 1979.
- [52] P. Najt and D. Foster, 'Compression-ignited homogeneous charge combustion', *SAE Trans.*, vol. 92, pp. 964–979, 1983.
- [53] R. H. Thring, 'Homogeneous-charge compression-ignition (HCCI) engines', SAE Technical paper, 1989.
- [54] D. Kothari, 'Experimental setup and controller design for an HCCI engine', 2014.
- [55] H. Zhao, 'Homogeneous charge compression ignition (HCCI) and controlled auto ignition (CAI) engines for the automotive industry', CRC Press, Boca Raton, Florida, 2007.
- [56] L. A. Gussak, V. P. Karpov, and Y. V. Tikhonov, 'The application of lag-process in prechamber engines', *SAE Trans.*, pp. 2355–2380, 1979.
- [57] M. Stockinger, H. Schaepertoens, and P. Kuhlmann, 'Investigations on a gasoline engine working with self-ignition by compression. Versuche an einem gemischansaugenden Verbrennungsmotor mit Selbstzündung', *Mot. Z.*, vol. 53, no. 2, 1992.
- [58] J.-O. Olsson, P. Tunestål, and B. Johansson, 'Closed-loop control of an HCCI engine', *SAE Trans.*, pp. 1076–1085, 2001.
- [59] D. Law, D. Kemp, J. Allen, G. Kirkpatrick, and T. Copland, 'Controlled combustion in an IC-engine with a fully variable valve train', *SAE Trans.*, pp. 192–198, 2001.
- [60] A. Fuerhapter, W. F. Piock, and G. K. Fraidl, 'CSI-Controlled auto ignition—the best solution for the fuel consumption—versus emission trade-off?', *SAE Trans.*, pp. 1142–1151, 2003.
- [61] xxxxxx, 'GM demonstrates new combustion technology'. </Read/8012/gm-demonstrates-new-combustion-technology> (accessed Apr. 10, 2021).
- [62] S. Nüesch, E. Hellström, L. Jiang, and A. G. Stefanopoulou, 'Mode switches among SI, SACI, and HCCI combustion and their influence on drive cycle fuel economy', in *2014 American control conference*, 2014, pp. 849–854.
- [63] M. Yao, Z. Zheng, and H. Liu, 'Progress and recent trends in homogeneous charge compression ignition (HCCI) engines', *Prog. Energy Combust. Sci.*, vol. 35, no. 5, pp. 398–437, 2009.
- [64] J. Dec and M. Sjöberg, 'Isolating the effects of fuel chemistry on combustion phasing in an HCCI engine and the potential of fuel stratification for ignition control', *SAE Tech. Pap.*, vol. 113, pp. 239–257, 2004.
- [65] D. Flowers, S. Aceves, C. K. Westbrook, J. R. Smith, and R. Dibble, 'Detailed chemical kinetic simulation of natural gas HCCI combustion: gas composition effects and investigation of control strategies', *J Eng Gas Turbines Power*, vol. 123, no. 2, pp. 433–439, 2001.

- [66] J. P. Angelos, M. Puignou, M. M. Andreae, W. K. Cheng, W. H. Green, and M. A. Singer, 'Detailed chemical kinetic simulations of homogeneous charge compression ignition engine transients', *Int. J. Engine Res.*, vol. 9, no. 2, pp. 149–164, 2008.
- [67] X. Lü, Y. Hou, L. Zu, and Z. Huang, 'Experimental study on the auto-ignition and combustion characteristics in the homogeneous charge compression ignition (HCCI) combustion operation with ethanol/n-heptane blend fuels by port injection', *Fuel*, vol. 85, no. 17–18, pp. 2622–2631, 2006.
- [68] M. Izadi Najafabadi and N. Abdul Aziz, 'Homogeneous charge compression ignition combustion: challenges and proposed solutions', *J. Combust.*, vol. 2013, 2013.
- [69] M. N. Schleppe, 'SI-HCCI mode switching optimization using a physics based model', 2011.
- [70] M. Christensen and B. Johansson, 'Influence of mixture quality on homogeneous charge compression ignition', *SAE Trans.*, pp. 951–963, 1998.
- [71] H. Zhao, Z. Peng, J. Williams, and N. Ladommatos, 'Understanding the effects of recycled burnt gases on the controlled autoignition (CAI) combustion in four-stroke gasoline engines', *SAE Trans.*, pp. 2100–2113, 2001.
- [72] A. Cairns and H. Blaxill, 'The effects of combined internal and external exhaust gas recirculation on gasoline controlled auto-ignition', SAE Technical Paper, 2005.
- [73] H. Persson, M. Agrell, J.-O. Olsson, B. Johansson, and H. Ström, 'The effect of intake temperature on HCCI operation using negative valve overlap', SAE Technical Paper, 2004.
- [74] S. S. Morimoto, Y. Kawabata, T. Sakurai, and T. Amano, 'Operating characteristics of a natural gas-fired homogeneous charge compression ignition engine (performance improvement using EGR)', SAE Technical Paper, 2001.
- [75] G. Singh, A. P. Singh, and A. K. Agarwal, 'Experimental investigations of combustion, performance and emission characterization of biodiesel fuelled HCCI engine using external mixture formation technique', *Sustain. Energy Technol. Assess.*, vol. 6, pp. 116–128, 2014.
- [76] P. G. Aleiferis, A. G. Charalambides, Y. Hardalupas, A. Taylor, and Y. Urata, 'Modelling and experiments of HCCI engine combustion with charge stratification and internal EGR', SAE Technical Paper, 2005.
- [77] P. S. Zoldak, 'Design of a research engine for homogeneous charge compression ignition (HCCI) combustion', 2005.
- [78] M. Christensen and B. Johansson, 'Supercharged homogeneous charge compression ignition (HCCI) with exhaust gas recirculation and pilot fuel', Jun. 2000, pp. 2000-01–1835.
- [79] K. Narayanaswamy and C. J. Rutland, 'Cycle simulation diesel HCCI modeling studies and control', SAE Technical Paper, 2004.
- [80] M. J. Atkins and C. R. Koch, 'The effect of fuel octane and diluent on homogeneous charge compression ignition combustion', *Proc. Inst. Mech. Eng. Part J. Automob. Eng.*, vol. 219, no. 5, pp. 665–675, 2005.
- [81] M. Fathi, R. K. Saray, and M. D. Checkel, 'The influence of exhaust gas recirculation (EGR) on combustion and emissions of n-heptane/natural gas fueled homogeneous charge compression ignition (HCCI) engines', *Appl. Energy*, vol. 88, no. 12, pp. 4719–4724, 2011.

- [82] N. Milovanovic, R. Chen, and J. Turner, 'Influence of the variable valve timing strategy on the control of a homogeneous charge compression (HCCI) engine', SAE Technical Paper, 2004.
- [83] Y. Urata, M. Awasaka, J. Takanashi, T. Kakinuma, T. Hakozaki, and A. Umemoto, 'A study of gasoline-fuelled HCCI engine equipped with an electromagnetic valve train', *SAE Trans.*, pp. 1263–1270, 2004.
- [84] M. Christensen, A. Hultqvist, and B. Johansson, 'Demonstrating the multi fuel capability of a homogeneous charge compression ignition engine with variable compression ratio', *SAE Trans.*, pp. 2099–2113, 1999.
- [85] S. Zhong, M. L. Wyszynski, A. Megaritis, D. Yap, and H. Xu, 'Experimental investigation into HCCI combustion using gasoline and diesel blended fuels', SAE Technical Paper, 2005.
- [86] N. Iida and T. Igarashi, 'Auto-ignition and combustion of n-butane and DME/air mixtures in a homogeneous charge compression ignition engine', SAE Technical Paper, 2000.
- [87] J. Hyvönen, G. Haraldsson, and B. Johansson, 'Operating conditions using spark assisted HCCI combustion during combustion mode transfer to SI in a multi-cylinder VCR-HCCI engine', SAE Technical Paper, 2005.
- [88] W. Gong, S. R. Bell, G. J. Micklow, S. B. Fiveland, and M. L. Willi, 'Using pilot diesel injection in a natural gas fueled HCCI engine', *SAE Trans.*, pp. 1911–1921, 2002.
- [89] J. E. Dec and M. Sjöberg, 'A parametric study of HCCI combustion—the sources of emissions at low loads and the effects of GDI fuel injection', *SAE Trans.*, pp. 1119–1141, 2003.
- [90] P. Strålin, F. Wåhlin, and H.-E. Ångström, 'Effects of injection timing on the conditions at top dead center for direct injected HCCI', SAE Technical Paper, 2003.
- [91] A. Helmantel and I. Denbratt, 'HCCI operation of a passenger car common rail DI Diesel engine with early injection of conventional diesel fuel', 2004, pp. 2004-01–0935.
- [92] J. Hyvönen, G. Haraldsson, and B. Johansson, 'Supercharging HCCI to extend the operating range in a multi-cylinder VCR-HCCI engine', *SAE Trans.*, vol. 112, pp. 2456–2468, 2003.
- [93] M. Christensen, B. Johansson, P. Amnéus, and F. Mauss, 'Supercharged homogeneous charge compression ignition', *SAE Trans.*, vol. 107, pp. 1129–1144, 1998.
- [94] M. Y. Au *et al.*, '1.9-Liter four-cylinder HCCI engine operation with exhaust gas recirculation', 2001, pp. 2001-01–1894.
- [95] T. Lee and R. D. Reitz, 'The effect of intake boost pressure on MK (Modulated Kinetics) combustion', *JSME Int. J. Ser. B*, vol. 46, no. 3, pp. 451–459, 2003.
- [96] J.-O. Olsson, P. Tunestål, G. Haraldsson, and B. Johansson, 'A turbo charged dual fuel HCCI engine', 2001, pp. 2001-01–1896.
- [97] S. Gharahbaghi *et al.*, 'Modelling and experimental investigations of supercharged HCCI engines', SAE Technical Paper, 2006.
- [98] D. Yap, M. L. Wyszynski, A. Megaritis, and H. Xu, 'Applying boosting to gasoline HCCI operation with residual gas trapping', SAE Technical Paper, 2005.
- [99] C. G. W. Sheppard, S. Tolegano, and R. Woolley, 'On the nature of autoignition leading to knock in HCCI engines', *SAE Trans.*, pp. 1828–1840, 2002.

- [100] M. Christensen, B. Johansson, and A. Hultqvist, 'The effect of combustion chamber geometry on HCCI operation', *SAE Trans.*, pp. 928–936, 2002.
- [101] M. Christensen and B. Johansson, 'The effect of in-cylinder flow and turbulence on HCCI operation', SAE Technical Paper, 2002.
- [102] R. P. Hessel, S. M. Aceves, and D. L. Flowers, 'A comparison of the effect of combustion chamber surface area and in-cylinder turbulence on the evolution of gas temperature distribution from IVC to SOC: a numerical and fundamental study', *SAE Trans.*, pp. 452–466, 2006.
- [103] R. X. Yu *et al.*, 'Effect of turbulence on HCCI combustion', *SAE Trans.*, pp. 217–229, 2007.
- [104] A. Vressner, R. Egnell, and B. Johansson, 'Combustion chamber geometry effects on the performance of an ethanol fueled HCCI engine', SAE Technical Paper, 2008.
- [105] S. S. Nathan, J. M. Mallikarjuna, and A. Ramesh, 'An experimental study of the biogas–diesel HCCI mode of engine operation', *Energy Convers. Manag.*, vol. 51, no. 7, pp. 1347–1353, 2010.
- [106] S.-C. Kong, R. D. Reitz, M. Christensen, and B. Johansson, 'Modeling the effects of geometry generated turbulence on HCCI engine combustion', *SAE Trans.*, pp. 1511–1521, 2003.
- [107] S. Q. Rizvi, 'Lubricant chemistry, technology, selection, and design', *ASTM Int. Conshohocken*, 2009.
- [108] M. Mofijur, M. M. Hasan, T. M. I. Mahlia, S. M. A. Rahman, A. S. Silitonga, and H. C. Ong, 'Performance and emission parameters of homogeneous charge compression ignition (HCCI) engine: A Review', *Energies*, vol. 12, no. 18, p. 3557, 2019.
- [109] D. Yap, J. Karlovsky, A. Megaritis, M. L. Wyszynski, and H. Xu, 'An investigation into propane homogeneous charge compression ignition (HCCI) engine operation with residual gas trapping', *Fuel*, vol. 84, no. 18, pp. 2372–2379, 2005.
- [110] K. Kobayashi *et al.*, 'Development of HCCI natural gas engines', *J. Nat. Gas Sci. Eng.*, vol. 3, no. 5, pp. 651–656, 2011.
- [111] Y. Zhang and H. Zhao, 'Investigation of combustion, performance and emission characteristics of 2-stroke and 4-stroke spark ignition and CAI/HCCI operations in a DI gasoline', *Appl. Energy*, vol. 130, pp. 244–255, 2014.
- [112] I. Lemberger and G. Floweday, '25cc HCCI engine fuelled with DEE', *SAE Int. J. Engines*, vol. 2, no. 1, pp. 1559–1573, 2009.
- [113] N. N. Al-Khairi, P. Naveenchan, and A. R. A Aziz, 'Comparison of HCCI and SI characteristics on low load CNG-DI combustion', *J. Appl. Sci.*, vol. 11, no. 10, pp. 1827–1832, 2011.
- [114] U. M. Elghawi, A. Mayouf, A. Tsolakis, and M. L. Wyszynski, 'Vapour-phase and particulate-bound PAHs profile generated by a (SI/HCCI) engine from a winter grade commercial gasoline fuel', *Fuel*, vol. 89, no. 8, pp. 2019–2025, 2010.
- [115] H. Li, W. S. Neill, W. Chippior, L. Graham, T. Connolly, and J. D. Taylor, 'An experimental investigation on the emission characteristics of HCCI engine operation using N-Heptane', 2007, pp. 2007-01–1854.
- [116] A. S. Silitonga *et al.*, 'Intensification of reutealis trisperma biodiesel production using infrared radiation: Simulation, optimisation and validation', *Renew. Energy*, vol. 133, pp. 520–527, 2019.

- [117] J. H. Mack, 'Investigation of homogeneous charge compression ignition (HCCI) engines fuelled with ethanol blends using experiments and numerical simulations'. University of California, Berkeley, 2007.
- [118] D. Polovina *et al.*, 'Steady-state combustion development of a downsized multi-cylinder engine with range extended HCCI/SACI capability', *SAE Int. J. Engines*, vol. 6, no. 1, pp. 504–519, 2013.
- [119] J. P. Szybist, K. D. Edwards, M. Foster, K. Confer, and W. Moore, 'Characterization of engine control authority on HCCI combustion as the high load limit is approached', *SAE Int. J. Engines*, vol. 6, no. 1, pp. 553–568, 2013.
- [120] N. Milovanovic, D. Blundell, R. Pearson, J. Turner, and R. Chen, 'Enlarging the operational range of a gasoline HCCI engine by controlling the coolant temperature', SAE Technical Paper, 2005.
- [121] H. Machrafi, S. Cavadias, and J. Amouroux, 'A parametric study on the emissions from an HCCI alternative combustion engine resulting from the auto-ignition of primary reference fuels', *Appl. Energy*, vol. 85, no. 8, pp. 755–764, 2008.
- [122] A. V. Domkundwar and V. M. Domkundwar, 'Internal combustion engines', *Dhanpat Rai CoP Ltd Publ. Delhi Pp7*, vol. 8, no. 7.15, p. 22.30, 2001.
- [123] R. K. Rajput, 'Internal combustion engines'. Laxmi Publications, 2005.
- [124] M. G. Nagargoje, S. S. Ragit, and K. P. Kolhe, 'Review on effect of exhaust gas recirculation (EGR) on NOx emission from C.I. engine', vol. 2, no. 3, p. 4, 2016.
- [125] J. Singh and V. Bansal, 'A review on exhaust gas recirculation (EGR) system in ic engines', p. 11.
- [126] x-engineer.org, 'Exhaust gas recirculation (EGR) complete guide – introduction – x-engineer.org'. <https://x-engineer.org/automotive-engineering/internal-combustion-engines/ice-components-systems/exhaust-gas-recirculation-egr-complete-guide-introduction/> (accessed Apr. 11, 2021).
- [127] N. Ladommatos, S. M. Abdelhalim, H. Zhao, and Z. Hu, 'The dilution, chemical, and thermal effects of exhaust gas recirculation on diesel engine emissions-part 1: effect of reducing inlet charge oxygen', SAE Technical Paper, 1996.
- [128] A. Maiboom, X. Tazua, and J.-F. Hétet, 'Experimental study of various effects of exhaust gas recirculation (EGR) on combustion and emissions of an automotive direct injection diesel engine', *Energy*, vol. 33, no. 1, pp. 22–34, 2008.
- [129] M. Lapuerta, J. J. Hernandez, and F. Gimenez, 'Evaluation of exhaust gas recirculation as a technique for reducing diesel engine NOx emissions', *Proc. Inst. Mech. Eng. Part J. Automob. Eng.*, vol. 214, no. 1, pp. 85–93, 2000.
- [130] M. Deqing, Q. Junnan, S. Ping, M. Yan, Z. Shuang, and C. Yongjun, 'Study on the combustion process and emissions of a turbocharged diesel engine with EGR', *J. Combust.*, vol. 2012, p. 932724, 2012.
- [131] K. Anand, R. P. Sharma, and P. S. Mehta, 'Experimental investigations on combustion, performance, and emissions characteristics of a neat biodiesel-fuelled, turbocharged, direct injection diesel engine', *Proc. Inst. Mech. Eng. Part J. Automob. Eng.*, vol. 224, no. 5, pp. 661–679, 2010.
- [132] GreatPersonality, 'What Is An Exhaust Gas Recirculation System?', *Mechanical Boost*, Feb. 26, 2021. <https://mechanicalboost.com/exhaust-gas-recirculation/> (accessed Jun. 18, 2021).

- [133] xxxxxxxx, 'Diesel Engine EGR System (Page 5) - Line.17QQ.com'. https://line.17qq.com/articles/athesstax_p5.html (accessed May 05, 2021).
- [134] P. C. Jain, 'Greenhouse effect and climate change: scientific basis and overview', *Renew. Energy*, vol. 3, no. 4–5, pp. 403–420, 1993.
- [135] A. K. Saxena, 'Greenhouse gas emissions: Estimation and reduction'. Asian Productivity Organization, 2009.
- [136] S. Vijaya Venkata Raman, S. Iniyar, and R. Goic, 'A review of climate change, mitigation and adaptation', *Renew. Sustain. Energy Rev.*, vol. 16, no. 1, pp. 878–897, 2012.
- [137] A. A. Lindley and A. McCulloch, 'Regulating to reduce emissions of fluorinated greenhouse gases', *J. Fluor. Chem.*, vol. 126, no. 11–12, pp. 1457–1462, 2005.
- [138] J. G. Olivier, J. A. Peters, G. Janssens-Maenhout, and J. Wilson, 'Long-term trend in global CO₂ emissions', 2011.
- [139] J. Lewtas, 'Air pollution combustion emissions: Characterization of causative agents and mechanisms associated with cancer, reproductive, and cardiovascular effects', *Mutat. Res. Mutat. Res.*, vol. 636, no. 1–3, pp. 95–133, 2007.
- [140] J. Figura, 'Modeling and state estimation of automotive SCR catalyst', DIPLOMA THESIS ASSIGNMENT, 2016.
- [141] G. A. Stratakis, 'Experimental investigation of catalytic soot oxidation and pressure drop characteristics in wall-flow diesel particulate filters', *Dr. Philos. Univ. Thessaly*, 2004.
- [142] xxxxxxxxxxxxxx, 'EU: Light-duty: Emissions | Transport Policy'. <https://www.transportpolicy.net/standard/eu-light-duty-emissions/> (accessed Jun. 04, 2021).
- [143] xxxxxxxxxxxxxx, 'Emission Standards: USA: heavy-duty onroad engines'. <https://dieselnet.com/standards/us/hd.php> (accessed Jun. 04, 2021).
- [144] T. Johnson, 'Vehicular emissions in review', *SAE Int. J. Engines*, vol. 7, no. 3, pp. 1207–1227, 2014.
- [145] xxxxxxxxxxxxxxxxxxxxxx, 'Emission Standards: Europe: Cars and Light Trucks'. <https://dieselnet.com/standards/eu/ld.php> (accessed Mar. 17, 2021).
- [146] B. P. Pundir, 'Engine emissions: pollutant formation and advances in control technology'. *Alpha Science International*, Limited, 2007.
- [147] A. Azama, S. Alia, and A. Iqbala, '134. emissions from diesel engine and exhaust after treatment technologies', In *4th International Conference on Energy, Environment and Sustainable Development*, 2016.
- [148] D. Bauner, S. Laestadius, and N. Iida, 'Evolving technological systems for diesel engine emission control: balancing GHG and local emissions', *Clean Technol. Environ. Policy*, vol. 11, no. 3, pp. 339–365, 2009.
- [149] L. Castoldi, N. Artioli, R. Matarrese, L. Lietti, and P. Forzatti, 'Study of DPNR catalysts for combined soot oxidation and NO_x reduction', *Catal. Today*, vol. 157, no. 1–4, pp. 384–389, 2010.
- [150] A. Sassi, R. Rohart, and G. Belot, 'Post-traitement des émissions polluantes des moteurs thermiques à combustion interne', *Mot. À Allumage Par Compression*, pp. 1–24, 2011.

- [151] M. Chen and K. Schirmer, 'A modelling approach to the design optimization of catalytic converters of I.C. engines', in *Design and Control of Diesel and Natural Gas Engines for Industrial and Rail Transportation Applications*, Erie, Pennsylvania, USA, 2003, pp. 201–207.
- [152] T. J. Wang, S. W. Baek, and J.-H. Lee, 'Kinetic parameter estimation of a diesel oxidation catalyst under actual vehicle operating conditions', *Ind. Eng. Chem. Res.*, vol. 47, no. 8, pp. 2528–2537, 2008.
- [153] M. Chen and K. Schirmer, 'A modelling approach to the design optimization of catalytic converters of I.C. engines', in *Design and Control of Diesel and Natural Gas Engines for Industrial and Rail Transportation Applications*, Erie, Pennsylvania, USA, 2003, pp. 201–207.
- [154] T. Kuki, Y. Miyairi, Y. Kasai, M. Miyazaki, and S. Miwa, 'Study on reliability of wall-flow type diesel particulate filter', SAE Technical Paper, 2004.
- [155] K. Ohno, N. Taoka, T. Furuta, A. Kudo, and T. Komori, 'Characterization of high porosity SiC-DPF', *SAE Trans.*, pp. 156–163, 2002.
- [156] A. P. Walker, 'Controlling particulate emissions from diesel vehicles', *Top. Catal.*, vol. 28, no. 1, pp. 165–170, 2004.
- [157] A. M. Stamatelos, 'A review of the effect of particulate traps on the efficiency of vehicle diesel engines', *Energy Convers. Manag.*, vol. 38, no. 1, pp. 83–99, 1997.
- [158] M. K. Khair, 'A review of diesel particulate filter technologies', 2003.
- [159] B. T. Johnson, 'Diesel engine emissions and their control', *Platin. Met. Rev.*, vol. 52, no. 1, pp. 23–37, 2008.
- [160] S. Biswas, V. Verma, J. J. Schauer, and C. Sioutas, 'Chemical speciation of PM emissions from heavy-duty diesel vehicles equipped with diesel particulate filter (DPF) and selective catalytic reduction (SCR) retrofits', *Atmos. Environ.*, vol. 43, no. 11, pp. 1917–1925, 2009.
- [161] R. B. GmbH, 'Denoxtronic 3.1 – Urea dosing system for SCR systems', p. 2.
- [162] xxxxxxxxxxxx, 'Les véhicules essence et Diesel', *IFPEN*. <https://www.ifpenergiesnouvelles.fr/enjeux-et-prospective/decryptages/transports/les-vehicules-essence-et-diesel> (accessed Jun. 19, 2021).
- [163] A. T. Hoang and V. V. Pham, 'A study of emission characteristic, deposits, and lubrication oil degradation of a diesel engine running on preheated vegetable oil and diesel oil', *Energy Sources Part Recovery Util. Environ. Eff.*, vol. 41, no. 5, pp. 611–625, 2019.
- [164] M. F. Al-Dawody and S. K. Bhatti, 'Optimization strategies to reduce the biodiesel NOx effect in diesel engine with experimental verification', *Energy Convers. Manag.*, vol. 68, pp. 96–104, 2013.
- [165] A. E. M. MATER, 'Prediction of NOx emission from turbocharged bio fuel engine', Doctoral dissertation, Sudan University of Science and Technology, 2017.
- [166] M. A. Hamdan and R. H. Khalil, 'Simulation of compression engine powered by Biofuels', *Energy Convers. Manag.*, vol. 51, no. 8, pp. 1714–1718, 2010.
- [167] A. S. Kuleshov, 'Multi-zone DI diesel spray combustion model and its application for matching the injector design with piston bowl shape', 2007, pp. 2007-01–1908.

- [168] H. Venu, V. D. Raju, and L. Subramani, 'Combined effect of influence of nano additives, combustion chamber geometry and injection timing in a DI diesel engine fuelled with ternary (diesel-biodiesel-ethanol) blends', *Energy*, vol. 174, pp. 386–406, 2019.
- [169] H.-A. Kochanowski, W. Kaiser, and D. Esche, 'Noise emission of air-cooled automotive diesel engines and trucks', 1979, p. 790451.
- [170] A. Datta and B. K. Mandal, 'Impact of alcohol addition to diesel on the performance combustion and emissions of a compression ignition engine', *Appl. Therm. Eng.*, vol. 98, pp. 670–682, 2016.
- [171] U. Rajak, P. Nashine, T. N. Verma, and A. Pugazhendhi, 'Performance, combustion and emission analysis of microalgae Spirulina in a common rail direct injection diesel engine', *Fuel*, vol. 255, p. 115855, 2019.
- [172] G. Woschni, 'A universally applicable equation for the instantaneous heat transfer coefficient in the internal combustion engine', SAE Technical paper, 1967.
- [173] A. S. Kuleshov, 'Use of multi-zone DI diesel spray combustion model for simulation and optimization of performance and emissions of engines with multiple injection', SAE Technical Paper, 2006.
- [174] M. F. Al-Dawody, 'Theoretical study for the influence of biodiesel addition on the combustion, performance and emissions parameters of single cylinder diesel engine', *J. Univ. Babylon*, vol. 25, no. 5, pp. 1830–1839, 2017.
- [175] A. C. Alkidas, 'Relationships between smoke measurements and particulate measurements', SAE Technical Paper, 1984.
- [176] A. Datta and B. K. Mandal, 'Engine performance, combustion and emission characteristics of a compression ignition engine operating on different biodiesel-alcohol blends', *Energy*, vol. 125, pp. 470–483, 2017.
- [177] K. Satyanarayana, V. K. Padala, T. H. Rao, and S. V. Umamaheswararao, 'Variable compression ratio diesel engine performance analysis', *Int. J. Eng. Trends Technol.*, vol. 28, pp. 1–12, 2015.
- [178] P. Singh *et al.*, 'Performance analysis and simulation of diesel engine on variable compression ratio', *Int. J. Automot. Eng. Technol.*, vol. 6, no. 1, pp. 9–17, 2017.
- [179] T. Ouksel, A. Chelghoum, and A. Mameri, 'Numerical investigation of the effect of cooled EGR on turbocharger HCCI engine performance fueled with methane', *Int. J. Automot. Eng.*, vol. 7, no. 1, 2017.
- [180] R. Design, 'CHEMKIN 10131', *San Diego*, 2013.
- [181] N. Jamsran and O. Lim, 'Effects of EGR and boosting on the auto-ignition characteristics of HCCI combustion fueled with natural gas', *J. Nat. Gas Sci. Eng.*, vol. 35, pp. 1015–1024, 2016.
- [182] G. P. Smith, 'GRI-Mech 3.0', *Httpwww Me Berkley Edugrimech*, 1999.
- [183] J. Chang *et al.*, 'New heat transfer correlation for an HCCI engine derived from measurements of instantaneous surface heat flux', *SAE Trans.*, vol. 113, pp. 1576–1593, 2004.
- [184] R. Design, 'CHEMKIN Tutorials Manual CHEMKIN® Software. 10112/15112', *React. Des. Livermore CA USA*, 2011.

- [185] M. E. Coltrin, R. J. Kee, and F. M. Rupley, 'Surface CHEMKIN (Version 4. 0): A Fortran package for analyzing heterogeneous chemical kinetics at a solid-surface---gas-phase interface', Sandia National Labs., Livermore, CA (United States), 1991.
- [186] R. Design, 'CHEMKIN theory manual', *San Diego CA*, 2007.
- [187] C. R. Ferguson and A. T. Kirkpatrick, 'Internal combustion engines: applied thermosciences'. John Wiley & Sons, 2015.
- [188] A. İSMAİLOV, S. HALİLOV, M. DOĞAN, and R. MEHDİYEV, 'DİZEL MOTORLARINDA SIKIŞTIRMA ORANININ OTOMATİK', presented at the AUTOMOTIVE TECHNOLOGIES CONGRESS- CONFERENCE PROCEEDINGS, 2004.
- [189] U. Rajak, P. Nashine, T. S. Singh, and T. N. Verma, 'Numerical investigation of performance, combustion and emission characteristics of various biofuels', *Energy Convers. Manag.*, vol. 156, pp. 235–252, 2018.
- [190] A. Gopinath, S. Puhan, and G. Nagarajan, 'Relating the cetane number of biodiesel fuels to their fatty acid composition: A critical study', *Proc. Inst. Mech. Eng. Part J. Automob. Eng.*, vol. 223, no. 4, pp. 565–583, 2009.
- [191] G. Singh, R. Bharj, and R. Kumar, 'Numerical investigation on performance and emission characteristics of a diesel engine fired with methanol blended diesel fuel', *J. Mech. Eng. JMechE*, vol. 16, no. 2, pp. 41–52, 2019.
- [192] Y. Jiao *et al.*, 'Comparison of combustion and emission characteristics of a diesel engine fueled with diesel and methanol-Fischer-Tropsch diesel-biodiesel-diesel blends at various altitudes', *Fuel*, vol. 243, pp. 52–59, 2019.
- [193] U. Rajak and T. N. Verma, 'Effect of emission from ethylic biodiesel of edible and non-edible vegetable oil, animal fats, waste oil and alcohol in CI engine', *Energy Convers. Manag.*, vol. 166, pp. 704–718, 2018.
- [194] P. Shrivastava, T. N. Verma, and A. Pugazhendhi, 'An experimental evaluation of engine performance and emission characteristics of CI engine operated with Roselle and Karanja biodiesel', *Fuel*, vol. 254, p. 115652, 2019.
- [195] T. S. Singh and T. N. Verma, 'Biodiesel production from *Momordica Charantia* (L.): Extraction and engine characteristics', *Energy*, vol. 189, p. 116198, 2019.
- [196] R. Ennetta, A. Yahya, and R. Said, 'Etude de la combustion du méthane enrichi à l'hydrogène', 2012.
- [197] A. Y. Nobakht, R. Khoshbakhi Saray, and A. Rahimi, 'A parametric study on natural gas fueled HCCI combustion engine using a multi-zone combustion model', *Fuel*, vol. 90, no. 4, pp. 1508–1514, 2011.
- [198] M. EL_Kassaby and M. A. Nemit_allah, 'Studying the effect of compression ratio on an engine fueled with waste oil produced biodiesel/diesel fuel', *Alex. Eng. J.*, vol. 52, no. 1, pp. 1–11, 2013.
- [199] R. Sindhu, G. Rao, and K. Murthy, 'Thermodynamic modelling of diesel engine processes for predicting engine performance', *Int. J. Appl. Eng. Technol.*, vol. 4, no. 2, pp. 101–114, 2014.

- [200] M. I. Najafabadi, N. A. Aziz, N. M. Adam, and A. M. Leman, 'Effects of intake temperature and equivalence ratio on HCCI ignition timing and emissions of a 2-stroke engine', *Appl. Mech. Mater.*, vol. 315, pp. 498–502, 2013.
- [201] A. Uyumaz, 'An experimental investigation into combustion and performance characteristics of an HCCI gasoline engine fueled with n-heptane, isopropanol and n-butanol fuel blends at different inlet air temperatures', *Energy Convers. Manag.*, vol. 98, pp. 199–207, 2015.
- [202] M. M. Hasan, M. M. Rahman, K. Kadirgama, and D. Ramasamy, 'Numerical study of engine parameters on combustion and performance characteristics in an n-heptane fueled HCCI engine', *Appl. Therm. Eng.*, vol. 128, pp. 1464–1475, 2018.
- [203] F. Hadia, S. Wadhah, H. Ammar, and O. Ahmed, 'Investigation of combined effects of compression ratio and steam injection on performance, combustion and emissions characteristics of HCCI engine', *Case Stud. Therm. Eng.*, vol. 10, pp. 262–271, 2017.
- [204] M. EL-Kasaby and M. A. Nemit-allah, 'Experimental investigations of ignition delay period and performance of a diesel engine operated with Jatropha oil biodiesel', *Alex. Eng. J.*, vol. 52, no. 2, pp. 141–149, 2013.
- [205] M. Canova, R. Garcin, S. Midlam-Mohler, Y. Guezennec, and G. Rizzoni, 'A control - oriented model of combustion process in a HCCI diesel engine', in *Proceedings of the 2005, American Control Conference, 2005.*, Portland, OR, USA, 2005, pp. 4446–4451.
- [206] K. Raitanapaibule and K. Aung, 'Performance predictions of a hydrogen-enhanced natural gas HCCI engine', in *Energy Conversion and Resources*, Orlando, Florida, USA, 2005, pp. 289–294.
- [207] I. D. Bedoya, S. Saxena, F. J. Cadavid, R. W. Dibble, and M. Wissink, 'Experimental study of biogas combustion in an HCCI engine for power generation with high indicated efficiency and ultra-low NO_x emissions', *Energy Convers. Manag.*, vol. 53, no. 1, pp. 154–162, 2012.
- [208] R. Pešić, 'The experimental VCR diesel engine and determination of double vibe function parameters, CAR 2005', in *Proceedings, 2005*, pp. 1–10.
- [209] B. Menacer and M. Bouchetara, 'Numerical simulation and prediction of the performance of a direct injection turbocharged diesel engine', *simulation*, vol. 89, no. 11, pp. 1355–1368, 2013.